NASA
Contractor Report 3825

AVSCOM
Technical Report 84-A-2

Helicopter Rotor Blade Design for Minimum Vibration

Robert B. Taylor

CONTRACT NAS2-11025
OCTOBER 1984

NASA

U.S. ARMY AVIATION SYSTEMS COMMAND

NASA
Contractor Report 3825

AVSCOM
Technical Report 84-A-2

Helicopter Rotor Blade Design for Minimum Vibration

Robert B. Taylor
United Technologies Research Center
East Hartford, Connecticut

Prepared for Aeromechanics Laboratory
U.S. Army Research and Technology Laboratories (AVSCOM)
and NASA Ames Research Center
under Contract NAS2-11025

National Aeronautics
and Space Administration

**Scientific and Technical
Information Branch**

1984

TABLE OF CONTENTS

PREFACE

This investigation was conducted by the United Technologies Research Center, East Hartford, Connecticut and was sponsored by the Aeromechanics Laboratory, U.S. Army Research and Technology Laboratories (AVRADCOM), Ames Research Center, California, under contract NAS2-11025. The Army technical representative for this contract was Donald L. Kunz of the Aeromechanics Laboratory. The principal investigator was Robert B. Taylor who is no longer at UTRC. For information regarding this contract activity contact Donald Kunz or Anton J. Landgrebe, Manager, Aeromechanics Research, UTRC.

SUMMARY

An analytical investigation was conducted to develop an understanding of the importance and role played by blade design parameters in rotor vibratory response and to design a minimum vibration blade based upon this understanding. Various design approaches were examined for a 4-bladed articulated rotor operating at a high speed flight condition. Blade modal shaping, frequency placement, structural and aerodynamic coupling, and intermodal cancellation were investigated to systematically identify and evaluate blade design parameters that influence blade vibratory airloads, blade modal responses, hub loads, and fuselage vibration.

The relative contributions of the various components of blade force excitation and response to the vibratory hub loads transmitted to the fuselage were determined in order to isolate primary candidates for vibration alleviation. For example, it was found that, due to cancellation effects, coupling of the elastic flatwise mode to produce elastic edgewise mode excitation can be a more important source of the important vibratory in-plane hub loads than the combination of drag, lag inertia and Coriolis excitation. Also, the blade torsion mode and a resonant frequency shift due to interharmonic coupling should be prime considerations for relieving elastic flatwise mode excitation. Findings such as these led to blade design changes based on modal shaping and frequency placement which do not follow established design criteria. Through blade design variations in mass distribution, stiffness, and outboard center-of-gravity location, a blade design was achieved which reduced the predicted fuselage vibrations from the baseline blade by approximately one-half. This analytical study indicates that new blade designs can be developed that offer significant reductions in vibration (and fatigue stresses) without resorting to special vibration alleviation devices, radical blade geometries, or weight penalties.

LIST OF FIGURES

LIST OF FIGURES (Cont'd)

LIST OF FIGURES (Cont'd)

LIST OF FIGURES (Cont'd)

LIST OF FIGURES (Cont'd)

LIST OF FIGURES (Cont'd)

LIST OF TABLES

LIST OF TABLES

LIST OF SYMBOLS

$C_{L\alpha}$	lift curve slope, N.D.
C_T	thrust coefficient, N.D.
c	blade chord, m(ft) or N.D.
CG	chordwise center of gravity, N.D. (percent chord)
dF	differential force, N/m (lb/in)
dm	differential blade mass, kg/m $\left(\frac{\text{lb-sec}^2}{\text{ft}^2}\right)$
dx	differential length in spanwise direction, m(ft)
EA	denotes elastic axis
EI	bending stiffness, N-m^2 (lb-in^2)
F	generalized blade airload, N (lb)
F_x	vibratory hub longitudinal force, N (lb)
F_y	vibratory hub lateral force, N (lb)
F_z	vibratory hub vertical force, N (lb)
j	index in modal shaping, Eq. (4), N.D.
K	airload coefficient, $1/2\rho c\ C_{L\alpha}V_T^2$, N/m (lb/ft), (see Tables 4 through 7)
MSP	modal shaping parameter, N.D.
M_x	vibratory hub roll moment, N-m (ft-lb)
M_y	vibratory hub pitch moment, N-m (ft-lb)
M_z	vibratory hub yaw moment, N-m (ft-lb)
N	denotes per rev frequency, N.D.
P	denotes per rev

q_{iN}	mode i generalized coordinate at harmonic N, N.D.
Q_{T1}	generalized coordinate of torsion mode, N.D.
Q_{V1}	generalized coordinate of first edgewise mode, N.D.
Q_{W1}	generalized coordinate of first flatwise mode, N.D.
Q_{W2}	generalized coordinate of second flatwise mode, N.D.
R	blade radius, m (ft)
V	airspeed, m/s (kt)
V_T	rotor tip speed, m/s (ft/s)
x	blade spanwise coordinate, m (ft) or N.D.
X	in-plane deflection due to edgewise mode deflection, m (ft)
z	amplification factor, N.D.
β	rigid flapping mode response at blade tip, nondimensionalized by blade radius, N.D.
μ	advance ratio, N.D.
ρ	air density, $\frac{kg\text{-}sec^2}{m^4}$ $\left(\frac{lb\text{-}sec^2}{ft^4}\right)$
σ	rotor solidity, N.D.
ϕ	mode shape, N.D.
Ω	rotor speed, rad/sec
ω	modal frequency, rad/sec

Subscripts

E	denotes edgewise mode
F	denotes flatwise mode
i	denotes ith mode
1,2,3	denotes first, second, or third mode

Superscript

( )'	denotes spatial differentiation

INTRODUCTION

Helicopter vibration has long been a problem that affects the performance, cost, and commercial acceptance of the helicopter. As helicopters fly faster, the vibration problem and its effects become more pronounced since helicopters notoriously vibrate more as air speed is increased.

Activity in the helicopter vibration area has increased strongly within the past five years with the advent of the new generation of commercial and military helicopters. The preponderance of this activity has been directed towards sophisticated and even exotic means of controlling vibration. In addition to the use of fixed and rotating system absorbers and various schemes for transmission isolation, the use of special blade tip geometries or designed-in elastic couplings have been theoretically and experimentally investigated. Also, active control of vibration is being vigorously pursued.

The potential for minimizing blade vibratory response through judicious blade design has not been fully exploited. Furthermore, the theoretical and experimental results of Refs. 1 through 3 indicate that the magnitude of the vibration reduction through better blade design is significant and worth pursuing. The need to understand and then determine the importance of all three blade dynamic characteristics, natural frequency, mode shapes and modal damping, is fundamental to improved blade design for vibration.

The investigation reported herein is also concerned with helicopter vibration, but the approach taken is fundamentally different from any that have been reported in the literature.

The premise of this investigation is that too little is known about the fundamentals of vibration, the sources of vibration, and the important parameters involved. Before advancements in vibration alleviation can be achieved, it is necessary to establish a basis of understanding upon which design criteria and approaches can be developed. Towards this end, the most important results reported are the qualitative results rather than the quantitative results.

The analytical study is centered on the main rotor in high speed flight. The main rotor is chosen because it is the prime source of vibration. Obviously, interference caused by proximity of the rotor to the fuselage affects vibration, but this is a problem beyond the scope of this study. Before such an effort can be understood and alleviated, there must first be an understanding of vibration from an isolated rotor. The same reasoning applies

to fuselage tuning. Fuselage frequency placement is quite important, but fuselage tuning will be much more effective if the main rotor loads and vibration are first decreased to the maximum extent possible.

The objective of this study is to develop a fundamental understanding of vibration in cruise, where most helicopters spend the largest percentage of flight time, and to determine the residual level of vibration that is still present after a rotor blade design has been optimized. Once the residual level is known, it is then possible to determine if and what other means are necessary (exotic designs, active control, isolation, etc.) to reduce vibration to the required level for a particular helicopter.

This report starts with a study of the vibratory airloads in cruise, with particular emphasis on the airloads produced by flexible blade motions. Vibration is then traced from the fuselage to the fixed system hub loads, to the rotating blade forces, to the key components involved in these forces, and finally, to the key mode shapes involved. The importance of mode shapes and modal frequency placement is investigated as is the interplay between various modes and between airloads and modes. Based upon the understanding of vibration that is developed, design modifications are made to the baseline blade, and the modified designs are analyzed for their effectiveness in reducing vibration and loads in the main rotor system.

DESIGN FLIGHT CONDITION

The design flight condition for this study is outlined in Table 1.

TABLE 1. - DESIGN FLIGHT CONDITION

Airspeed	82.3 m/s (160 kt)
Rotor Tip Speed	205.7 m/s (675 ft/sec)
Air Density	S.L. std.
Lift	4903 N (10800 lb)
Propulsive Force	538 N (1186 lb)
Shaft Tilt	-4.7 deg
Cyclic Pitch	
Longitudinal	8.2 deg
Lateral	-4.4 deg

The lift and propulsive force are representative for a helicopter rotor system of this size. The flight speed was chosen as 82.3 m/s (160 kt) because it is at the upper limit or slightly higher than level flight cruise speeds on today's helicopters. The combination of this flight speed and a moderately high thrust level ($C_T/\sigma = 0.089$) results in considerable vibration and vibratory loads for a rotor without vibration alleviation devices, and thus presents a challenge for improved blade design.

BASELINE ROTOR SYSTEM

The baseline rotor system that has been used for this investigation is a 4-bladed articulated rotor system similar to the S-76 rotor system without vibration alleviation devices and tip sweep. Table 2 below presents the general characteristics of the baseline blade that has been modeled in the theoretical simulation.

TABLE 2. - GENERAL CHARACTERISTICS OF BASELINE BLADE

Radius	6.71 m (264 in)
Chord	0.396 m (15.6 in)
Twist	-10 deg (nonlinear)
Hinge Offset from Hub Center	0.254 m (10 in)
Mass (outboard of flapping pin)	45.4 kg (100 lb)

The spanwise mass and elastic stiffness properties for the baseline blade are shown in Fig. 1, and the spanwise torsional inertia and stiffness properties are shown in Fig. 2. The blade pitch axis is located at 25 percent chord, and the blade CG and shear center are also nominally located at 25 percent chord. The blade planform is conventional with no sweep or droop.

The blade dynamic characteristics are standard for a conventional articulated rotor blade, as shown in Table 3.

TABLE 3. - BASELINE BLADE NATURAL FREQUENCIES

	per rev
Flatwise Frequencies	
Rigid Body	1.032
First Flexible	2.747
Second Flexible	4.883
Third Flexible	7.728
Edgewise Frequencies	
Rigid Body	0.263
First Flexible	4.769
Torsion Frequency	5.303

THEORETICAL SIMULATION

The theoretical simulation that has been used for this analytical study is the G400 analysis documented in Ref. 4. The G400 analysis, which is based on the Galerkin method, uses uncoupled normal blade modes which are calculated by the eigen portion of the analysis based on blade physical properties. The normal modes can also be input externally. The analysis calculates a time history solution for the rotor, and a harmonic analysis of vibration stresses, airloads, etc. is performed after the solution has converged. The analysis can be run in the coupled rotor-airframe mode. For this study, the hub was fixed, and fuselage vibrations were developed by means of a mobility transfer matrix between the hub and locations in the airframe. This approach was used to isolate rotor design effects from hub impedance and airframe dynamic effects. Further studies would be necessary to determine the effect of hub impedance and airframe dynamics separately on vibration for the rotor design that has been developed in this study.

Uniform inflow is used in the theoretical simulation to model the rotor downwash in high speed flight. This is a reasonable first order approximation in high speed flight, and the use of uniform inflow instead of a variable inflow wake model reduces computer time by a factor of 4-5. But more important than the savings of computer time is the necessity to demonstrate that high vibration levels can occur in high speed flight without variable inflow effects and, furthermore, that the resulting vibration is largely self-induced by rigid and flexible motions of the rotor blade. This will be discussed extensively throughout following sections of the report.

VIBRATORY AIRLOADS IN HIGH SPEED FLIGHT

Figures 3 and 4 show the predicted vibratory lift and drag airloads, respectively, for the high speed flight condition, V = 82.3 m/s (160 kt). The simulated inflow through the rotor disk is uniform, which is a reasonable first order approximation at high speed. The amplitude of the 3, 4, and 5 per rev airloads are shown along the blade span. These airloads are important for a 4-bladed rotor, since they are the primary source of vibratory forcing of the blade natural modes. The vibratory response of these modes, along with the forcing, results in vibratory blade root shears and moments which in turn cause helicopter vibration.

The primary characteristic of Figs. 3 and 4 is the high loading near the blade tip. Note that, for nearly every harmonic shown for both lift and drag, the loading increases along the blade span and is highest at the blade tip. The other notable characteristic is that the magnitude of the airloading decreases with increasing harmonic number. Both of these characteristics are not surprising and intuitively follow from linear 2-dimensional aerodynamic theory for helicopter rotors. What is interesting is that a significant percentage of the vibratory airloads shown is due to airloads induced by the blade rigid and flexible motions. This will be shown in the following section.

Vibratory Airloads Due to Blade Motions

The vibratory lift airloads due to blade motions can be calculated from 2-dimensional linear quasistatic aerodynamic theory for rotor systems in forward flight. The approach that has been taken to show the spanwise shape of these harmonic airloads is to express the equations of blade motion in harmonic form, solve for each harmonic of airload in terms of the appropriate mode shape (or derivative), select characteristic mode shapes for the blade rigid and flexible modes, and substitute the analytic mode shapes in each harmonic airload expression.

Tables 4 through 7 show the form of the harmonic lift airloads due to motion of the rigid body flatwise mode, the first and second flexible flatwise modes, and the flexible torsion mode, respectively. The equations for the mode shapes $\phi(x)$ in Tables 4 through 7 are based on representative spanwise mode shape distributions for an articulated rotor. Each table shows the airload function at N per rev, the amplitude of the airload at the blade tip, and the spanwise shape of the airload that is created. The airload can be of any harmonic N that is one or greater. Note that in all four tables there are four separate airload functions, denoting four separate airload terms. Three of the four terms in all four tables are caused by advance ratio (μ) so that these terms only occur in forward flight. The effect of the presence of

Table 4
N Per Rev Lift Airloads Produced by Motion of the Rigid Body Flatwise Mode

$K = 1/2\ \rho c C_{L\alpha} V_T^2$

$\phi(x) = x$

PER REV MODE MOTION NEEDED TO PRODUCE N PER REV LIFT AIRLOADS	AIRLOAD FUNCTION	AIRLOAD AMPLITUDE AT TIP FOR UNIT MODE DEFLECTION
N	$-Kx\phi(x)$	$-K$
$N \pm 1$	$\frac{K\mu\phi(x)}{2}$	$\frac{K\mu}{2}$
$N \pm 1$	$\frac{-K\mu x\phi'(x)}{2}$	$\frac{-K\mu}{2}$
$N \pm 2$	$\frac{-K\mu^2\phi'(x)}{4}$	$\frac{-K\mu^2}{4}$

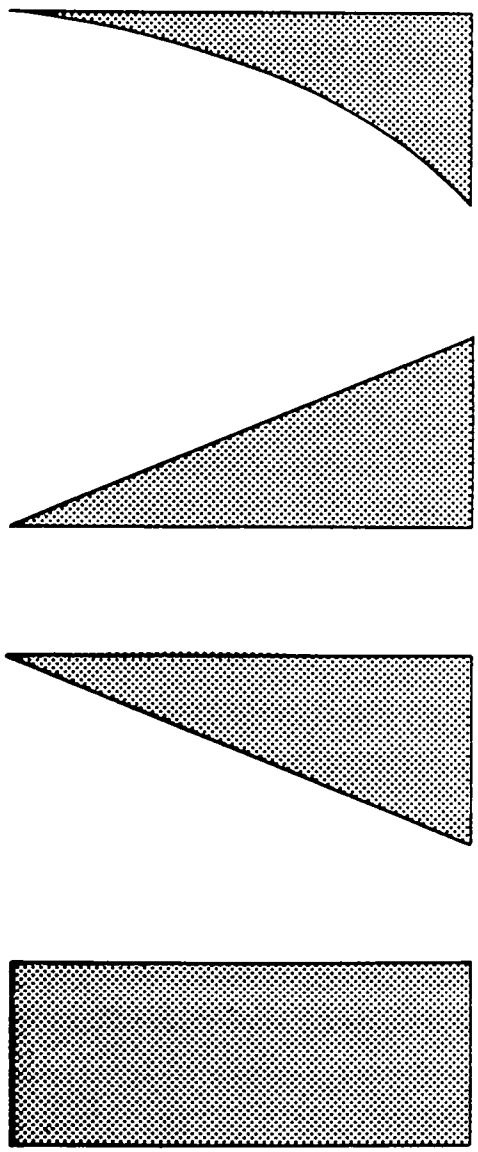

82-11-15-1

Table 5
N Per Rev Lift Airloads Produced by Motion of the First Flexible Flatwise Mode

$K = 1/2\ \rho c C_{L\alpha} V_T^2$

$\phi(x) = 4x^2 - 3x$

PER REV MODE MOTION NEEDED TO PRODUCED N PER REV LIFT AIRLOADS	AIRLOAD FUNCTION	AIRLOAD AMPLITUDE AT TIP FOR UNIT MODE DEFLECTION
N	$-Kx\phi(x)$	$-K$
$N \pm 1$	$\frac{K\mu\phi(x)}{2}$	$\frac{K\mu}{2}$
$N \pm 1$	$\frac{-K\mu x\phi'(x)}{2}$	$\frac{-5K\mu}{2}$
$N \pm 2$	$\frac{-K\mu^2\phi'(x)}{4}$	$\frac{-5K\mu^2}{4}$

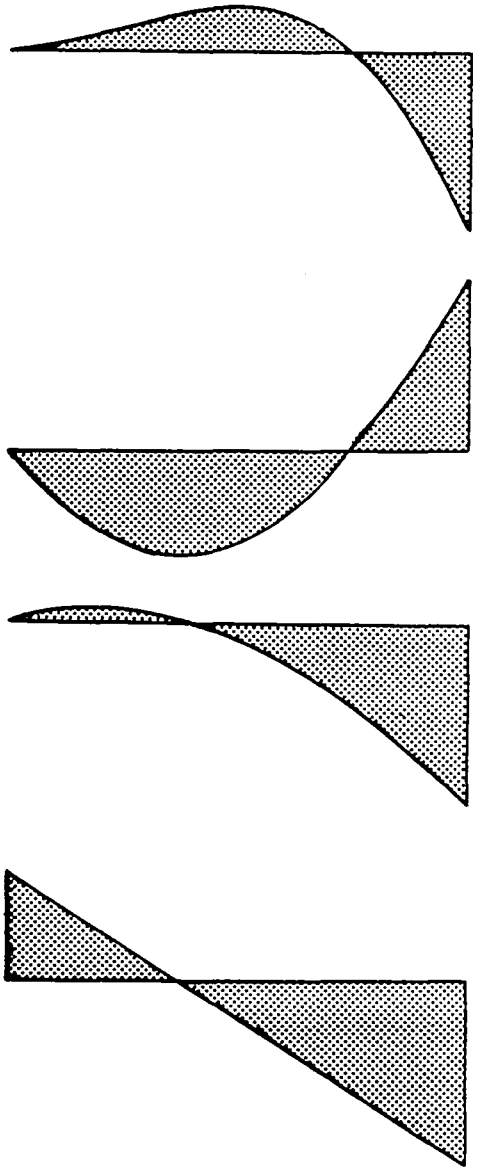

82-11-15-2

Table 6
N Per Rev Lift Airloads Produced by Motion of the Second Flexible Flatwise Mode

$$K = 1/2\ \rho c C_{L\alpha} V_T^2$$

$$\phi(x) = (8x - 26x^2 + 19x^3)$$

PER REV MODE MOTION NEEDED TO PRODUCE N PER REV LIFT AIRLOADS	AIRLOAD FUNCTION	AIRLOAD AMPLITUDE AT TIP FOR UNIT MODE DEFLECTION
N	$-Kx\phi(x)$	$-K$
$N \pm 1$	$\frac{K\mu\phi(x)}{2}$	$K\mu$
$N \pm 1$	$\frac{-K\mu\phi'(x)}{2}$	$\frac{-13K\mu}{2}$
$N \pm 2$	$\frac{-K\mu^2\phi'(x)}{4}$	$\frac{-13K\mu^2}{4}$

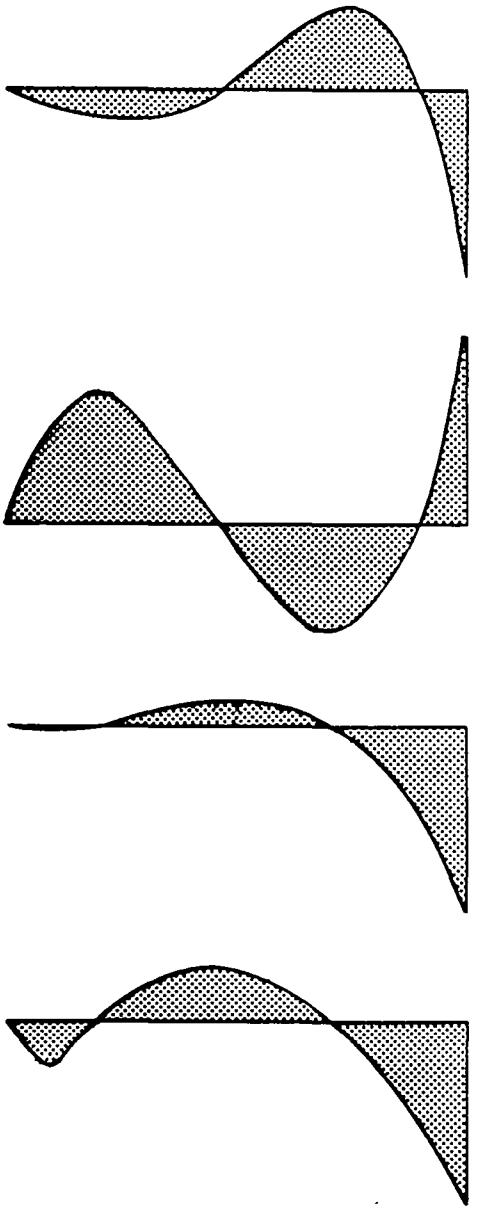

82-11-15-3

Table 7
N Per Rev Lift Airloads Produced by Motion of the First Flexible Torsion Mode

$K = 1/2\ \rho c C_{L\alpha} V_T^2$

$\phi(x) = (2 + 11x - 5x^2)$

PER REV MODE MOTION NEEDED TO PRODUCE N PER LIFT AIRLOADS	AIRLOAD FUNCTION	AIRLOAD AMPLITUDE AT TIP FOR UNIT MODE DEFLECTION
N	$Kx^2\phi(x)$	K
N	$\frac{K\mu^2}{2}\ \phi(x)$	$\frac{K\mu^2}{2}$
N ± 1	$K\mu x\phi(x)$	$K\mu$
N ± 2	$\frac{-K\mu^2}{4}\ \phi(x)$	$\frac{-K\mu^2}{4}$

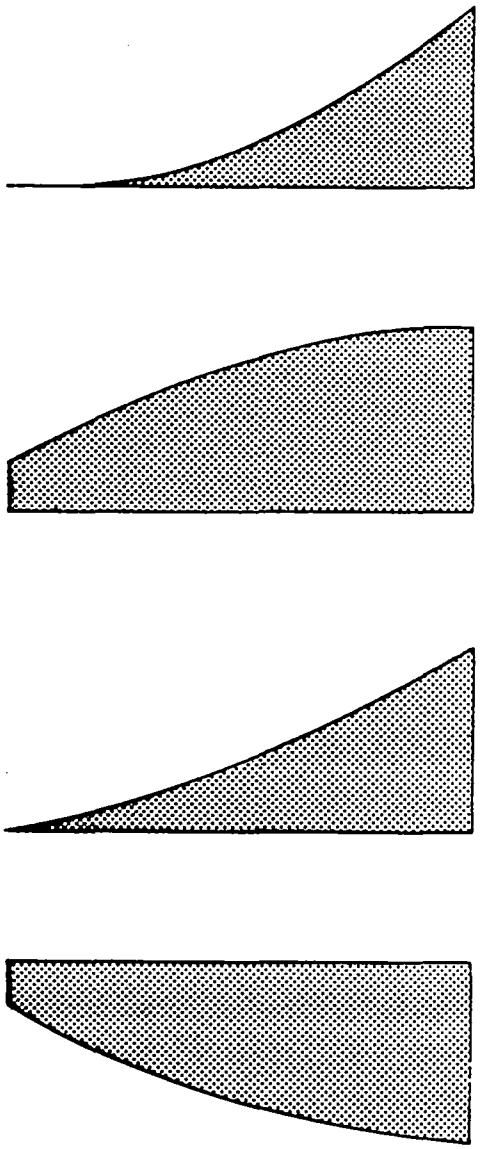

82-11-15-4

advance ratio in these terms is to cause interharmonic coupling between blade motions and the airloads produced by the same blade motions. This is true for all of the advance ratio terms in Tables 4 through 7 except for one term in Table 7 for the torsionally induced airloads. These interharmonic coupling terms arise from the multiplication in the blade equations of motion of a harmonically varying angle of attack and a square of a one per rev variation in the local blade element velocity. These are the same terms that are the source of the periodically varying coefficients in the blade equations of motions. The impact of the interharmonic coupling is to cause blade motions at $N\pm1$ or $N\pm2$ to induce airloads at N per rev in addition to the airloads at N per rev caused by blade motion at N per rev. When the airload function contains μ to a unity power the motion-airload coupling is $N\pm1$ for N per rev airloads. When μ is squared the coupling is $N\pm2$. Since μ is less than 1, terms containing μ are reduced in magnitude compared to the nonforward flight terms, and when μ is squared, the terms are even smaller. However, it will be shown later that the forward flight airload terms are quite significant.

A few other comments are necessary before the shape of the airload induced by blade motion is discussed. First, a linear unstalled lift curve with slope of .1/deg is assumed. Second, mode shapes $\phi(x)$ for each of the modes in Tables 4 through 7 are assumed and are shown at the top of each table. Obviously, the shape of the airloads caused by the harmonic response of these modes will vary as the mode shapes change, but the important point being made in this section is that, for characteristic mode shapes for an articulated rotor, characteristic airload distributions are created by the harmonic motions of the modes. The different airload spanwise shapes that are created are discrete, are definable in terms of spanwise distribution, and are a direct function of the mode shape or the spatial derivative of the mode shape, the advance ratio, and the tip deflection of the mode shape. Third, the airload shapes that are shown in Tables 4 through 7 are normalized for nondimensional unit tip deflection of the mode shapes.

The spanwise airload shapes shown in Tables 4 through 7 provide important information on the influence of blade motions on the harmonic airloads. Without exception, the largest airload amplitude always occurs at the blade tip. This is expected since local section velocity is highest at the blade tip. Even though this result is obvious, it has important implications for vibration induced by these airloads. For vibration, the response of the flexible blade modes is quite important, and since the blade tip is the location of the maximum modal deflection for the flexible modes, this means that maximum energy in the form of harmonic airloads induced by motion of any mode shown occurs at the same spanwise location where the flexible modes can absorb the most energy. Conversely, if the maximum airloads occurred at a blade mode antinode, the mode would not absorb any energy. Another way of viewing it is that the generalized airload (differential airload times modal deflections) for flexible modes is largest at the blade tips.

It is recognized that consideration of wake induced variable inflow would influence the tip loading somewhat, but the airloads due to uniform inflow are assumed to provide a reasonable first order representation for this vibratory study.

Another observation relating to the airloads for blade flatwise motion (Tables 4 through 6) is that the airloads vary more along the blade span as the mode number is increased. For example, airloads due to motion of the second flexible flatwise mode vary more along the blade span than those for the first flexible flatwise mode, and so on. The spanwise variation is directly due to the variation in mode shapes; the higher the mode, the more nodes and antinodes involved. The impact is to cause both positive and negative spanwise airloads for a positive modal tip deflection. From the viewpoint of forced response of the flexible flatwise modes for vibration, this means that the integrated effect along the blade span is reduced.

It is possible that the generalized airload is not reduced, however. For example, the second airload term in Table 5 is a function of the mode shape, so in this case, the spanwise airload changes sign at the same radial location as the mode shape. Therefore, the spanwise generalized airload is always positive or always negative, depending upon the sign of the modal tip deflection.

Probably the most important observation of all is that harmonic airloads, which will force the flexible flatwise modes and ultimately cause vibration, can result from motion of all the modes shown, and not solely from the particular flexible flatwise mode involved. For example, if 3 per rev vibratory response of the blade is of interest, then 3 per rev vibratory response of the first flexible flatwise mode is of prime interest, since it is the mode that is most highly amplified at 3 per rev due to mode frequency placement. In forward flight, 3 per rev airloads are also created by 1, 2, 3, 4, and 5 per rev motion of the rigid body flatwise mode, the second flexible flatwise mode, and the torsion mode. In this example, 3 per rev airloads created by motion of the rigid body flatwise mode are significant because 1 and 2 per rev motion (induced by trimming the rotor with cyclic pitch, collective pitch, and shaft tilt), which are large, are important contributions to the 3 per rev airloads. Trimming the rotor to null the 1 per rev flapping is of little consequence, since it can be shown with 2 dimensional aerodynamic theory in forward flight that cyclic pitch and shaft tilt needed to null the flapping create harmonic airloads also of equal importance. Therefore, a major portion of the 3 per rev airloading due to blade motion can be traced back to the trimming of the rotor in forward flight. It will be shown later that the 3 per rev airloading due to blade motion is a significant portion of the total 3 per rev airloads. Therefore, it can be said that a major portion of the <u>total</u> 3 per rev airloading that causes 3 per rev vibratory response of the blade is due to the

phenomenon of trimming the rotor with cyclic pitch or flapping in forward flight. As airspeed increases, one and two per rev flapping also increase, or the amplitude of cyclic pitch increases to maintain a fixed level of flapping. In either case, it is apparent that 3 per rev airloads and hence 3 per rev vibration will rise as airspeed is increased, simply due to the fundamental phenomenon of helicopters having a periodically varying blade section velocity in forward flight.

Continuing this example even further, it is interesting to note that one and two per rev motion of the first flexible flatwise mode also cause 3 per rev airloading which in turn forces the first flexible mode to respond at 3 per rev. Normally the airloads produced by flexible blade motions are thought of as damping airloads. This is true for 3 per rev motion inducing 3 per rev airloads. But beyond this damping airload, it is interesting to see that modal motions at one harmonic induce modal motions at another harmonic for the same mode because of the interharmonic coupling between motions and airloads. Furthermore, the 3 per rev airloads that are created in this manner are comparable in magnitude to the damping airload simply because the one and two per rev airloads that force the one and two per rev motion of the first flexible flatwise mode are large.

In summary, the airloads in Tables 4 through 7 clarify a primary source of vibratory airloads in forward flight. The total phenomenon can be viewed as a cascade effect, starting with the basic characteristic of helicopter rotors in forward flight. The cascade effect is as follows. One per rev airloads are created by either blade flapping or cyclic pitch. The one per rev airloads cause one per rev response of the blade modes. The resulting one per rev motions create 2 and 3 per rev airloads. These airloads in turn cause 2, 3, 4, and 5 per rev response of the blade modes and so on. Different blade modes respond more than others due to resonant type responses, and vibration results from the combination of inertial, elastic, and raw airloading. It is clear that in forward flight there is no need for stall induced or variable inflow airloads to have significant vibration levels. As speed increases, the effect of advance ratio on the magnitude of the terms in Tables 4 through 7 also increases. The end result is that the rotor is exciting itself to a large degree. With hindsight, this makes sense when compared to the voluminous wind tunnel and flight test data available for helicopters. A fundamental characteristic of helicopter vibration (hingeless, bearingless and teetering included) is that vibratory rotor loads and vibration increase sharply as airspeed increases above 40-50 m/s (80-100 kts). Vibration below 40 m/s (80 kts) is associated with wake interference effects and is not directly associated with the high speed vibration phenomenon being investigated. With hindsight, it also makes sense that variable inflow effects are not the primary source of high speed vibration since the rotor inflow becomes more uniform with increases in airspeed. Thus, from a vibratory rotor load and

vibration viewpoint, the helicopter rotor is the source of its own problems. The challenge is to design the rotor system dynamic response to alleviate these problems inherently; that is, to alleviate the motion-airload cascade effect to the maximum extent possible through improved blade design.

Amplitude of Vibratory Airloads Due to Blade Motions

The previous section showed the types of harmonic airloads that are induced by blade motions for unit modal tip deflection. In this section, the dimensional harmonic airloads due to blade motions are shown. These airloads were obtained by multiplying the nondimensional airload terms in Tables 4 through 7 by the predicted modal motions for the high speed flight condition.

Figures 5 through 8 show the predicted 3, 4, and 5 per rev lift airloads created by 1, 2, 3, 4, and 5 per rev motions of the rigid body flatwise mode, the first and second flexible flatwise modes, and the torsion mode, respectively. The amplitudes of the airloads are shown along the blade span, and a tip and root loss factor has been applied to the results. These airloads are comparable to the total vibratory lift airloads shown in Fig. 3.

It is apparent that the amplitudes of the blade motion induced airloads can be similar to those of the total harmonic airloads shown in Fig. 3. For 3 per rev, the rigid body flapping induced airloads in Fig. 5 even exceed the total 3 per rev airloads. It is clear that the rigid body flapping mode motion is an important source of vibratory airloading to excite the flexible flatwise modes, even at 4 and 5 per rev. These airloads are due to the cascade effect discussed previously. Even the motion of the flexible flatwise modes induces significant harmonic airloads, for example the 3 and 4 per rev airloading shown in Fig. 6.

When all of the blade motion induced airloads are added taking phase into account, the resultant amplitudes of airloads are shown in Fig. 9. Comparing this figure with Fig. 3, it is clear that blade motions account for a large portion of the harmonic airloads in forward flight. For 3, 4, and 5 per rev, the amplitudes of blade motion induced airloads are approximately 2/3, 3/4 and 1/3 of the total airloads, respectively.

Two additional points should be made with regard to these results. First, motion of the rigid body flatwise mode is the dominant contributor to the airloads caused by blade motions. This is shown in Table 8. Except for 5 per rev airloads for which the second flexible flatwise mode is the largest contributor, the contributions of the rigid body flatwise mode are the largest. This is important because it is difficult to change the response of the rigid body mode due to its low frequency and high damping characteristics.

Table 8
Percent Contribution of Individual Blade Modes to Lift Airloads Created by All Blade Motions

	1/REV	2/REV	3/REV	4/REV	5/REV
RIGID BODY FLAT	53	40	46	34	26
1ST FLEXIBLE FLAT	16	35	18	34	16
2ND FLEXIBLE FLAT	2	2	8	20	42
TORSION	29	23	28	12	16

NOTE: VALUES SHOWN ARE FOR AMPLITUDES AT BLADE TIP

Table 9
Percent of Lift Airloads Due to Blade Motions That Are Induced by Interharmonic Coulping

	1/REV	2/REV	3/REV	4/REV	5/REV
RIGID BODY FLAT	22	34	65	53	42
1ST FLEXIBLE FLAT	54	49	58	87	80
2ND FLEXIBLE FLAT	91	52	84	31	59
TORSION	24	40	41	48	50

NOTE: VALUES SHOWN ARE FOR AMPLITUDES AT BLADE TIP

Second, a major portion of the airloads induced by blade motion is due to interharmonic coupling effects; that is, airloads created at N per rev by blade motions at N±1 or N±2 per rev. Whereas N per rev airloads induced by N per rev blade motions are characterized as damping airloads, the interharmonic coupling airloads can be characterized as effective spring and inertia airloads. This is shown in Table 9. The magnitude of these airloads, which are a function of advance ratio (μ or μ^2), are surprisingly large in comparison to the damping airloads which are not a function of μ. For example in Table 9, 65 percent of the 3 per rev airloads (tip amplitude) that are induced by motion of the rigid body flatwise mode are due to motions of the mode at 1, 2, 4, and 5 per rev. Likewise, for the first flexible flatwise mode, 58 percent of the 3 per rev airloads induced by motion of this mode are due to harmonic motions at 1, 2, 4, and 5 per rev. This result is quite important, since the response of a blade mode to blade motion induced airloading is indifferent to the source as long as it is not a damping airloading (N per rev airloading due to N per rev motion of the same mode). Taking the first flexible flatwise mode as an example, this mode will respond to the 3 per rev airloading caused by its own 1, 2, 4, and 5 per rev motion just as if the source of the airloading was the motion of another mode or variable inflow effects. Actually, this is not entirely true; the qualification that is needed is the interharmonic coupling effect on the dynamic amplification. Since, for example, two per rev motion induces 3 per rev airloading, an effective spring is created which alters the apparent mode frequency from its uncoupled frequency in vacuum. This effect can be strong, as will be discussed later. For now, it is sufficient to note that interharmonic coupling from the cascade effect, and not damping airloads alone, dominates the airloads induced by blade motions.

An additional point should be made concerning the harmonic airloads induced by motion of the blade torsion mode. The amplitude of the 3 per rev airloads in Fig. 8 is large compared to the amplitude of the total 3 per rev lift airloads in Fig. 3. This indicates that blade torsion motion is an important source of 3 per rev airloading. The source of the torsion induced 3 per rev airloading is even more revealing. Figure 10 separates the 3 per rev airloading induced by motion of the torsion mode into the contributions due to 2 per rev and 3 per rev torsional motions. The spanwise shapes and amplitudes of these components are similar, but what is even more interesting is the phase of each of these components, noted on Fig. 10. The components are nearly in phase so that they nearly add directly. Apparently, 2 and 3 per rev blade torsion motion are phased so that the 3 per rev induced airloads strongly add from torsional motion at these two harmonics. This could be a coincidence, but the shape of the blade torsion time history response around the azimuth indicates that the two phases are strongly correlated. Figure 11 shows the time history response of the torsion mode. The dominant characteristic of this waveform is the strong nose-down response on the advancing side

of the rotor disk. In Fig. 12, this time history waveform is separated into the individual harmonic components, and the harmonic components starting with 1 per rev are added one at a time until all harmonics through 10 per rev are included.

In Figure 12, the total nose-down amplitude on the advancing side is reached with only 1, 2, and 3 per rev components. The 2 and 3 per rev components necessarily add with a fixed phase, together with the one per rev component, to produce the nose down motion. It is easier to see the phase correlation when the periodic time history is broken down into harmonic components with phase rather than adding harmonic components to produce a periodic waveform. In reality, this matches the actual physical phenomenon. On the advancing side of the rotor disk, the blade section aerodynamic center moves aft with increasing Mach number, and the blade experiences a sharp nose-down induced moment. The blade recovers as it approaches the front of the rotor disk near 180 degrees azimuth. When this blade torsional motion is Fourier analyzed, harmonic amplitude and related phases result. But the phases of these harmonics are closely linked and necessary to produce the fundamental characteristics of the waveform. In this case, this sharp nose-down motion of the blade torsion motion on the advancing side of the rotor disk results in 2 and 3 per rev components of motion which in turn add strongly to produce a 3 per rev airload of large amplitude. The significance of this particular airload contribution in relation to the rotor vibratory response will be discussed later.

PREDICTED BLADE PEAK-TO-PEAK STRESSES

The predicted 1/2 peak-to-peak blade stresses for the baseline blade at the high speed flight condition are shown in Fig. 13. These stresses are indicative of the fatigue loading that must be considered in the rotor blade design. The peaks in the flatwise stresses at 10 and 75 percent span are primarily due to response of the second flexible flatwise mode, since these spanwise locations correspond to the locations for peak spanwise modal moments for this mode. The peak in the edgewise stresses at 15 percent span is primarily due to the lag damper. The remainder of the edgewise stresses is due to response of the first flexible edgewise mode.

Figure 14 presents a harmonic breakdown of the blade stresses at key spanwise stations. For the flatwise stress at 71 percent radius, one per rev response is the largest; stress amplitudes decrease for the higher harmonics. For the edgewise stress at 49 percent radius and the torsional stress at 6.5 percent radius, the amplitude of the 3 per rev stress dominates.

PREDICTED VIBRATION AND HUB LOADS FOR THE BASELINE BLADE

Fuselage Vibrations

The predicted 4 per rev fuselage vibrations for the baseline blade at the high speed flight condition are shown in Fig. 15. The 4 per rev vibration levels, in the cockpit and cabin are shown. Note that no vibration treatment (bifilers, absorbers, etc.) is included in the prediction. While the dominant vibrations are the heel-slide vertical vibrations for the pilot and copilot, the most important vibrations are those affecting crew and passenger comfort, the pilot and copilot vertical vibrations and the cabin vertical vibrations. A good objective would be to reduce the cockpit seats and cabin vibrations to .1 g or lower while reducing the heel-slide vibrations by the maximum extent possible.

Vibratory Fixed System Hub Loads

The predicted vibratory 4 per rev fixed system hub loads for the baseline blade at the high speed flight condition are shown in Fig. 16. The three hub shears are shown along with the three hub moments. Reducing these vibratory loads is the fundamental objective of this study, since they are the source of the fuselage vibrations shown in Fig. 15. The vibratory hub load components with the most influence on fuselage vibration are the three shears. In order of importance they are the longitudinal, lateral, and vertical shears. On other helicopters which may have a different mobility matrix than that being used in this report, the vertical shear may be more important than the two inplane shears. In any case, the three shears have much more influence on fuselage vibration for articulated rotors than the three moments, especially the hub, pitch, and roll moments. These moments are quite small due to the small hinge offset on articulated rotor systems. For hingeless or bearingless rotor systems, the pitch and roll moments become more important, since the effective hinge offset is further outboard than for typical articulated rotor systems.

Rotating Blade Root Shears

Since the 4 per rev hub fixed system shears are the dominant contributors to rotor induced vibration on an articulated rotor, it is important to determine what shears in the rotating blade system contribute to the fixed system shears. On a 4 bladed rotor, the 4 per rev hub fixed system vertical shear results directly from the summation of the 4 per rev blade root rotating shear, assuming the rotor is in a steady-state condition and all blades are performing the same motions and have the same dynamic response. The 4 per rev hub fixed system inplane shears (longitudinal and lateral) result from the

summation of 3 per rev and 5 per rev blade root rotating inplane shears, assuming the same steady-state condition for the rotor. The 3 and 5 per rev root components add together trigonometrically into 2 per rev and 4 per rev components in the fixed system. When the contributions of all four blades are added in the fixed system, the 2 per rev components cancel and the 4 per rev components add. Figure 17 shows the blade root rotating inplane shears for the baseline blade at the high speed flight condition. These are the inplane rotating components that form the 4 per rev fixed system inplane shears shown in Fig. 16.

There are two components of rotating blade inplane shear, a lateral component in the chordwise direction and a radial component in the blade spanwise direction. Figure 17 shows the 3 and 5 per rev contributions for each of these components. The most important result in this figure is the dominance of the 3 per rev shears over the 5 per rev shears. This makes sense for a high speed flight condition. It was shown previously that the 3 per rev blade airloading was approximately 3 times larger than the 5 per rev airloading, so it is logical that the shears should also reflect the dominance of 3 per rev. This result indicates that the best method to reduce the vibratory 4 per rev fixed system hub inplane longitudinal and lateral shears is to reduce the 3 per rev rotating blade root lateral and radial shears. The next most important result of Fig. 17 is that the rotating blade lateral and radial shears are approximately equal. The lateral and radial shears are formed from different inertial, elastic, and airloading components, as will be shown later. This result indicates that many individual contributors must be reduced simultaneously and not, for example, only those components in the chordwise direction that contribute to the lateral shear alone.

Source of Rotating Blade Root Inplane Shears

With the origin of the vibratory 4 per rev hub fixed system inplane shears traced to the 3 per rev rotating blade root shears, the next step is to determine the source of the components contributing to the rotating inplane shears. Figures 18 and 19 break down the blade lateral and radial shears into the basic contributing components, respectively. The results are presented in polar form showing the amplitude and phase of the shears and contributing components. For the blade lateral shear in Fig. 18, the total lateral shear is shown as well as each individual component. The components are added vectorially, and the sum of all the components equals the total blade lateral shear. The most important component is the inertia of the rigid body edgewise mode, denoted lag inertia in Fig. 18. In fact, its amplitude equals the amplitude of the total lateral shear. The next two components are the 3 per rev drag and the 3 per rev coriolis force due to flapping of the rigid body flatwise mode. The 3 per rev coriolis can result from 1, 2, and/or 3 per rev

flapping combined with coning. It is important to see that the sum of the drag and coriolis is nearly equal to the amplitude of the lag inertia; therefore, the sum of the first three components is small. With hindsight, this is logical since the lag mode has such a low frequency (.26 per rev) that it effectively responds as a zero frequency mode. Even with a large amount of damping from the lag damper, this mode has a mass-like response at 3 per rev and nearly cancels the sum of the two components that are causing the mode to respond, the drag and rigid flapping coriolis. In effect, the large contributor to inplane shear is cancelling its source of forcing so the residual is small and inconsequential. This should be true for all articulated rotor systems and should also apply to a large degree for hingeless and bearingless systems with low first mode inplane frequencies, say less than 1 per rev. The next component shown in Fig. 18 is the lag coriolis due to foreshortening caused by rigid edgewise motion; this term is small. The next component is the elastic edgewise inertia due to response of the first edgewise inplane mode. This term is about equal in magnitude to the drag component for the baseline blade. The reason why this mode responds will be discussed later. The next component is the coriolis contribution due to response of the first and second elastic flatwise modes. This term can result from 1, 2, and 3 per rev response of these modes. The next component shown in Fig. 18 is termed the coupled flatwise-edgewise elastic inertia. This term results from inplane inertias that are the product of torsional and vertical displacements and velocities. Another name for this term is the complementary part of X the inplane deflection due to edgewise mode deflection, since when the second derivative of the total inplane deflection is taken to form the inertia, the second derivative of X results plus complementary parts from vertical and torsional deflections. If the blade did not deflect vertically and was not twisted, this term would not be present. The amplitude of this term is of the same order as the lag coriolis and is inconsequential for the baseline blade. The last component shown is the third largest contributor to the rotating blade 3 per rev lateral shear. This term is the elastic flatwise inertia term. This term arises simply because the blade is operating with collective pitch and the blade is also twisted. Therefore, there are inplane components of the flatwise inertial response just as there are vertical components of the edgewise inertial response.

The magnitude of the elastic flatwise inertia is surprising when compared to the magnitude of the elastic edgewise inertia. It has been presumed in the past in the helicopter industry that the source of blade lateral shears in the chordwise direction is the response of the elastic edgewise mode. There is no mention in the literature of the importance of flatwise inertia contributions. And yet the result in Fig. 18 shows that the elastic flatwise inertia contribution, which is due to response of the first flexible flatwise mode, is roughly twice that of the elastic edgewise mode. More will be said about these two terms later.

Summarizing Fig. 18, 3 components effectively cancel: the lag inertia, drag, and rigid flapping coriolis. The remaining two important components are the elastic edgewise inertia and the inplane component of the elastic flatwise inertia. In order to reduce the rotating blade lateral shear these two terms must be reduced.

The components contributing to the blade rotating 3 per rev radial shear are shown in Fig. 19. There are four main components. The first component shown is the lag centrifugal force, which is due to foreshortening caused by rigid edgewise mode motion. The next component is the rigid body flapping acceleration. This term results from 1, 2, and 3 per rev rigid flapping motions. Note that it is orthogonal in phase and about 1/3 the magnitude of the rigid flapping coriolis component shown in Fig. 18. These two terms are closely related. The next component is the centrifugal force due to foreshortening of the elastic flatwise modes. This term is the largest contributing component of all. The last component shown, which is small in magnitude, is the elastic flatwise acceleration. These results also point to the importance of the elastic flatwise modal response in the formation of the inplane shears. It is evident that reduction of the vibratory hub fixed system 4 per rev inplane longitudinal and lateral shears is heavily dependent upon reduction in the response of the elastic flatwise modes, in particular the first elastic flatwise mode.

PREDICTED BLADE NATURAL MODE RESPONSE FOR THE BASELINE BLADE

The harmonic response of the blade natural modes is the key element in the generation of vibratory hub shears and moments which ultimately cause fuselage vibrations. This was indicated by the results of the previous section. For the baseline 4-bladed rotor, the blade modal responses at 3, 4 and 5 per rev are the most important. These are shown in Figs. 20, 21, and 22, respectively. The amplitudes of the mode generalized coordinates (nondimensional modal tip amplitude) are shown for 3 flatwise modes (rigid body and first and second elastic), the first flexible edgewise mode, and the torsion mode. Note that, for the flatwise response, the first flexible mode has the largest amplitude at 3 per rev, due largely to the proximity of its natural frequency to 3 per rev. Based on the results of the previous section, this will have a large impact on the hub inplane shears. For 4 and 5 per rev, the second flexible flatwise mode has the largest amplitude of the three flatwise modes shown. This will have an impact on the hub 4 per rev vertical shear. A surprising result is the large response of the rigid body flatwise mode. For 3, 4, and 5 per rev responses, this modal damping is supercritical and therefore has an apparent low amplification factor. There are two possible reasons for the large rigid body flatwise response at these harmonics. First, the generalized airload for this mode (integration of the distributed harmonic airload times the mode shape) is large. This is a logical result, since the amplitude of the rigid body mode increases approximately linearly along the span to the blade tip and has no antinodes. Second and more important, interharmonic coupling between blade motions and induced airloads increases the effective frequency of this mode, which increases its amplification factor for the higher frequencies. One and two per rev motion of this mode create a 3 per rev airload which acts as an effective spring at 3 per rev for this mode. This will be discussed in more detail later. The large 3 per rev response of this mode has a direct impact on the rotating inplane shears through Coriolis and acceleration, discussed in the previous section.

Summarizing Figs. 20 through 22, there are effectively four modal responses that should be reduced to reduce the vibratory hub 4 per rev fixed system vertical and inplane shears: the rigid body flatwise mode 1, 2, and 3 per rev response, the first flexible flatwise mode 3 per rev response, the first flexible edgewise mode 3 per rev response, and the second flexible flatwise mode 4 per rev response. Table 10 summarizes the influence of these modes on vibratory loads that produce vibration.

TABLE 10. - INFLUENCE OF BLADE NATURAL MODES ON VIBRATORY LOADS THAT PRODUCE VIBRATION

Mode	Harmonic Response	Affected Blade Rotating Shear	Affected Fixed System Hub Shear
Rigid Body Flapping	1P,2P,3P	3P lateral 3P radial	4P lateral 4P longitudinal
First Flexible Flatwise	3P	3P lateral 3P radial	4P lateral 4P longitudinal
Second Flexible Flatwise	4P	4P vertical	4P vertical
First Flexible Edgewise	3P	3P lateral	4P lateral 4P longitudinal

MODAL SHAPING FOR REDUCED FLATWISE MODE RESPONSE

This section discusses changes made to the baseline blade design in order to reduce the dynamic 4 per rev response of the second flexible flatwise mode by altering the shape of the mode. As shown previously, the response of this mode at 4 per rev is the most important source of 4 per rev vertical hub shears which contribute to fuselage vibrations.

There are three basic ways to alter the dynamic response of a blade natural mode at some fixed frequency of forcing. First, the dynamic amplification can be changed by altering the mode natural frequency. This changes the mode amplification factor with, it is hoped, a reduction at the forcing frequency. Frequency placement is the rotor blade design method most commonly used in the helicopter industry today.

The second method is to change the modal damping. Modal damping can be altered by changes in the mode natural frequency and by changes in the mode shape. In terms of generalized coordinates of the blade flatwise natural modes, the mode critical damping ratio is inversely proportional to the mode natural frequency, ω, and is also inversely proportional to the mode generalized mass, $\int\phi^2 dm$, where ϕ is the spanwise mode shape and dm is the mass distribution. The damping ratio is directly proportional to the integral $\int\phi^2 x dx$ where x is the blade spanwise coordinate. For the blade flatwise modes, the source of damping is aerodynamic due to velocity induced airloading caused by modal motion. The integral $\int\phi^2 x dx$ is a measure of the amount of modal damping that can be achieved per unit modal tip displacement. Note that the frequency of modal displacement must be the same as the frequency of forcing. For example, the 2 per rev flatwise mode does not dampen the flatwise modal response at 3 per rev; only 3 per rev motion will create modal aerodynamic damping at 3 per rev.

The third way to alter the blade mode dynamic response is to change the level of modal forcing. This is the subject of this section. In terms of generalized coordinates for the flatwise modes, the level of modal forcing is the generalized airload $\int\phi \frac{dF}{dx} dx$ where $\frac{dF}{dx}$ is the spanwise distributed aerodynamic loading along the blade span x. The integral is independent of the mode natural frequency. This is important because it will be shown that the flatwise mode shapes can be changed substantially without significantly changing the mode natural frequency. The value of the integral is then a function of the product of the spanwise mode shape and the distributed harmonic airloading, regardless of the harmonic of the airloading. If this integral is to be reduced to decrease the modal dynamic response, then the spanwise shape of the airloading is important.

In Ref. 1*, a modal shaping parameter (MSP) was developed as an aid in determining how the mode shape should be tailored in order to decrease the level of harmonic forcing. This modal shaping parameter has been used in this investigation to determine what changes in the baseline blade design are necessary to reduce the level of harmonic loading on the flatwise modes. The MSP results directly from solving the modal equation of motion for the harmonic root shear due to the modal response:

$$\text{Root shear due to mode i} = R \cdot q_{iN} \cdot \omega_i^2 \int \phi_i dm \quad \text{(1)}$$
$$\text{At harmonic N}$$

$$q_{iN} = \frac{1}{[z]_{iN}} \quad \frac{\int \phi_i \frac{dF}{dx} dx}{R(N\Omega)^2 \int \phi_i^2 dm} \quad \text{(2)}$$

where q_{iN} is the mode i generalized coordinate at harmonic N and z is the dynamic amplification of mode i at harmonic N. Then

$$\text{Root shear due to mode i} = \frac{1}{[z]_{iN}} \quad \frac{\omega_i^2 \int \phi_i dm \cdot \int \phi_i \frac{dF}{dx} dx}{(N\Omega)^2 \int \phi_i^2 dm} \quad \text{(3)}$$
$$\text{At harmonic N}$$

The MSP is a form of the triple integral product in equation (3). The MSP is defined as

$$MSP = \frac{\int \phi dm \cdot \int \phi x^j dx}{\int \phi^2 dm} \quad \text{(4)}$$

*Reference 1, "Helicopter Vibration Reduction by Rotor Blade Modal Shaping" includes a more detailed derivation of the modal shaping parameter along with a description and initial application of the modal shaping concept.

The first integral in the numerator is proportional to the root modal shear per unit tip deflection of the mode. The integral in the denominator is the generalized mass of the mode, where dm is the distributed blade spanwise mass. The second integral in the numerator is a form of the generalized airload integral, where x is the blade spanwise coordinate and j indicates the assumed spanwise shape of the harmonic airloading. For example, if j = 0, the harmonic airload is uniform along the blade span. If j = 1, the harmonic airload spanwise shape is triangular; zero at the blade root and 1 at the blade tip (the integral is normalized for a maximum harmonic airload amplitude of 1). If j = 2, the harmonic airloading distribution is quadratic. As the value of j increases the harmonic airloading becomes more and more concentrated at the blade tip.

The usefulness of the MSP lies in its ability to quickly determine the best spanwise shape the mode should have in order to reduce the level of forcing for a given harmonic airload distribution. For example, if it is known that the harmonic airloading distribution of interest is essentially uniform, then j can be assigned the value of zero and the mode shape appropriately tailored. If the harmonic airloading is concentrated at the blade tip, j can be assigned a higher value, say 2 or 3, to determine the best mode shape to minimize the MSP. Minimizing the MSP in this manner essentially minimizes the amount of energy the mode can absorb from the impressed harmonic airloading. The concept is not peculiar to rotor blade modes with aerodynamic forcing; it applies to all beams with distributed dynamic loading. The key to successful use of the MSP is to shape the most resonant mode at the harmonic of interest and to model the aerodynamic loading correctly in the MSP. Note that the amplitude of the airloading is not involved in the MSP, so only the spanwise shape of the harmonic airloading is important.

In order to model the harmonic aerodynamic loading correctly for use in the MSP, the predicted spanwise lift airloading shown previously has been used and appropriately altered to account for damping effects. Figures 23 and 24 show the predicted spanwise harmonic airloading distributions at 3, 4, and 5 per rev after the damping airloads have been vectorially subtracted. Figure 23 shows the resulting airloads for the first flexible flatwise mode, and Fig. 24 shows the airloads for the second flexible flatwise mode. The damping airloads were removed from these figures by calculating the harmonic airloading produced by motion of the modes at the same harmonic. The mode generalized coordinates were taken from the predicted results for the baseline blade design. The resulting airloads are then what the modes would perceive as harmonic forcing, which includes airloads produced by other modes and even airloads produced by the same mode but not by motions of the mode at the same harmonic since these are the damping airloads.

The primary characteristic of Figs. 23 and 24 is that the highest airloading occurs at the blade tip, except for 3 per rev airloading for the first flexible flatwise mode. The objective of this section is to reduce the response of the second flexible flatwise mode at 4 per rev in order to reduce the 4 per rev vertical hub shear. In Fig. 24, the 4 per rev airloading is strongly concentrated at the blade tip. Only the 5 per rev airloading shows more tip concentration. In terms of the MSP, the 4 per rev airloading can be characterized by a value of 2 or 3 for j in Eq. (4), indicating a quadratic or cubic airloading distribution. A value of 3 was selected for j in the MSP and a concentrated mass was placed at different locations along the blade span to alter the second flexible flatwise mode shape and change the MSP. The results are shown in Fig. 25.

Two values of concentrated mass were used: 2.27 kg (5 lb) and 4.53 kg (10 lb). Placing the concentrated mass near the blade tip is the most effective approach, and the 4.53 kg (10 lb) mass is more effective than the 2.27 kg (5 lb) mass.

Based on these results a radial location of .909 R was chosen for the location of a concentrated mass, and the G400 analysis was used to predict the change in 4 per rev modal response and 4 per rev vertical hub shear as the amount of mass was changed. Figures 26 and 27 show the predicted results for the modal response and vertical shear, respectively. There is a strong correlation between the results shown in the two figures. Adding the 2.27 kg (5 lb) weight reduces the modal response by over 70 percent (Fig. 26) and reduces the vertical shear by 80 percent (Fig. 27). Adding additional weight further decreases the modal response and vertical shear; however, for concentrated masses greater than about 5.44 kg (12 lb), the effect is detrimental. The reason this happens is clearly shown in Fig. 26 and also in Fig. 25. In Fig. 26, the modal response phase is changing rapidly for concentrated masses between 4.53 kg (10 lb) and 6.80 kg (15 lb). For the given shape of spanwise 4 per rev airloading, the amount of energy that the mode can absorb has been minimized. Adding more weight changes the sign of the MSP as it passes through an effective null point (see Fig. 25), and the mode absorbs more and more energy from the impressed 4 per rev airloading. Only the phase of absorbed energy is reversed, since the sign of the generalized airload integral in Eq. (2) is reversed. It should be noted that adding tip weight increases the mode natural frequency from 4.89 per rev for the baseline to 5.33 per rev for the 4.53 kg (10 lb) weight. This reduces the modal amplification at 4 per rev. However, further increases in weight continue to increase the frequency (5.54 per rev for 15 lb) and reduce the modal amplification. Therefore, the effect shown in Figs. 26 and 27 is due to a fundamental change in the generalized airloading and not to dynamic amplification.

Based on the results of Fig. 27, the baseline design was modified by adding a 4.53 kg (10 lb) weight at .909 R. This design is called modified design No. 1. The predicted effect of the added 4.53 kg (10 lb) weight on the blade mode generalized coordinates is shown in Fig. 28. The 4 per rev response of the second flexible flatwise mode has been reduced by about 80 percent compared to the baseline. In fact, the response of all of the modes has been reduced, except for the first flexible flatwise mode response at 4 per rev. The predicted 4 per rev fixed system hub loads for modified design No. 1 are shown in Fig. 29. Compared to the baseline, the 4 per rev vertical shear is decreased by 70 percent. There are also substantial reductions in the inplane shears due to the reduction in the 3 per rev edgewise mode response and first flexible flatwise mode response, as shown in Fig. 28. The only increases are in the pitch and roll moments. As previously mentioned, these hub moments are low for articulated rotors and have small effect on fuselage vibrations.

The predicted fuselage vibrations for modified design No. 1 are shown in Fig. 30. In general, the fuselage vertical vibrations have been decreased by about 40 percent (except the pilot seat which is about .05 g's). This vibration reduction is attributed not only to a reduction in the response of the second flexible flatwise mode which caused a reduction in the vertical hub shear, but also to a decrease in the lateral and longitudinal shears, as shown in Fig. 29.

The reason for the reduction in these two inplane shears is shown in Figs. 31 and 32. These figures show the 3 per rev rotating lateral and radial shears and the individual components that vectorially add to form the shears. These figures for modified design No. 1 can be compared directly with Figs. 18 and 19 for the baseline blade design. For the lateral shear (Fig. 31), all of the individual components have been reduced, except for the 3 per rev drag. However, the vectorial sum of the first three components (lag inertia, drag, and rigid flapping Coriolis) is small, just as it was for the baseline.

The reduction in the rigid body flapping Coriolis is due to a combined reduction in 1 and 2 per rev flapping (particularly 2 per rev), not in 3 per rev flapping which remains about the same as for the baseline. Apparently, the change in the 2 and 3 per rev airloads, resulting from the reduced response of the first flexible flatwise mode, reduces the forcing of the rigid flapping mode at 2 per rev. This results in a reduced 3 per rev Coriolis, and a reduced lag mode response, which responds to the Coriolis forcing. The reduction in the rigid flapping and lagging responses also affects the 3 per rev radial shear (Fig. 19), as expected. This is a good indication of the strong influence of elastic mode response on the airloads. Another way of viewing this is that the blade flatwise modes are strongly coupled through the airloads, resulting in the cascade effect mentioned previously.

The reduction in contributions due to the elastic flatwise and edgewise modes ranges from 40 to 50 percent. A major portion of the reduction in the first flexible flatwise mode response clearly comes from a reduction in the generalized airload for this mode. The generalized airload (with damping airload removed from raw airload) is reduced by 20 percent compared to the baseline, so about half of the 40 percent reduction in the 3 per rev response of the first flexible flatwise mode (Fig. 28) is due to a reduction in the generalized airload. The other half comes from a reduction in the dynamic amplification factor at 3 per rev for this mode, even though the uncoupled natural frequency for this mode in vacuum increased from 2.736 to 2.938 per rev for this mode. On the surface, this should substantially increase the 3 per rev response of this mode, but it will be shown later that the natural frequency of this mode is much higher than 3 per rev due to an airspring effect. Therefore, increasing the uncoupled frequency actually reduces the 3 per rev response of this mode.

The source of the 50 percent reduction in the 3 per rev response of the first flexible edgewise mode (Fig. 28) is not so easily determined. It was noted previously that the 3 per rev drag did not change between the baseline and modified blade designs, so a change in drag forcing could not be the source of the reduction in the edgewise mode response. Furthermore, drag forcing has only a small effect on the response for this mode. This conclusion is reached by calculating the 3 per rev generalized airload for this mode by integrating the predicted 3 per rev drag from G400 and the predicted first flexible edgewise mode shape along the blade span. The drag is the inplane aerodynamic component and includes induced as well as pressure drag. Even if no damping is assumed for this mode, the dynamic response for the calculated generalized airload due to drag is only 14 percent of the G400 predicted response. Three per rev drag is not an important source of forcing for this mode.

Another possible source of forcing for the edgewise mode is Coriolis due to rigid body flapping. To calculate its effect on the response of the edgewise mode, the 3 per rev Coriolis force is treated as a generalized force by integrating the Coriolis and the edgewise mode shape along the blade span. The result shows that Coriolis forcing has even less effect (1/20) on edgewise response at 3 per rev than drag. The edgewise response due to Coriolis is less than 1 percent of the G400 predicted response.

This result is obvious, with hindsight, because it is the integrated Coriolis effect that forces the edgewise mode. Since the spanwise Coriolis force at a blade radial station is proportional to the rigid body flatwise mode shape, weighted by the mass distribution, the edgewise mode generalized force is proportional to the integral of the rigid body flatwise mode and the first flexible flatwise mode. This integral is quite small, simply because these two modes are nearly orthogonal. The first flexible edgewise mode is

orthogonal to the rigid lag mode and the rigid lag mode is quite similar to the rigid flapping mode, so it makes sense that the rigid flapping mode and the flexible edgewise mode should also be nearly orthogonal. This is not true for the rigid lag mode, since the lag mode and the rigid flapping mode are quite similar. Therefore, Coriolis through rigid body flapping is a prime source of forcing for the rigid lag mode. Looking at it another way, the first flexible edgewise mode looks like the first flexible flatwise mode, so again orthogonality between the rigid flatwise mode and the flexible edgewise mode can be expected.

To summarize, neither 3 per rev drag nor Coriolis force excite the flexible edgewise mode to any great extent. The source of the response of this mode is related to the response of the first flexible flatwise mode. These two modes are strongly coupled inertially because of blade twist and collective pitch, so the response of one mode strongly influences the response of the other mode. More will be said about this effect later.

The last result to be shown for modified blade design No. 1 is the effect on the blade fatigue stresses. Figure 33 shows the predicted change in blade peak-to-peak flatwise, edgewise, and torsional stresses along the blade span for the modified blade design. The peak outboard flatwise stresses, the most critical on the blade design, have been reduced by 37 percent. The peak mid-span edgewise stresses, also critical, have also been reduced by 37 percent. The peak inboard torsional stresses have been reduced by 33 percent with the modified blade design. Obviously, the reduced 3, 4, and 5 per rev harmonic blade mode response contributes to this stress reduction, but more importantly, the stress reduction is primarily due to a reduction in 1 and 2 per rev response of these modes. This result demonstrates that blade fatigue stress benefits as well as vibration reduction can be obtained with the modified blade design.

EFFECT OF FLAPPING ON VIBRATORY HUB LOADS

In the last section, it was noted that, for modified design No. 1, with 4.53 kg (10 lb) at .90 R, there is a reduction in the rigid flapping Coriolis force and the rigid lag mode inertial force components in the 3 per rev lateral shear. Also, the rigid body flapping acceleration and the rigid lag mode centrifugal force components in the 3 per rev radial shear are reduced. The reduction in the flapping induced 3 per rev force components is due to a reduction in the two per rev flapping, since 1 and 2 per rev flapping combine to produce a 3 per rev Coriolis lateral shear and a 3 per rev radial acceleration. The lag mode components are reduced, since the Coriolis forces induced by flapping are a primary source of forcing for the rigid lag mode. Since flapping induced Coriolis is such a strong source of forcing for the lag mode, and the lag response is a large component in the 3 per rev rotating blade lateral and radial shears, it is worthwhile to investigate the effect of reduced Coriolis through reduced flapping and the resultant effect on lag mode response and blade rotating shears. In this section, the 3 per rev Coriolis force is reduced by reducing 1 per rev flapping while holding a constant tip path plane, remembering that 3 per rev Coriolis comes not only from coning times 3 per rev flapping, but also from the product of 1 and 2 per rev flapping. The 1 per rev flapping is reduced by adjusting cyclic pitch while at the same time adjusting shaft tilt to maintain a constant tip path plane angle. The results are shown in Figs. 34 and 35. These figures show the 3 per rev amplitude of the rotating blade lateral and radial forces along with the prime components of these forces as a function of 1 per rev blade flapping. In Fig. 34, the rigid body flapping Coriolis force reduces linearly with reduced flapping. The Coriolis force for zero flapping is that due to coning times 3 per rev flapping. The rigid body lag inertia also reduces with flapping. The 3 per rev drag remains essentially constant as does the elastic edgewise inertia force. A constant elastic edgewise inertial force implies no change in the response of this mode with changes in flapping. This is further confirmation of the insensitivity of the mode to Coriolis.

Even though there are large changes in the Coriolis and lag inertia forces, there is essentially no change in the 3 per rev rotating blade lateral force. The obvious reason is that the lag inertia force and the Coriolis force cancel each other in combination with the drag (cf. Fig. 31). For moderate flapping, there is a vectorial cancellation of large numbers; for small flapping, there is a cancellation of small numbers. In both cases, the residual remains about the same.

The same results hold true for the 3 per rev rotating blade radial force, shown in Fig. 35. The 3 per rev flapping acceleration component reduces with flapping, since it is a function of the product of 1 and 2 per rev flapping as

is the Coriolis force. The rigid lag centrifugal force proportionately decreases with flapping, but the rotating blade radial force remains essentially unchanged with flapping, although a near zero flapping condition does reduce the radial force by about 16 percent compared to that for moderate flapping. For the radial force, the vectorial cancellation between flapping and lag induced forces is not as strong (cf. Fig. 32) as that for the lateral force, but is still generally true.

The predicted effect of flapping on the 4 per rev fixed system hub loads is shown in Fig. 36 for modified blade design No. 1. There is essentially no change in the hub longitudinal and lateral shears with flapping. This result demonstrates that reductions in hub loads and vibration cannot be achieved by minimizing blade flapping in high speed flight.

EFFECT OF EDGEWISE FREQUENCY ON VIBRATORY HUB LOADS

It has been previously noted that the 4 per rev hub fixed system inplane shears are an important source of vibratory forcing on 4-bladed rotor systems. The elastic edgewise mode response is a significant contributor to the inplane loads. In Fig. 31, the 3 per rev elastic edgewise mode response was shown to be an important contributor to the 3 per rev blade rotating lateral shear, which combines with the 5 per rev rotating lateral shear to form the hub fixed system inplane 4 per rev shear. The 4 per rev elastic edgewise mode response is also important, since this response is the source of hub 4 per rev yaw moment and torque of the drive system. Therefore, reduction of the response of this mode is beneficial from both a vibration and a loads point of view. One major way of reducing the response of this mode is to alter its frequency, either through stiffness or mass.

This approach was investigated for modified blade design No. 1, and the results are shown in Fig. 37. The amplitude of the edgewise mode generalized coordinate at 3, 4, and 5 per rev is shown as a function of the edgewise mode frequency for the high speed flight condition. The capability in the G400 analysis to change the frequency while holding the mode shape constant was used so that the effect of frequency alone could be isolated. The edgewise mode shape used is that for modified design No. 1. The results are generally as expected. The highest 3 per rev response is when the frequency is at 3 per rev. The same holds true for the 4 and 5 per rev response.

The most notable result of Fig. 37 is that it clearly shows that the best edgewise mode tuning to reduce edgewise mode response at all 3 harmonics (3, 4, 5) is above 5 per rev, not between 3 and 4 or between 4 and 5 per rev. Compared to the edgewise mode response for modified design No. 1 there is a significant reduction in the response of the edgewise mode for a 5.5 per rev tuning. This is shown in Table 11.

TABLE 11. - PREDICTED REDUCTION IN THE EDGEWISE MODE RESPONSE FOR 5.5 PER REV EDGEWISE MODE TUNING

V = 82.3 m/s (160 kt)

3/rev	4/rev	5/rev
39%	54%	9%

Note: edgewise mode frequency for modified design No. 1 is 4.64/rev.

The reduction in the 3 per rev response indicates that the inplane shears, which contribute to 4 per rev fixed system hub inplane shears, should decrease. Also, the reduction in the 4 per rev response indicates that the hub 4 per rev yaw moment and torque of the drive system should decrease significantly.

Figure 38 shows that the expected hub inplane shears do decrease when the edgewise frequency is increased, but there is essentially no reduction between the modified blade design No. 1 tuning of 4.64 per rev and the 5.5 per rev tuning. With hindsight, this result could be expected because there are many individual contributions to the 3 per rev rotating blade lateral shear; therefore, the vectorial sum as affected by vectorial cancellation becomes important. For example, in Fig. 31 for modified blade design No. 1, the elastic edgewise inertia contribution is orthogonal to the total shear, which is the sum of all the components. Even if the elastic edgewise inertia was reduced to zero, the total 3 per rev inplane shear amplitude would not be significantly affected; the only indication would be a change in the response phase by about 20 to 30 degrees. This result emphasizes the fact that there are many sources of inplane shear, and reducing the edgewise mode response by 39 percent by means of frequency tuning cannot guarantee a proportionate reduction or any reduction for that matter.

Nevertheless, it is desirable to reduce the edgewise mode response as much as possible, since there is not only a reduction in edgewise stresses with a reduction in the modal response, but also because it is more desirable to vectorially form a residual (total shear) from small components rather than from large ones. The 9 percent reduction in the 5 per rev response is not large, but it should help to reduce load and vibration in the low speed region where the rotor wake significantly influences the rotor vibratory response. In this low speed flight region, 5 per rev edgewise mode response has been known to be quite high. Furthermore, there is still a significant reduction in the 4 per rev edgewise mode response with a tuning of 5.5 per rev. This has a direct impact on the hub 4 per rev yaw moment, since the edgewise mode response is the major contributor to this hub load. This is shown in Fig. 39, which presents the predicted 4 per rev fixed system hub loads for the high speed flight condition. The results for the baseline design and modified design No. 1 are shown. Also shown are the results for a blade design in which the edgewise stiffness was increased for modified blade design No. 1. The target edgewise frequency was 5.5 per rev; the result is 5.23 per rev. There is little change in the longitudinal and lateral shears, but the hub yaw moment has significantly decreased due to a reduction in the 4 per rev edgewise mode response. This design change has a small impact on vibration, but the benefits for drive system loads clearly demonstrate the desirability of high edgewise mode tuning.

In summary, tuning the edgewise mode higher than 5 per rev decreases edgewise mode response significantly compared to tuning between 3 and 5 per rev. This is especially true for 3 and 4 per rev response. There is little benefit derived from the high tuning for the hub inplane shears, because the contribution of this mode is not as large as other components involved and vectorial cancellation plays an important role. However, there is a significant benefit for the hub yaw moment and also for blade edgewise stresses. These results form the basis for a new blade design criteria which places the edgewise mode frequency higher than 5 per rev for a 4-bladed rotor.

EFFECT OF FLATWISE FREQUENCY ON EDGEWISE RESPONSE

In the last section, the importance of edgewise mode tuning on edgewise vibratory response was discussed. It was shown that a frequency higher than 5 per rev was desirable, particularly for 4 per rev response. However, the question of what forces the edgewise mode still remains. Changing the edgewise mode tuning changes the amplified modal response, but the source of excitation still has not been identified. It was shown previously that drag and coriolis are not the source of the 3 per rev excitation for the elastic edgewise mode. In this section, it will be shown that the primary source of 3 per rev elastic edgewise mode response is due to elastic and inertial coupling with the first elastic flatwise mode. Blade twist and collective pitch are the source of this coupling.

To determine the effect of flatwise frequency on edgewise mode 3 per rev response, the flatwise frequency was varied while keeping the flatwise mode shape fixed. This was done in order to isolate the effect of frequency from the effect of mode shape. The results are shown in Fig. 40 for modified blade design No. 1 at the high speed flight condition. The amplitude of the 3 per rev edgewise mode response is shown as a function of flatwise frequency. Also shown is the phase angle between the edgewise mode response and the flatwise mode response at 3 per rev. The amplitude response clearly shows a strong correlation with the flatwise frequency. Starting with a resonant type response (which will be explained later) for a flatwise frequency of 2.2 per rev, the edgewise mode response decreases sharply with increased flatwise frequency. For modified design No. 1, the flatwise frequency is 2.94, an increase from 2.75 per rev for the baseline blade. Increasing the frequency further sharply decreases the edgewise mode response. For example, for a flatwise frequency of 3.2 per rev, the edgewise mode 3 per rev response has decreased by 33 percent.

The phase angle of the edgewise mode response with respect to the flatwise response shows an essentially smooth change with a change in flatwise frequency. Both flatwise and edgewise response phases are changing so the phase shown in Fig. 40 is the difference between these two phases. What is important is that the change in flatwise frequency directly affects both the amplitude and the phase of the edgewise mode response. For low flatwise frequencies, the two modes are essentially out of phase (flap up-lagging). For high flatwise frequencies the two modes are essentially in phase (flap up-leading).

Figure 41 shows the change in edgewise mode response with changes in the flatwise mode response as the flatwise frequency is varied. There is a strong correlation between these two responses. For high 3 per rev flatwise response, the edgewise response is high and vice versa.

The mechanism for this strong correlation is coupling between the modes. Combining the built-in twist and collective pitch results in local inboard blade section pitch angles of 25 to 30 degrees with respect to the disk plane. The blade neutral axes are also oriented by this same angle, so the result is a strong coupling between those two modes. The flatwise mode has a strong source of aerodynamic forcing at 3 per rev, so when this mode responds at 3 per rev, the edgewise mode also responds.

The reduction in the edgewise mode response at 3 per rev obviously results from a reduction in the 3 per rev flatwise mode response. This is important from the point of view of reducing the edgewise mode response by flatwise tuning, but it is even more important from the point of view of reducing the flatwise mode response at 3 per rev. Figures 31 and 32 showed the importance of the elastic flatwise mode 3 per rev response in the 3 per rev blade rotating inplane shears. So it is apparent that the 3 per rev rotating blade inplane shears can be affected by tuning of the elastic flatwise mode. This is the subject of the next section.

EFFECT OF FLATWISE FREQUENCY ON VIBRATORY LOADS AND VIBRATION

Based on the results previously discussed, the major source of the vertical vibration in the cockpit and cabin of the baseline 4-bladed articulated helicopter has been traced to the 4 per rev hub fixed system inplane shears and further to the 3 per rev rotating blade inplane shears. It has also been shown that a major contribution to these rotating blade inplane shears is the 3 per rev response of the first flexible flatwise mode. As the blade design has progressed from the baseline blade to modified blade design No. 1, other major contributions to the rotating inplane shears have decreased (e.g., elastic edgewise mode, coriolis and its induced blade modal inertial responses), so the relative importance of the elastic flatwise mode contribution becomes even greater.

Figure 41, discussed in the previous section, shows that the 3 per rev elastic edgewise response decreases as the 3 per rev flatwise response decreases. Both responses decrease when the flatwise mode frequency is increased. The subject of this section is the nature of the decrease in the flatwise response with the objective of incorporating a change in the blade design to take advantage of this characteristic.

Figure 42 shows the change in the 3 per rev elastic flatwise mode response as the frequency of this mode is varied over a range from 2 to 4.4 per rev. These data were taken from the same analytical results used to develop Figs. 40 and 41. The flatwise mode shape is fixed in order to separate frequency effects from mode shape effects. In the lower half of Fig. 42, the solid line shows the amplitude of the 3 per rev flatwise response. The response peaks near 2.2 - 2.3 per rev and decreases for flatwise frequencies greater than 2.3 per rev. The peak flatwise response at 2.2 - 2.3 per rev explains why the 3 per rev edgewise response in Fig. 40 also peaks at the same flatwise frequency. There is a plateau effect in the response near 3 per rev frequency. For frequencies greater than 3 per rev, the response drops sharply.

The most important result in Fig. 42 is that the 3 per rev response does not peak at 3 per rev as expected. From an uncoupled in-vacuum viewpoint, the mode should be resonant at 3 per rev for this frequency and have the largest dynamic amplification factor. However, the peak response is near 2.2 - 2.3 per rev which indicates that the mode frequency in air for 3 per rev response is much higher than the vacuum frequency. A flatwise mode airspring effect equivalent to 0.7 - 0.8 per rev has increased the modal frequency for 3 per rev response such that, when the frequency in vacuum is 2.2 - 2.3 per rev, the frequency in air for 3 per rev response is 3 per rev. Thus, this mode is

resonant at 3 per rev when the uncoupled frequency is 2.2 - 2.3 per rev. The mechanism for this airspring effect will be discussed shortly. However, it is important to note that the phenomenon observed is only related to frequency, not mode shape, since the mode shape was fixed while the frequency was varied.

In order to prove that an airspring is involved, the 3 per rev generalized coordinate for the flatwise mode was normalized by the generalized airload. The result is a type of transfer function (inches of modal amplitude per pound of loading). The important point is that the generalized airload, which was computed by summing the fixed mode shape and the spanwise aerodynamic lift, includes all 3 per rev airloading, the 3 per rev airloading due to forward flight as well as the 3 per rev airloading due to blade motions. The damping airload was vectorially subtracted (3 per rev elastic flatwise motion inducing 3 per rev airloading) so that the net 3 per rev airloading includes motion induced 3 per rev airloading from the rigid body flatwise, second flexible flatwise, and torsion modes plus 3 per rev airloading due to 1, 2, 4, and 5 per rev motion of the first flexible flatwise mode. This is summarized in Table 12 below.

TABLE 12. - BLADE MOTION INDUCED AIRLOADS INCLUDED IN THE 3 PER REV GENERALIZED AIRLOAD FOR THE FIRST FLEXIBLE FLATWISE MODE

	Harmonic of Blade Motion				
	1	2	3	4	5
Rigid flatwise	x	x	x	x	x
First flexible flatwise	x	x		x	x
Second flexible flatwise	x	x	x	x	x
First flexible torsion	x	x	x	x	x

Therefore, all the airspring effects, particularly the off diagonal airspring effects of the first flexible flatwise mode due to advance ratio, are included in the generalized airload. When the generalized coordinate of the 3 per rev flatwise response is divided by this generalized airload, the net effect is to treat the airspring airloads as loading rather than as effective springs, so the dynamic response can then be viewed as a response in vacuum. With this normalization, the result is as expected. The normalized response peaks at 3 per rev and has a characteristic dynamic response for a second order system. This is shown by the dotted line in Fig. 42. Also the phase (dotted line in upper half of Fig. 42) confirms the 3 per rev resonance when the frequency in vacuum is 3 per rev, since the phase is 90 degrees at this point. For frequencies lower than 3 per rev, the mode damping is supercritical; above 3 per rev, it is subcritical.

There are two important conclusions to be drawn from this figure. First, maximum 3 per rev response of the flatwise mode occurs for frequency placements below 3 per rev. This is ironic since for typical rotor blade designs this frequency is normally in the 2.7 - 2.9 per rev range and considerable design efforts are expended (mass and stiffness adjustments) to lower the frequency (i.e., increase its separation from a 3 per rev tuning). In fact, there are blade design frequency placement criteria used in the helicopter industry that state how low this frequency should be. The results of Fig. 42 show that this is an invalid design criterion; in fact, it increases the 3 per rev response of this mode.

The second important conclusion to be drawn from Fig. 42 is that the best tuning frequency to reduce 3 per rev response is above 3 per rev; the higher, the better. Obviously, this is a radical change from present day blade design practices. Tuning this mode above 3 per rev presents design problems not previously encountered since most, if not all, rotor blades produced by major helicopter manufacturers are tuned to below 3 per rev at design rotor speed, regardless of the number of rotor blades used for the main rotor system. However, it will be shown later that flexible blade designs can be achieved in which the frequency for this mode is greater than 3 per rev. Based on Fig. 42, a reasonable objective is to tune this mode to 3.4 per rev. Figure 42 shows that the 3 per rev modal response for this frequency is reduced by 30 to 40 percent compared to the baseline blade frequency (2.75 per rev) and the frequency for modified design No. 1 (2.95 per rev). More will be said in this regard later.

Source of 3 per rev Airspring

The airspring effect which strongly influences the 3 per rev flatwise response as the frequency is changed can be traced to the 1 and 2 per rev responses. It was shown in Table 9 for the baseline blade that 58 percent of the 3 per rev airloads created by motion of the flatwise mode are due to motions of that mode at harmonics other than 3 per rev (1, 2, 4, and 5 per rev) due to advance ratio. The strongest contributor of these is the 2 per rev response. The spanwise shape of the 3 per rev airloads created by 2 per rev response is shown in Table 5, the second and third terms.

The mechanism by which these airloads affect the dynamic 3 per rev response of the flatwise mode as the flatwise frequency is changed is as follows. When the frequency of this mode is decreased, say from 3 per rev towards 2 per rev, the dynamic amplification of this mode at 2 per rev is increased as the mode becomes more resonant at 2 per rev. The increased 2 per rev response results in increased 3 per rev airloads, and the phasing of the 2 per rev response and resultant 3 per rev airloads creates a positive airspring effect. The phasing of the 2 and 3 per rev responses of the flatwise mode are at least moderately coupled in forward flight, simply because a large proportion of the airloads that are forcing the modes at 2 and 3 per rev come from blade motions induced by interharmonic coupling of airloads and blade modal motions, as shown in Table 4. However, when the modal frequency is reduced towards 2 per rev while keeping all other parameters fixed, including the mode shape, the phase coupling between 2 and 3 per rev becomes even stronger, because the response at one frequency becomes more closely tied to the response and resultant airloads created at another frequency. In other words, when the mode frequency is reduced towards 2 per rev, the induced interharmonic coupling airloads become more dominant.

A measure of how strong an influence the 2 per rev response of the flatwise mode has on the 3 per rev response because of the induced 3 per rev airloads can be obtained from Fig. 43. This figure shows how the 1, 2, and 4 per rev response of the flatwise mode changes as the frequency of this mode is varied while keeping the mode shape fixed. All these harmonic responses increase as the frequency is reduced towards 3 per rev, but the 2 per rev response increases strongly. The 3 per rev airloads induced by this 2 per rev response increase proportionately. At a frequency of 2.2 - 2.3 per rev, the 2 per rev response (and 3 per rev induced airloads) is about 3-4 times as large as that for modified blade design No. 1 with a frequency of 2.95 per rev.

In summary, the frequency in air of the flexible flatwise mode for 3 per rev response is strongly affected by interharmonic coupling in forward flight. The apparent frequency in air is tied directly to the response frequency, so that the apparent frequency for 2 per rev response or other harmonics will most likely be different. In fact, negative springs may be created for responses at different harmonics. Another important point is that this effect on the frequency is a direct function of advance ratio; therefore, in hover, the modal frequency for all harmonics of response will be the same as the frequency in vacuum.

All of these results re-emphasize the fact that blade motions and harmonic airloading are strongly coupled and that the resultant harmonic airloading has a strong influence on the dynamic response of the rotor blade and hence also on vibration. This fact must be considered in the blade design process to minimize vibration.

Blade Design with Increased Flatwise Frequency

Based on the results of the previous section, two blade designs (modified design Nos. 2 and 3) were developed to have frequency placements greater than 3 per rev for the first flexible flatwise mode. In addition, the edgewise frequency was also increased above 5 per rev for both designs to take advantage of reduced dynamic response, particularly at 3 and 4 per rev. The flatwise frequency was increased primarily by modifying the blade spanwise mass distribution. Weight was increased outboard at the same time weight was decreased inboard, but not below that needed to provide strength for centrifugal forces. The edgewise frequency was also increased by increasing edgewise stiffness along the span.

Figure 44 shows the spanwise distribution of mass, flatwise stiffness, and edgewise stiffness for modified design No. 3. The inboard mass has been restricted to no less than 0.036 kg/cm (0.20 lb/in) in order to allow adequate mass needed to provide strength for centrifugal stresses. The outboard mass has been restricted to no more than 0.16 kg/cm (0.9 lb/in) to ensure that the mass can fit within the airfoil shape. The flatwise stiffness has changed little from the baseline, and the edgewise stiffness has increased by approximately 50 percent.

The weight and frequencies of the two new blade designs are compared to those for the baseline design and modified design No. 1 in Table 13.

TABLE 13. - BLADE WEIGHT AND FREQUENCY PLACEMENTS FOR BLADE DESIGN MODIFICATIONS

	Baseline	Design No. 1	Design No. 2	Design No. 3
Weight, N (lb)	445 N (100 lb)	463 N (110 lb)	436 N (98 lb)	463 N (104 lb)
Flatwise Frequency, per rev	2.75	2.95	3.20	3.40
Edgewise Frequency, per rev	4.77	4.64	5.65	5.5

For modified design No. 2, the weight is slightly less than that for the baseline, and the flatwise frequency is 3.2 per rev. For modified design No. 3, the weight is 18 N (4 lbs) heavier than the baseline and the flatwise frequency is 3.4 per rev. The blade designs shown in Table 13 demonstrate a wide range in frequency placement with judicious tailoring of the blade properties while maintaining a feasible design.

Figure 45 shows the predicted 4 per rev vibrations in the cockpit and cabin for the baseline blade and the three modified blade designs for the high speed flight condition. Both modified designs No. 2 and No. 3 show an improvement in vibration over the baseline and modified design No. 1. The largest reductions are in the heelslide vibrations, but the copilot seat and cabin vibrations also show appreciable reductions. The heelslide vibrations have been reduced by over 50 percent and the cockpit seat and cabin vibrations are now approaching the 0.1 g goal, an arbitrary goal that was set for improved blade design without any hub or fuselage vibration treatment.

The vibratory hub loads that cause the fuselage vibrations are shown in Fig. 46 for the baseline blade and all three modified blade designs for the high speed flight condition. The two inplane forces for modified designs No. 2 and No. 3 are both lower than those for modified design No. 1 with the 4.53 kg (10 lb) weight at the blade tip. Furthermore, they are 55 to 70 percent lower than the baseline inplane shears. This reduction is predominantly due to a reduction in the 3 per rev rotating blade inplane shears since the 5 per rev rotating shears are smaller in magnitude.

Tables 14 and 15 compare the components that contribute to the 3 per rev rotating lateral and radial inplane shears, respectively. The results for the baseline blade and modified designs No. 1 and No. 3 are compared. All of the lateral components for design No. 3 with the 3.4 per rev flatwise tuning have been reduced compared to modified design No. 1, except for the elastic flapping Coriolis. However, the elastic flatwise inertia contribution is not reduced as much as expected. More will be said in this regard later. In Table 15, the major components of the 3 per rev rotating radial shear have been reduced appreciably. The elastic flapping acceleration is reduced because of the change in the blade spanwise mass distribution (more mass outboard) even for a constant 3 per rev response of this mode. The lag centrifugal force is reduced because the lag 3 per rev response is reduced. This is also reflected in the lag inertia contribution to the rotating lateral shear in Table 14 for modified design No. 3.

It is interesting to see how a change in the 3 per rev lag response affects the inplane shears. For the lateral shear, the lag mode responds to the distributed loading of drag and Coriolis from rigid and elastic flapping. The inertial response nearly equals the vectorial sum of these loads as shown in Fig. 47, which shows the vectorial addition of the components that form the rotating lateral shear for modified design No. 3. Thus, for the lateral shear, the lag response is inconsequential. But this is not so for the radial force, shown in Fig. 48 for modified design No. 3. In the radial direction, only the rigid flapping acceleration is out of phase with the lag centrifugal force caused by 3 per rev lag mode response, and the lag centrifugal force component is much larger in magnitude. Therefore, it is important to reduce the 3 per rev lag mode response in order to reduce the 3 per rev rotating lateral shear. The most direct method of reducing the 3 per rev lag forcing is to reduce the 3 per rev rigid flapping Coriolis, but Fig. 47 shows that the applied force to the lag mode was reduced by cancellation between the rigid flapping and elastic flapping Coriolis components.

Referring back to the 4 per rev hub fixed system loads for designs No. 2 and No. 3 in Fig. 46, the hub pitching moment has increased by about 50 percent, but the magnitude of the vibratory moment is so low that it has only a small influence in vibration. The vibratory yaw moment is substantially reduced for designs No. 2 and No. 3, and this is primarily due to a proportionate reduction in the 4 per rev edgewise mode response. The 4 per rev vertical hub shear for blade design No. 3 is about the same level as that for blade design No. 2 (80 percent reduction compared to the baseline), but the vertical shear for design No. 3 has increased and is almost at the same level as that for the baseline.

Table 16 shows the amplitude of the blade generalized coordinates for the three modified blade designs and helps explain the change in the vibratory hub loads shown in Fig. 46.

Table 14
Predicted Amplitude of Components in 3 Per Rev Blade Rotating Lateral Shear for the High Speed Flight Condition

	BASELINE	MODIFIED DESIGN NO. 1	MODIFIED DESIGN NO. 3
LAG INERTIA	197	107	65
DRAG	62	60	47
RIGID FLAPPING CORIOLIS	132	60	59
LAG CORIOLIS	17	8	4
ELASTIC EDGEWISE INERTIA	69	40	17
ELASTIC FLAPPING CORIOLIS	34	12	34
COUPLED ELASTIC F-E INERTIA	22	18	13
ELASTIC FLATWISE INERTIA	112	77	71
TOTAL	198	106	72

Table 15
Predicted Amplitude of Componets in 3 Per Rev Blade Rotating Radial Shear for the High Speed Flight Condition

	BASELINE	MODIFIED DESIGN NO. 1	MODIFIED DESIGN NO. 3
LAG CENTRIFUGAL FORCE	113	64	35
RIGID FLAPPING ACCELERATION	43	19	20
ELASTIC FLATWISE CENTRIFUGAL FORCE	103	51	27
ELASTIC FLATWISE ACCELERATION	6	2	6
TOTAL	172	101	42

TABLE 16. - PREDICTED HARMONIC AMPLITUDE OF BLADE GENERALIZED COORDINATES FOR THE HIGH SPEED FLIGHT CONDITION

	Baseline	Modified Design No. 1	Modified Design No. 2	Modified Design No. 3
First Flexible Flatwise Mode 3/rev	.0052	.0032	.0037	.0035
First Flexible Flatwise Mode 4/rev	.00032	.00037	.00042	.00048
Second Flexible Flatwise Mode 4/rev	.00082	.00012	.00011	.000075
First Flexible Edgewise Mode 3/rev	.00075	.00032	.00018	.00012
First Flexible Edgewise Mode 4/rev	.00029	.00026	.00013	.00012

As shown in Table 16, modified design No. 3 has reduced the 4 per rev generalized coordinate for the second flatwise mode by 91 percent of the baseline value. This would indicate a large reduction in the 4 per rev hub vertical shear, since the second flatwise mode response is the primary source of this shear. Yet Fig. 46 shows that the vertical shear for this design is about the same as the baseline.

The reason for this apparent anomaly is in the vectorial cancellation at the blade root between the 4 per rev responses for the first and second flexible flatwise modes. The 4 per rev response phase of these two modes is such that beneficial cancellation in shear can be achieved at the blade root, but when the response of the most important contributor (the second flatwise mode) is reduced to such a large extent, the shear amplitude is then controlled by the first flexible flatwise mode. Table 16 shows that the 4 per rev response of this mode has increased at the same time that the response of the second flatwise mode has decreased. When looking at the baseline 4 per rev responses for these two modes, it is apparent that the second flatwise mode is the most important contributor, particularly when the blade root shear that this mode

contributes is approximately 2.6 times as large as that for the first flatwise mode for equal modal tip displacements. Therefore, this is a case in which the most important mode for 4 per rev shear was actually made too insensitive. Retuning this mode to increase its 4 per rev response would actually decrease the 4 per rev root shear. Analytically this may be true, but in an actual blade design it is better to desensitize the prime mode for a particular vibratory hub load and not depend upon this type of beneficial vectorial cancellation. Changes in aircraft configuration or flight condition could alter the phase relationship between these two modes and negate any load cancellation. Therefore, it is felt that the best design for hub vertical shear is actually modified design No. 3.

Table 16 also explains the substantial decrease in the 4 per rev hub yaw moment. This moment comes from the edgewise mode 4 per rev response, and Table 16 shows a large reduction in the 4 per rev response of this mode for blade designs No. 2 and 3. For blade design No. 3, the 4 per rev response has been reduced to 41 percent of that for the baseline blade.

Table 16 does not explain the reduction in the longitudinal and lateral shears shown in Fig. 46 for blade designs No. 2 and 3. The 3 per rev response of the edgewise mode is reduced substantially, but it has been shown before, for blade design No. 2, that the inertial root force from the 3 per rev response of this mode is a moderately small component of the rotating blade 3 per rev inplane shear. Furthermore, the 3 per rev response of the first flexible edgewise mode has increased for blade designs No. 2 and 3 compared to that for design No. 1, even though Fig. 42 has shown that increasing the flatwise frequency above 3 per rev would reduce the response of this mode at 3 per rev. Blade design No. 2 has a flatwise tuning of 3.2 per rev while blade design No. 3 has a tuning of 3.4 per rev.

The reason for this anomaly lies in the change in mode shape when the blade mass and stiffness distributions were modified for designs No. 2 and 3. In Fig. 42, the mode shape is fixed, so any change in the generalized airload is due only to a change in the airload. In the actual blade design, the mode shape changes with change in frequency so that the generalized airload is a function of both the change in mode shape and the change in the generalized airload. For blade designs No. 2 and 3, the change in mode shape was sufficient to increase the generalized airload to negate the beneficial effect of reduced dynamic response at 3 per rev due to tuning at 3.2 and 3.4 per rev. This is shown in Table 17.

TABLE 17. - PREDICTED 3 PER REV FLATWISE MODE GENERALIZED AIRLOAD FOR THE HIGH SPEED FLIGHT CONDITION

	Baseline	Modified Design No. 1	Modified Design No. 2	Modified Design No. 3
3/rev Generalized airload	173	141	201	259

The generalized airload for the three modified blade designs is calculated by integrating the product of the 3 per rev spanwise lift including lift due to blade motions and the flatwise mode shape. The generalized damping airload for this mode (3 per rev lift due to 3 per rev mode response) is then subtracted, as discussed previously. Table 17 shows that the generalized airload for modified blade designs No. 2 and 3 has increased substantially.

The impact of the generalized airload on the normalized 3 per rev response of the flatwise modes is shown in Fig. 49. The dashed line in this figure is the same as the dashed line in Fig. 42. It represents the predicted normalized response of the flatwise mode for a fixed mode shape and is calculated by dividing the flatwise mode generalized coordinate by the generalized airload. Also shown in this figure are the calculated normalized coordinate responses for blade designs 1, 2, and 3. These normalized responses are calculated in the same manner except that the generalized airload for these designs is a function of the mode shape change as well as the airload change. The normalized response for these three blade designs correlate well with that predicted for a fixed mode shape. This result demonstrates that the dynamic response amplification of the flatwise mode at 3 per rev is reduced as expected. But since the generalized airload increases sharply the coordinate response remains about the same (Table 16).

The increase in the generalized airload for the modified blade designs is due to two factors: an increase in the 3 per rev lift airload, and a change in the flatwise mode shape. The change in the 3 per rev airload can be seen by comparing Figs. 50, 51, and 52. These figures show the spanwise distribution of the amplitude of the 3 per rev lift airload for the baseline blade and for modified blade designs No. 1 and No. 3. In addition to the total amplitude, each figure also shows the amplitude of the airload due to blade motions. This amplitude cannot be subtracted directly from the total airload, since the airload phase varies along the blade span. That portion of the airloads due to blade motions which results from 3 per rev response of the

flatwise mode is also shown. Finally, the residual airload which is defined as the total airload minus (vectorially subtracted) the damping airload is shown. The residual airload is the airload distribution that forces the flatwise mode and is used in calculating the generalized airload for this mode.

The most obvious change in the 3 per rev lift airload for the modified designs is a change in the peak amplitude of airload near the blade tip. For the modified designs, the airload amplitude has nearly doubled compared to that for the baseline blade. Moreover, the residual airload (total minus damping for flatwise mode) has nearly doubled, so it is obvious that the generalized airload for the flatwise mode has increased even for a fixed flatwise mode shape. Note that the damping airload amplitude has decreased for the modified designs, reflecting a decrease in the flatwise mode response, even though the generalized airload has increased. The reduced response at 3 per rev is due to reduced amplification at frequencies greater than 3 per rev, as discussed earlier. If the residual airload had not increased, the reduction in the response of this mode would have been even greater.

The increase in generalized airload for the modified designs is also due to a change in the mode shape. Figure 53 shows how the flatwise mode shape for modified designs No. 1 and No. 3 changes from that for the baseline design. The node point moves outboard as the flatwise frequency is increased and the depth of the antinode near midspan increases substantially. The change in the depth of the antinode is the primary cause for the increase in the generalized airload. This can be shown by the following example.

Assume that the 3 per rev modal tip deflection for the flatwise mode is positive, as shown in Fig. 53, and that the phase of the residual airload in Figs. 50, 51 and 52 is constant along the blade span. Then the airload inboard of the mode shape node point, near 75 to 80 percent span, forces the mode down at the tip in proportion to the negative area of the mode shape. Outboard of the node point the opposite is true. The airload forces the mode up at the tip in proportion to the positive area of the mode shape. The net generalized force is the integrated sum of the mode shape from the root to the node point times the airload over that portion of the blade span (a negative value) plus the integrated sum of the mode shape from the node point to the blade tip times the airload over that portion of the blade span (a positive value). If the net sum of these two values is zero, the generalized force is zero and the mode will not respond. This was discussed previously in the section on modal shaping. But as the node point moves outboard and the depth of the antinode increases, the area under the mode shape inboard of the node point increases and the area outboard of the node point decreases. Thus, for a fixed spanwise airload shape, the generalized force increases (negatively) so as to pull the blade tip down.

This is basically what has happened for the modified blade designs, although the airload shape has changed and is larger at the blade tip. This is a compensating factor, increased outboard airload with decreased area under the mode shape. But the compensation is not sufficient to negate the increased area under the mode shape inboard of the node point combined with increased airload amplitude over the same portion of the blade span.

The net result is that the generalized airload inboard of the node point is dominant and increases because of the change in the form of the flatwise mode shape. Therefore, further reductions in the 3 per rev response of the flatwise mode must be directed at reducing the generalized airload. The increased frequency of 3.4 per rev for modified design No. 3 reduced the dynamic amplification. Clearly, the next step is to combine the reduced dynamic amplification with reduced forcing.

EFFECT OF BLADE CG LOCATION ON VIBRATORY HUB LOADS

In the last section, it was shown that reduced dynamic amplification of the flatwise mode at 3 per rev achieved by tuning to 3.4 per rev (modified blade design No. 3) was negated by an increase in the generalized airload for the mode. The increase in the generalized airload was due to a change in the flatwise mode shape and also due to an increase in the 3 per rev lift distribution. It was also shown that the increase in the lift airload was primarily induced by flexible blade motions. In this section, the 3 per rev airloads due to blade flexible motions are altered by modifying the blade chordwise CG location. The primary impact of this design change is a change in the torsion mode response, which has a strong effect on the airloads. A secondary result is a change in the rigid flapping response, which also alters the spanwise 3 per rev airload.

The effect of chordwise CG location was investigated by changing the CG for modified design No. 3 with 3.4 per rev frequency for the first flatwise mode. Figure 54 shows the spanwise distribution of the chordwise CG location for modified design No. 3. The CG location of this design has not been altered from the baseline, so all of the modified blade designs discussed so far have the same CG distribution. The CG is aft of the quarter chord (also the elastic axis) inboard and ahead of the quarter chord from 60 to 80 percent blade radius. Outboard, the CG is approximately at 26 percent chord. For the sake of distinction, the CG location for this blade design will be designated as 26 percent chord.

Four different CG locations were investigated in addition to modified blade design No. 3. All of these design variations have the CG at the quarter chord from 0 to 80 percent blade span; then the CG is at a constant distance from the quarter chord from 80 to 100 percent blade span. Table 18 summarizes the variations in CG investigated for modified blade design No. 3.

TABLE 18. - CG LOCATIONS INVESTIGATED FOR MODIFIED BLADE DESIGN NO. 3

	CG Location	
Modified design No. 3	26%	
Variation 1	25%	
2	24%	NOTE: CG is at 25% chord
3	22%	from 0-80% span, then is
4	20%	varied as shown.

The predicted effect of CG location on 3 per rev blade modal response is shown in Fig. 55. The results for modified design No. 3 are plotted at 26 percent chord, and the variations in CG ahead of the quarter chord are also shown. The strongest effect of CG location is on the 3 per rev blade torsional response. Moving the CG forward results in a sharp decrease in 3 per rev torsional response, until the 3 per rev torsional response is nearly nulled at a CG location of 23.5 percent chord. Further movement of the CG location towards the leading edge results in increased 3 per rev torsional response. The torsional response has, in fact, changed phase by 180 degrees. This is shown in Fig. 55 by the arrows on each theoretical data point for the torsional response. The arrows indicate the response phase at 3 per rev (0 degrees phase is down, 90 degrees phase is on the right). The edgewise, flatwise, and rigid flapping response all show the same trend of decreasing amplitude with forward CG locations. The response of these modes is obviously coupled to the response of the torsion mode and the link is the effect on the airloads. The reduction in the rigid flapping response with forward CG will also be modified by the change in the flapping motions, since it was shown previously that harmonic flapping creates large airloads.

The variation in modified design No. 3 with the CG at 24 percent chord over the outboard 20 percent of the blade span is called modified blade design No. 4. The predicted change in the torsion response time history around the azimuth for this blade design is shown in Fig. 56. For the baseline design, the torsion response is characterized by a strong nose-down angular deflection on the advancing side of the blade azimuth. It was shown previously that the nose-down response is a combination of 1, 2, and 3 per rev response. For modified blade design No. 4, with the outboard CG at 24 percent chord, there is no nose down response on the advancing side. Instead the waveform consists of a 1 per rev response, maximum nose down at 180 degrees azimuth plus smaller contributions of higher harmonics. Moving the CG forward for modified blade design No. 4 has nearly nulled the 3 per rev response and has also reduced the 1 and 2 per rev torsional responses. This is shown in Table 19. The combination of reduced 2 and 3 per rev responses has eliminated the advancing side nose down characteristic. When the CG is moved further forward, the 3 per rev response increases with a 180 degree phase change, and the 2 per rev response has the same characteristic. In effect, an advancing side nose-up response can result.

TABLE 19. - REDUCTION IN HARMONIC TORSIONAL RESPONSE FROM THE BASELINE FOR MODIFIED DESIGN NO. 4

	1/rev	2/rev	3/rev
Percent decrease in torsional response	31	57	89

The mechanism involved in this phenomenon is the CG-EA offset. When the blade tip bends downward on the advancing side, a forward CG induces a nose-up torsion increase on the blade near the blade tip. This moment counteracts the nose-down aerodynamic pitching moment due to high Mach number on the advancing side. An accurate prediction of the best CG location to induce this cancellation requires accurate simulation of the unsteady pitching aerodynamics on the advancing side. But the results shown for quasi-steady aerodynamics certainly show the mechanisms involved and the sensitivity of torsion response to CG placement.

The effect of reduced 2 and 3 per rev torsion responses for modified design No. 4 on the 3 per rev spanwise lift distribution is shown in Fig. 57. The peak airload near the blade tip for design No. 4 is approximately 1/3 less than that for design No. 3. The difference is due to a change in the outboard CG from 26 to 24 percent chord. Moving the CG further forward results in even further reductions in the tip airload. In fact, for a CG placement at 20 percent chord, the airload distribution has the characteristics of the damping airload for the flatwise mode (see Fig. 52).

The reduction in the 3 per rev airload with forward CG and the corresponding reduction in the 3 per rev flatwise mode response indicate that the 3 per rev rotating inplane shears should also decrease. However, this is not the case, as shown in Table 20.

TABLE 20. - PREDICTED CHANGE IN 3 PER REV ROTATING BLADE LATERAL AND RADIAL SHEARS WITH BLADE CHORDWISE CG LOCATION

	Baseline	Modified Design No. 3 (26% CG)	Modified Design No. 4 (24% CG)
Lateral shear N (lb)	877N (197 lb)	320N (72 lb)	307N (69 lb)
Radial shear N (lb)	770N(173 lb)	187N (42 lb)	227 (51 lb)

Comparing modified designs No. 3 and No. 4, the lateral shear has decreased slightly with the forward CG location and the radial shear has increased. The reason for this disparity is shown in Figs. 58 and 59, which present the amplitude and phase of the components that form the lateral and radial shears for modified design No. 4. Comparing these two figures with Figs. 47 and 48 for modified design No. 3, it is apparent that the reduction in the inplane shear components due to flatwise response has not ocurred as expected with the reduction in the flatwise 3 per rev response. Comparing designs No. 3 and No. 4, the elastic flatwise inertia contribution to the lateral shear for design No. 4 has decreased by only 8 percent, and the elastic flatwise centrifugal force contribution to the radial shear has increased by 60 percent. The increase in the elastic flatwise centrifugal force contribution explains the increase in the radial shear shown in Table 20. The reason for this predicted increase is not yet understood.

SUMMARY OF VIBRATION, HUB LOADS, BLADE LOADS AND MODAL RESPONSES

This section summarizes the vibration, loads, and modal responses for the blade design modifications that were considered in this analytical study for an articulated rotor operating at the high speed flight condition.

The primary contributors to helicopter vibration, as determined in this study, are summarized in Fig. 60. The primary harmonics of airloads, blade response, blade root shears, hub shears, and fuselage vibrations are shown along with their principal inter-relationships.

Table 21 summarizes the blade frequencies and weights for the four blade design modifications.

Figure 61 shows a comparison of the predicted cockpit and cabin vibrations for the four blade design modifications. In general, the vibrations for modified designs No. 3 and No. 4 have been reduced by about 50 percent (except the pilot seat vertical vibration) compared to the baseline vibrations. Of particular importance are the seat and cabin vibrations, which are approaching a 0.1g level. These results indicate that acceptable seat and cabin vibration levels can be attained by improved blade design and without the use of vibration treatment equipment. Further study in the area of improved blade design for vibration should result in vibrations lower than 0.1g for high speed flight.

The vibratory hub loads that produced this vibration are shown in Fig. 62 In general, these hub loads have been reduced by at least 50 percent except for the pitch and roll moments, which are low in magnitude and have a small influence on vibration.

It is important to understand that, even though the pitch and roll moments increased, the blade design procedure that was used in this study and the blade design modifications that followed are directly applicable to hingeless and bearingless rotor designs in which the pitch and roll moments are fundamental sources of forcing and vibration. For the articulated rotor design studied, these moments which come from 3 per rev rotating vertical shears (again, primarily the first flexible flatwise mode) are small because the hinge offset is small. The inertial shears roughly balance the airloads, so the result can be considered a residual level. On a hingeless or bearingless rotor, moment is carried into the hub, in addition to the shear. The moment is quite large and overcompensates the 3 per rev airload. Thus, the primary consideration is to reduce this bending moment, even without regard to

Table 21
Summary of Blade Frequencies and Weight for Baseline and Modified Blade Designs

	BASELINE	MODIFIED DESIGN NO. 1	MODIFIED DESIGN NO. 2	MODIFIED DESIGN NO. 3	MODIFIED DESIGN NO. 4
FLATWISE FREQUENCIES (PER REV)					
RIGID BODY	1.03	1.03	1.03	1.03	1.03
FIRST FLEXIBLE	2.75	2.94	3.20	3.41	3.41
SECOND FLEXIBLE	4.88	5.32	5.57	5.56	5.56
THIRD FLEXIBLE	7.73	8.32	8.10	8.52	8.52
EDGEWISE FREQUENCIES (PER REV)					
RIGID BODY	0.26	0.26	0.25	0.25	0.25
FIRST FLEXIBLE	4.77	4.64	5.65	5.79	5.79
TORSION FREQUENCY (PER REV)	5.30	5.30	5.30	5.30	5.30
BLADE WEIGHT	445 N (100 lb)	490 N (110 lb)	436 N (98 lb)	463 N (104 lb)	463 N (104 lb)

83-6-38-3

any cancellation with the airload because the moment is so much larger. Reducing the 3 per rev flatwise mode response for a hingeless or bearingless rotor, as was done in this study for an articulated rotor, will directly reduce the bending moment and the 4 per rev hub moments. If these moments can be reduced to levels on the order of even the largest pitch and roll moments shown in Fig. 62, the vibration will be considerably reduced, and other vibration sources should then be considered, e.g., inplane and vertical shears.

The 3, 4, and 5 per rev harmonic response of the blade modes are shown in Figs. 63, 64, and 65 for the four modified blade designs. Comparing results for design No. 4 with those for the baseline, it is apparent that the vibratory blade modal response is considerably reduced. Moreover, the most important responses for vibration (3 per rev first flatwise mode, 4 per rev second flatwise mode, 3 and 4 per rev edgewise mode) show some of the largest reductions. For example, the 4 per rev second flatwise mode response has been reduced to such an extent that it is no longer the primary contributor to 4 per rev vertical hub shear. Also, the 3 per rev edgewise mode response has decreased to the point where it can no longer be considered a contributor to 3 per rev rotating inplane shears.

Finally, Fig. 66 shows the blade spanwise peak-to-peak vibratory stresses for the four blade design modifications. Modified designs No. 3 and No. 4 show about a 50 percent reduction in the critical stress areas: outboard flatwise stress, midspan edgewise stress, and inboard torsional stress. These reductions resulted from reduced 3, 4, and 5 per rev modal responses, but also because of decreased 1 and 2 per rev responses. This result indicates that reductions in stress and vibration can be achieved simultaneously by improved blade design.

CONCLUDING REMARKS

This analytical study has served to develop new blade designs that offer significant reductions in vibration and fatigue stresses without resorting to radical design procedures or blade geometries and without paying significant weight penalties. The baseline blade that was used has a standard planform without tip sweep or droop and with moderate built-in twist. The torsion frequency is moderately high, so development of elastic couplings by reduced stiffness is not involved. In fact, there is nothing too different or pronounced in the baseline blade or the design modifications made. This is the key to the value of this investigation. The results have shown that considerable advancements can be made by tailoring a basic blade design. In fact, it can be argued that government and the helicopter industry have not optimized the basic helicopter blade design before resorting to exotic and sophisticated approaches and devices. The fundamentals of vibration have not been understood, and before radical planform changes, elastic couplings, and active control are implemented, there must be a basis of fundamental understanding based on analysis and experiment.

In addition to the development of promising designs, this study has served to develop a fundamental understanding of helicopter vibration produced by the main rotor system. This understanding was developed by means of an analytical tool (G400) which provided more than the bottom line vibration and load results. Any forced response analysis used in the industry would serve the same purpose as long as it was possible to use the analysis as a diagnostic tool to trace the source of the vibration and loads and identify the important contributing components. In this sense, the analysis has been used in a different manner than that normally used in government and industry. In a nutshell, the analysis was used to understand the parameters involved in the problem. The quantitative results are not nearly as important as the qualitative results. The predicted absolute vibration and load levels are approximate as are the predictions of all other forced response helicopter analyses in use today. But the importance of many parameters involved in the vibration problem certainly has been identified, and a method to control the important sources has been developed, regardless of the absolute value of vibration.

A most gratifying result of this study is that the role played by certain parameters involved in vibration that was identified by using G400 as a diagnostic tool can be confirmed with "back of the envelope" calculations. Also, with hindsight, many of the results became obvious that were not previously obvious. For example, analytical results show that neither 3 per rev Coriolis nor drag provide substantial forcing for the edgewise mode; the first is due to the spanwise shape of forcing and the latter is due to the magnitude

of the forcing. Both results can be confirmed with simple calculations. The same is true for modal shaping of the second flatwise mode for 4 per rev response. The importance of reducing the integrated generalized force is easily determined. Another example is the role played by the lag mode in the 3 per rev inplane shears. It is obvious that this mode absorbs large forces from drag and Coriolis because of its mode shape, but because of the very low frequency, the inertial response essentially cancels the applied forcing as with any second order supercritical system.

This analytical study also uncovered results that are not so obvious. The best example is the role played by flatwise motion in forcing the edgewise mode at 3 per rev. It now seems clear that the best method of reducing the response of the edgewise mode, after it is tuned to greater than 5 per rev to reduce its dynamic amplification, is to reduce the response of this flatwise mode. The result implies, particularly for hingeless and bearingless rotor systems, that inplane and out-of-plane vibration are closely related. Another not so obvious result is the magnitude and role played by vibratory airloading induced by blade flexible motions. This result was uncovered by performing simple calculations of the airloads due to blade motions based on 2-dimensional unstalled aerodynamics. Even with this simple tool, the interdependence of blade motions and airloads became clear. More sophisticated aerodynamics with stall and unsteady effects will undoubtedly increase the understanding in this area, but the basic fundamentals can be determined with simple calculations, hindsight, and an understanding of the fundamentals. It is then obvious that aerodynamics affect the frequency of the flatwise mode in air. The importance of interharmonic coupling is understood in relation to the vibration problem.

A last observation is that vibration on a helicopter in forward flight is predominantly produced by the machine itself, in fact by the rotor itself, even without fuselage rotor interference effects and tail vibration effects. The increase in vibration with airspeed that is characteristic of helicopters is a phenomenon traced to the rotor characteristics. Non-uniform inflow is not needed in cruise to produce the preponderance of vibration experienced. Wake effects and interference effects are only added aggravation to a fundamental problem. Before these aggravations can be dealt with, it is necessary to understand and then solve the fundamental vibration problem in forward flight. The results presented in this report are provided to advance the fundamental understanding needed to improve helicopter rotor blade designs.

REFERENCES

1. Taylor, R. B.: Helicopter Vibration Reduction by Rotor Blade Modal Shaping, Proceedings of the 38th Annual Forum of the American Helicopter Society, May 1982.

2. Blackwell, R. H.: Blade Design for Reduced Helicopter Vibration, Journal of the American Helicopter Society, Vol. 28, No. 3, July 1983.

3. Blackwell, R. H. and K. C. Frederickson: Wind Tunnel Evaluation of Aeroelastically Conformable Rotors, USAAVRADCOM-TR-80-D-32, Applied Technology Laboratory, U.S. Army Research and Technolo;gy Laboratories, January 1981.

4. Bielawa, R. L.: Aeroelastic Analysis for Helicopter Rotor Blades with Time-Variable, Nonlinear Structural Twist and Multiple Structural Redundancy - Mathematical Derivation and User's Manual, NASA CR-2638, October 1976.

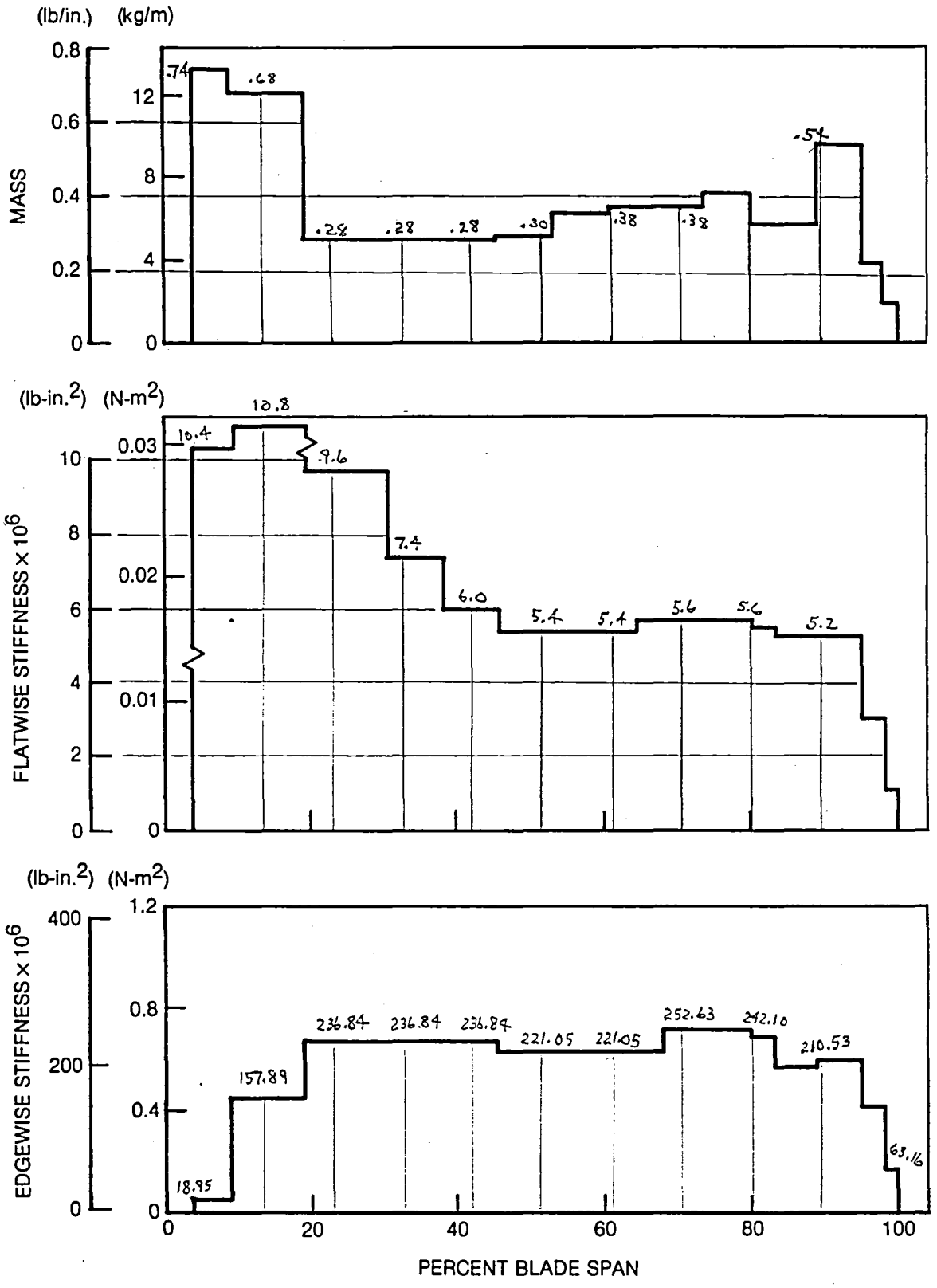

Figure 1. Spanwise Mass and Elastic Bending Stiffness for the Baseline Blade

82-11-15-34

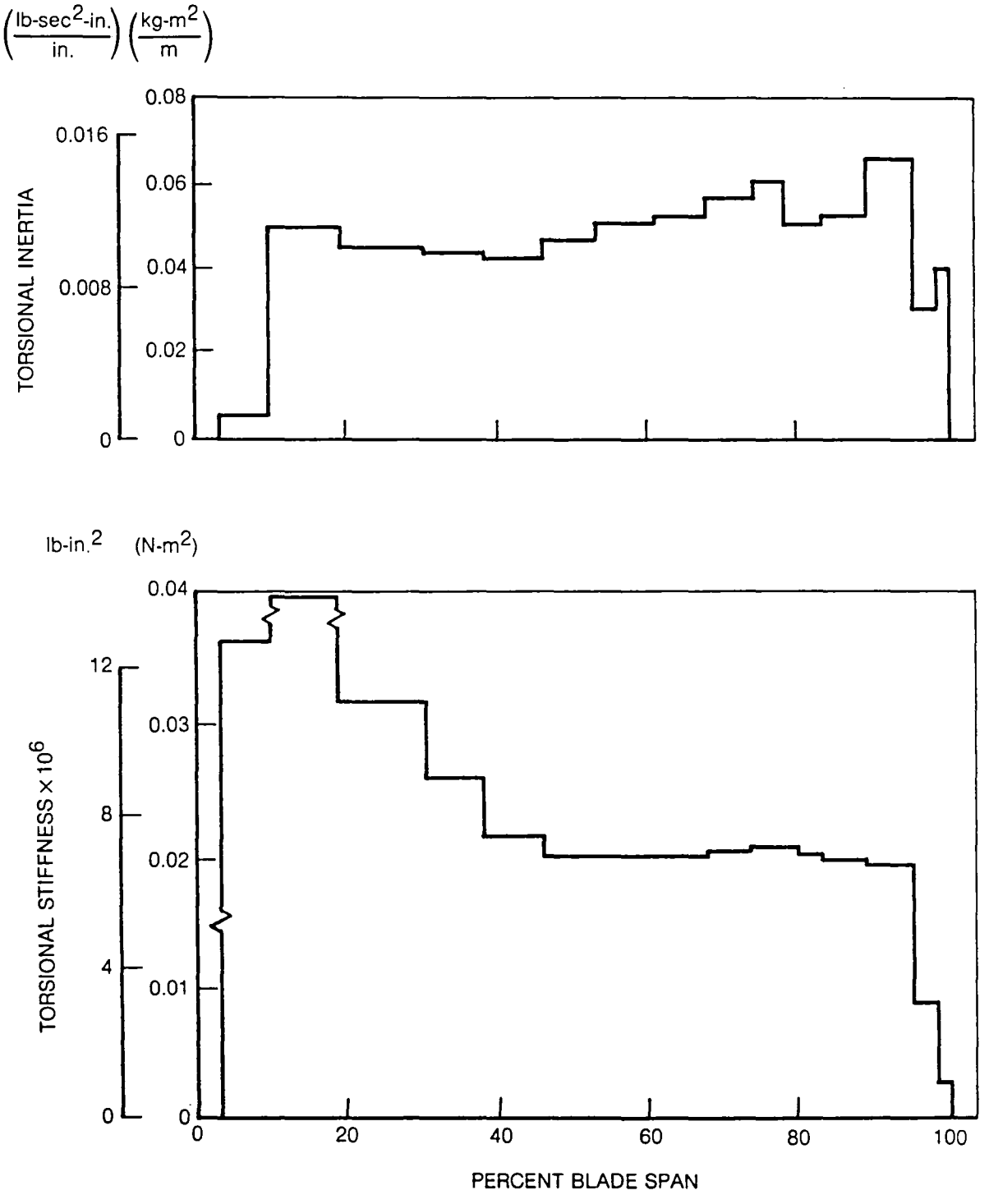

Figure 2. Spanwise Torsional Inertia and Stiffness for the Baseline Blade

82-11-15-33

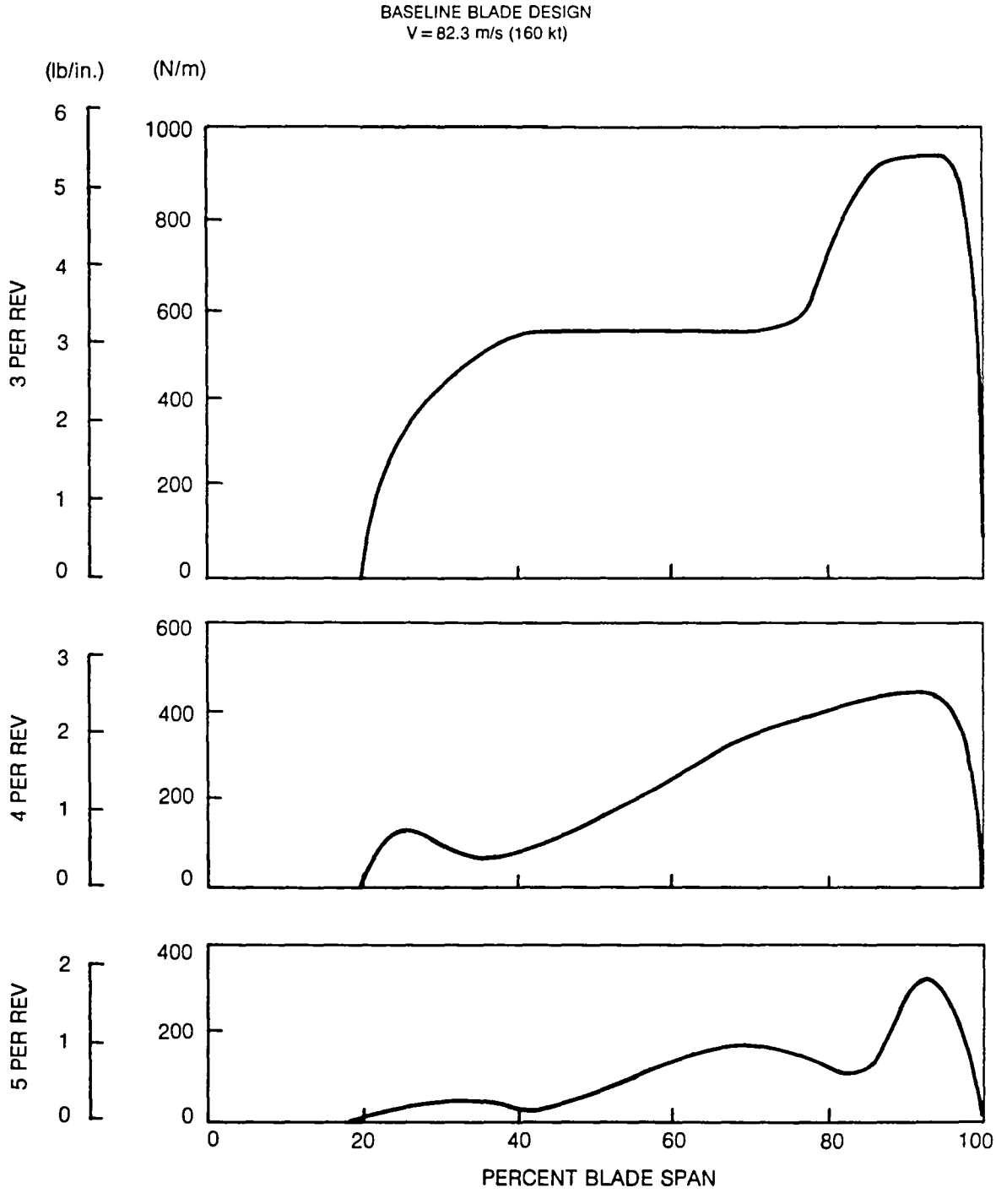

Figure 3. Predicted Amplitude of Vibratory Lift Airloads for the High Speed Flight Condition

82-11-15-6

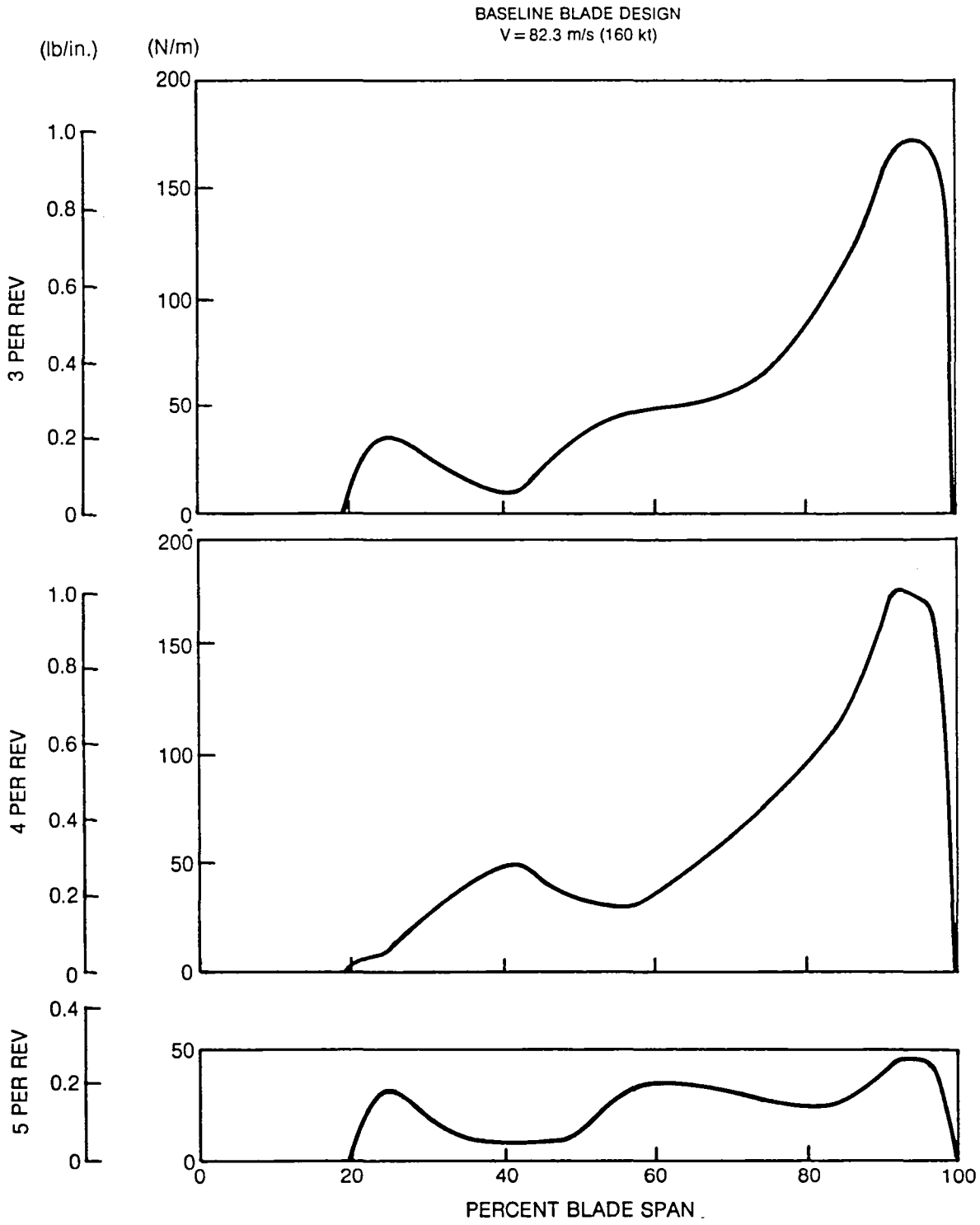

Figure 4. Predicted Amplitude of Vibratory Drag Airloads for the High Speed Flight Condition

82-11-15-7

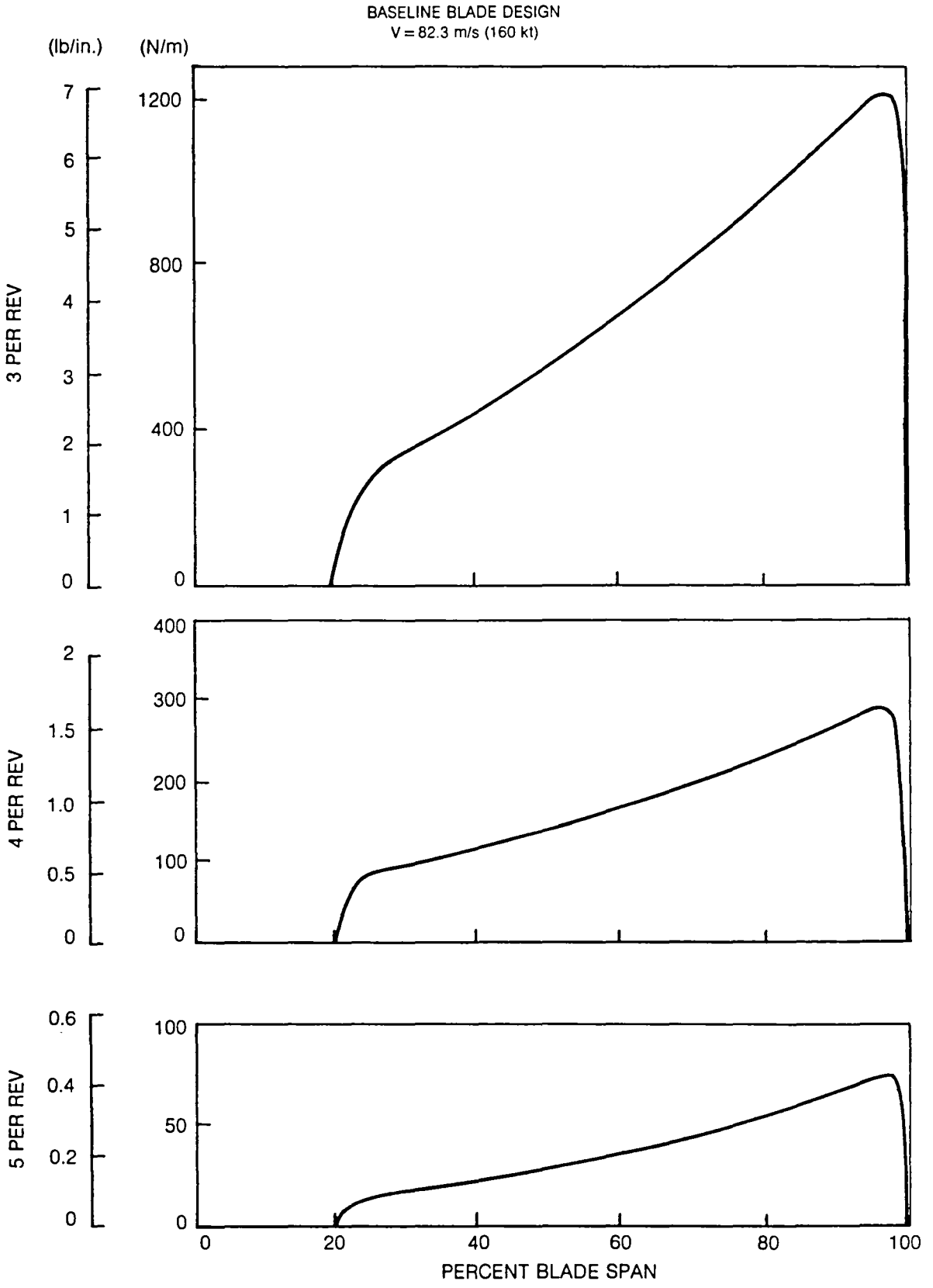

Figure 5. Predicted Amplitude of Vibratory Lift Airloads Due to Rigid Flapping Motion for the High Speed Flight Condition

82-11-15-5

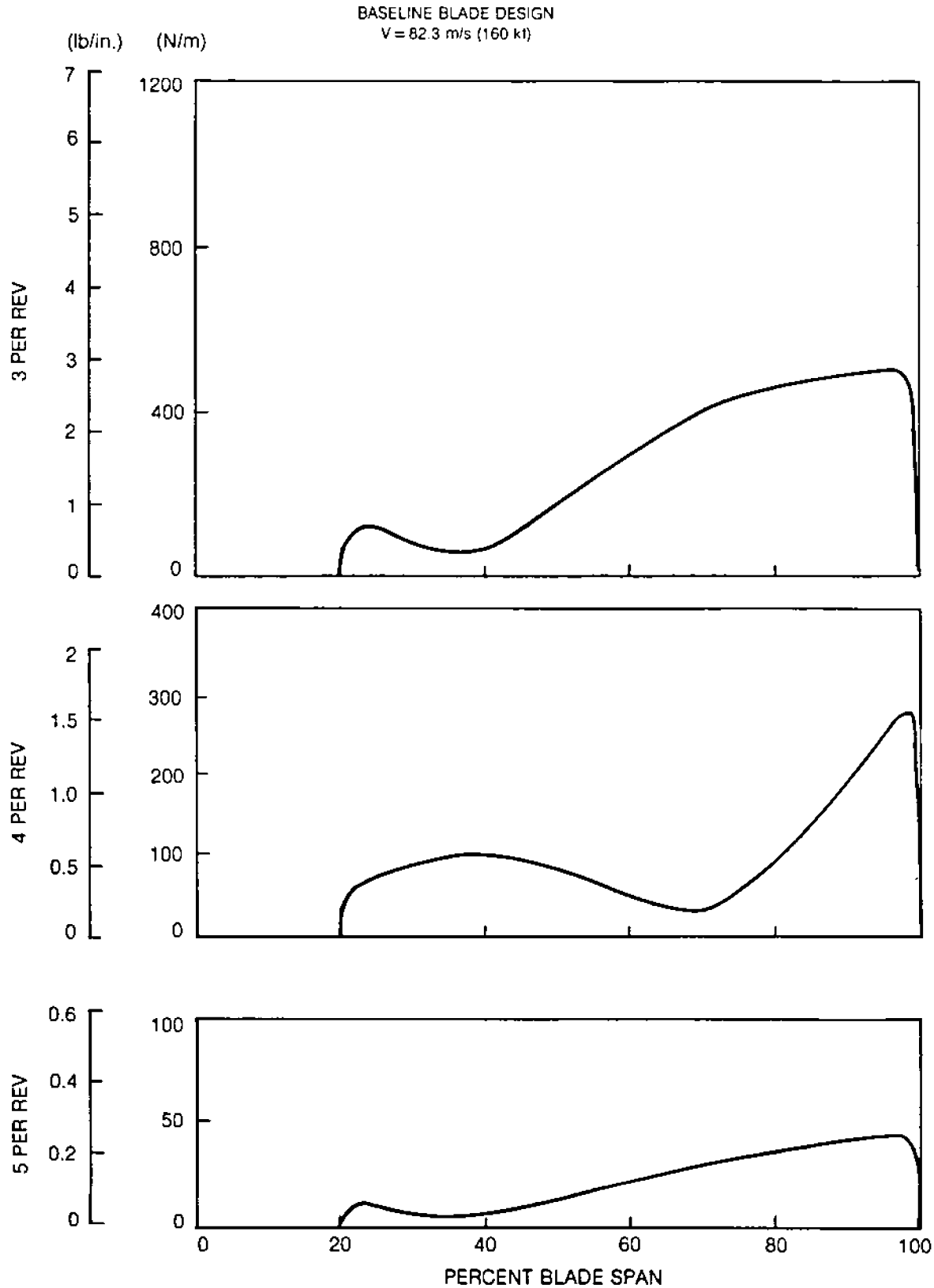

Figure 6. Predicted Amplitude of Vibratory Lift Airloads Due to First Flexible Flatwise Mode Motion for the High Speed Flight Condition

82-11-15-13

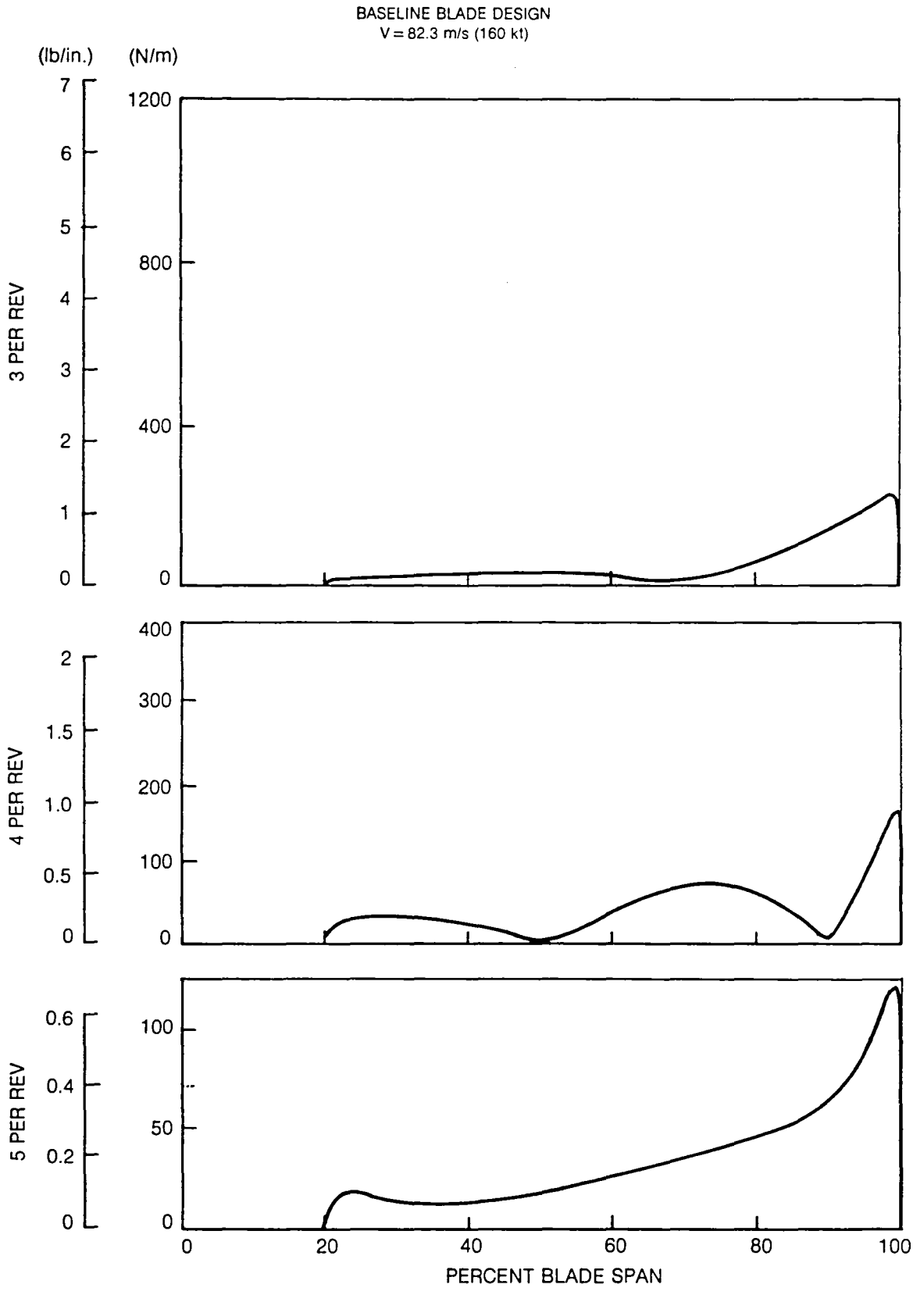

Figure 7. Predicted Amplitude of Vibratory Lift Airloads Due to Second Flexible Flatwise Mode Motion for the High Speed Flight Condition

82-11-15-15

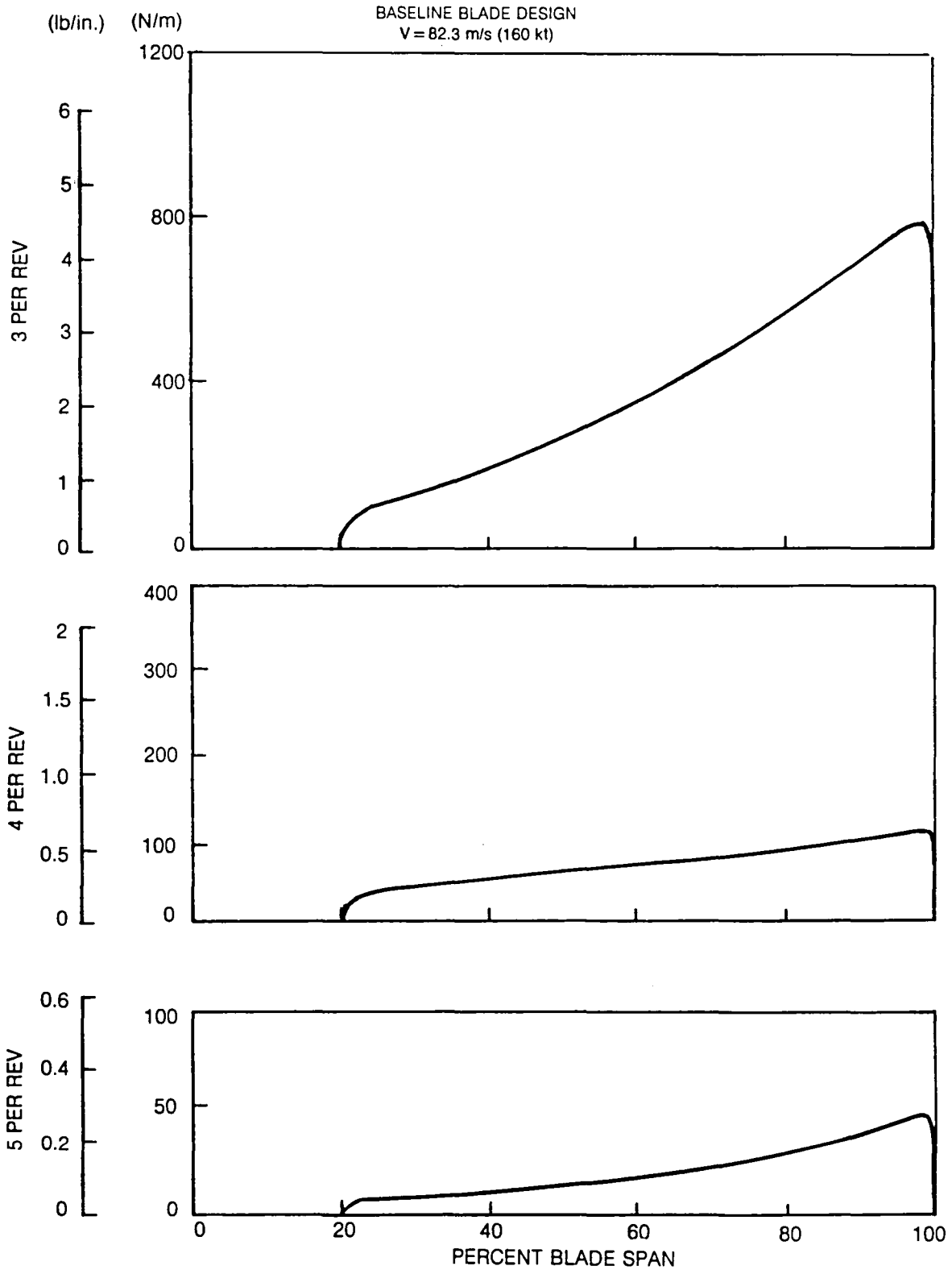

Figure 8. Predicted Amplitude of Vibratory Lift Airloads Due to First Flexible Torsion Mode Motion for the High Speed Flight Condition

82-11-15-14

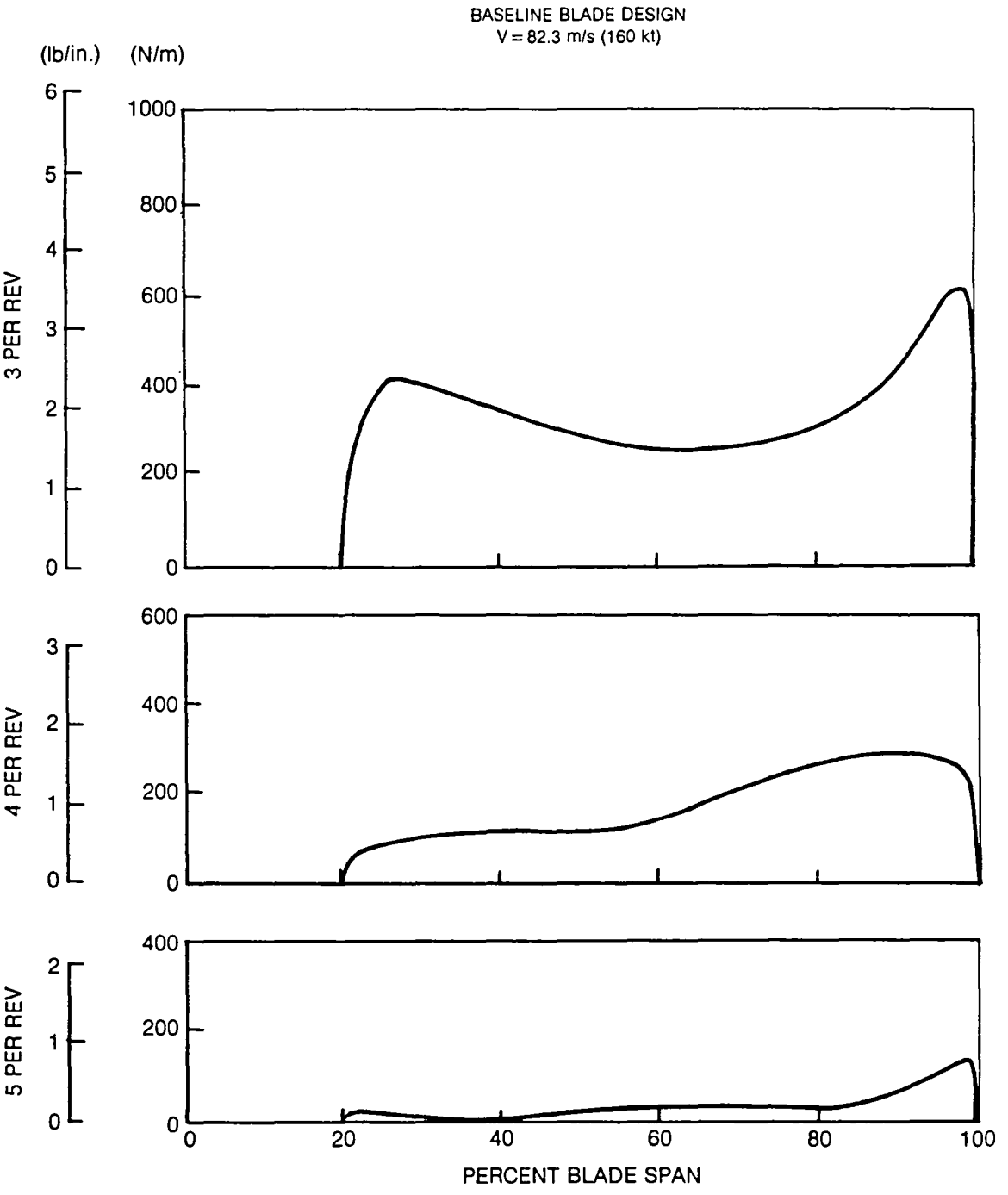

Figure 9. Predicted Amplitude of Vibratory Lift Airloads Due to Blade Rigid and Flexible Motions for the High Speed Flight Condition

82-11-15-11

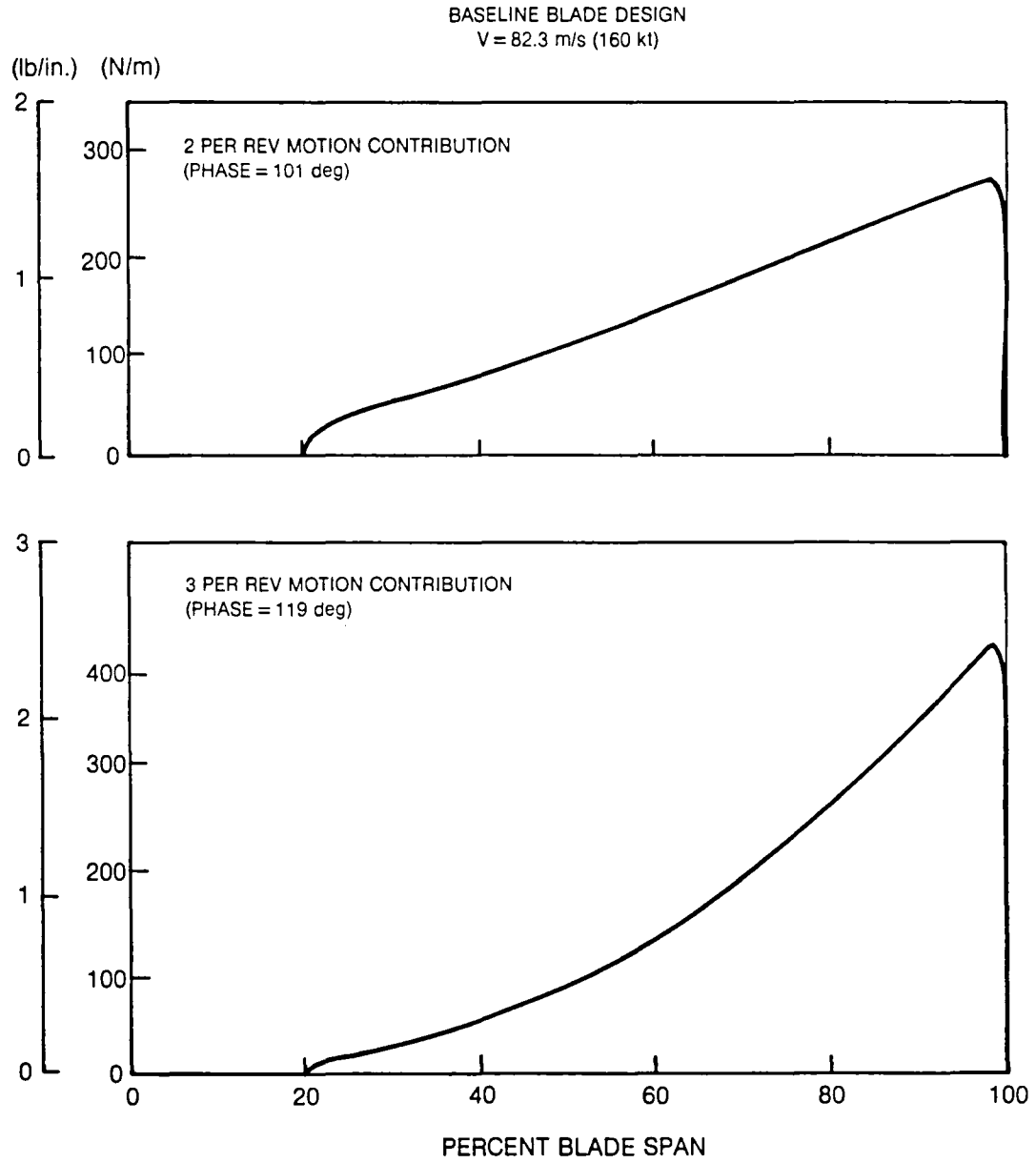

Figure 10. Predicted Amplitude of 3 Per Rev Vibratory Lift Airloads Due to 2 and 3 Per Rev Motion of the Torsion Mode for the High Speed Flight Condition

82-11-15-17

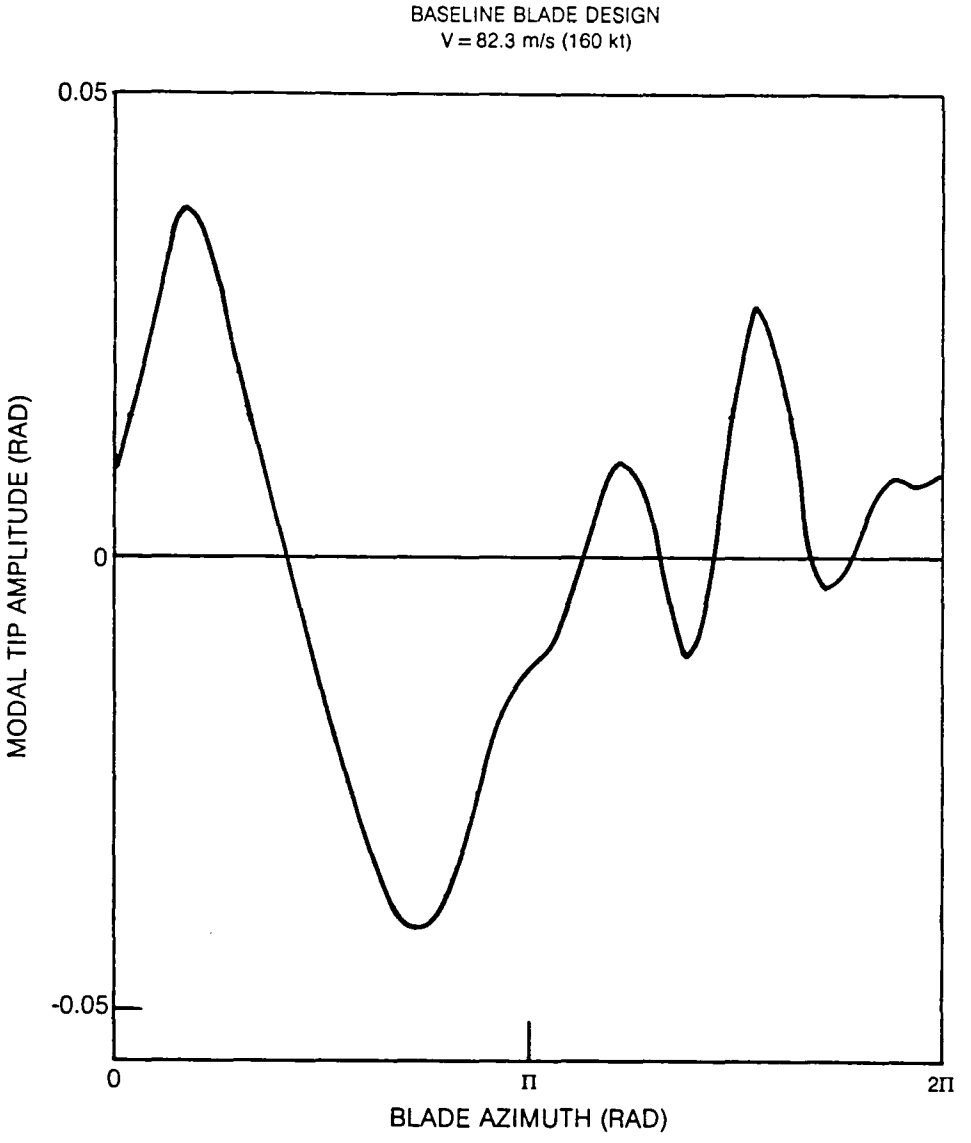

Figure 11. Predicted Time History of Torsion Mode Response for the High Speed Flight Condition

82-11-15-22

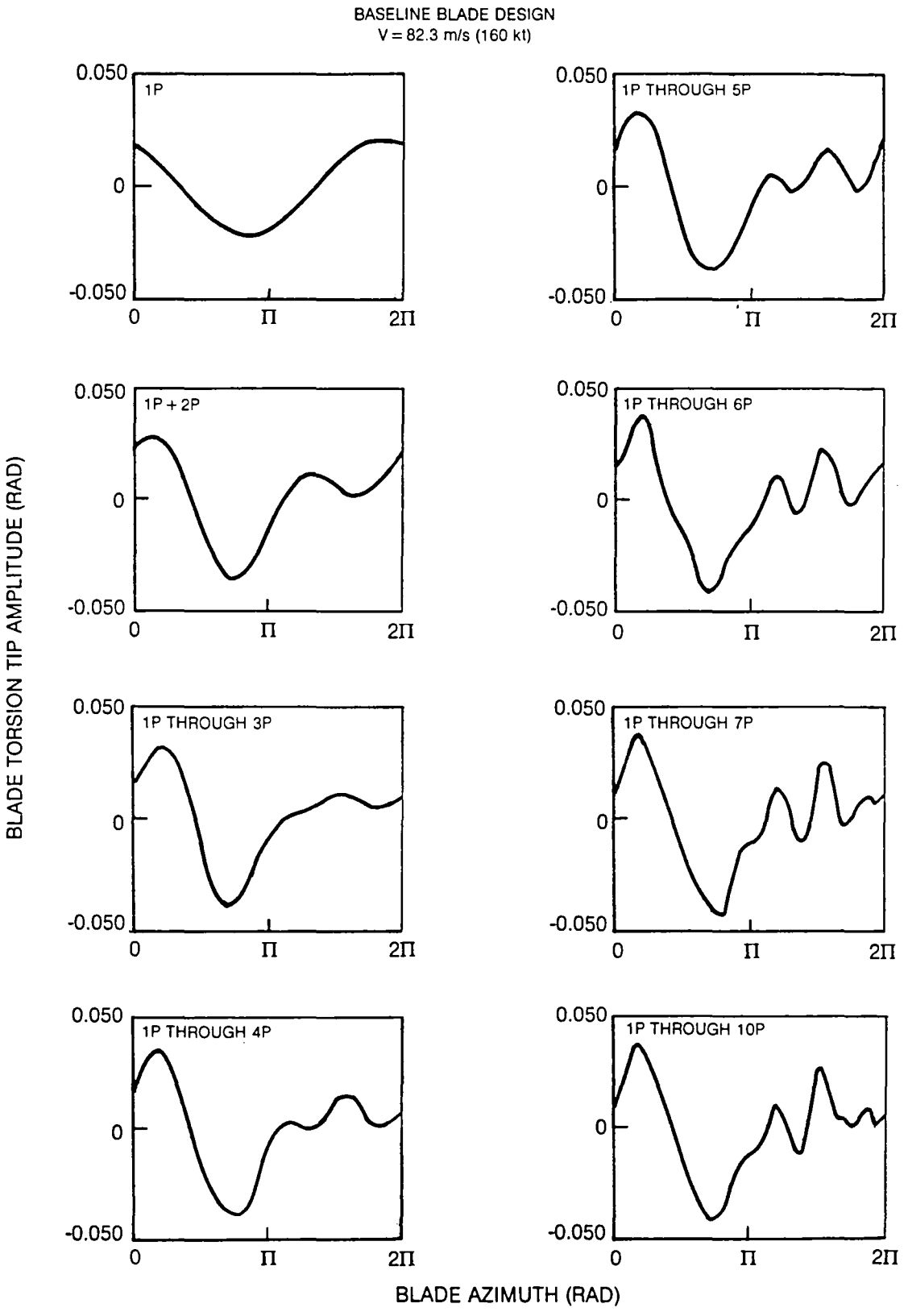

Figure 12. Predicted Effect of Harmonic Contributions to Blade Torsion Time History for the High Speed Flight Condition

82-11-15-24

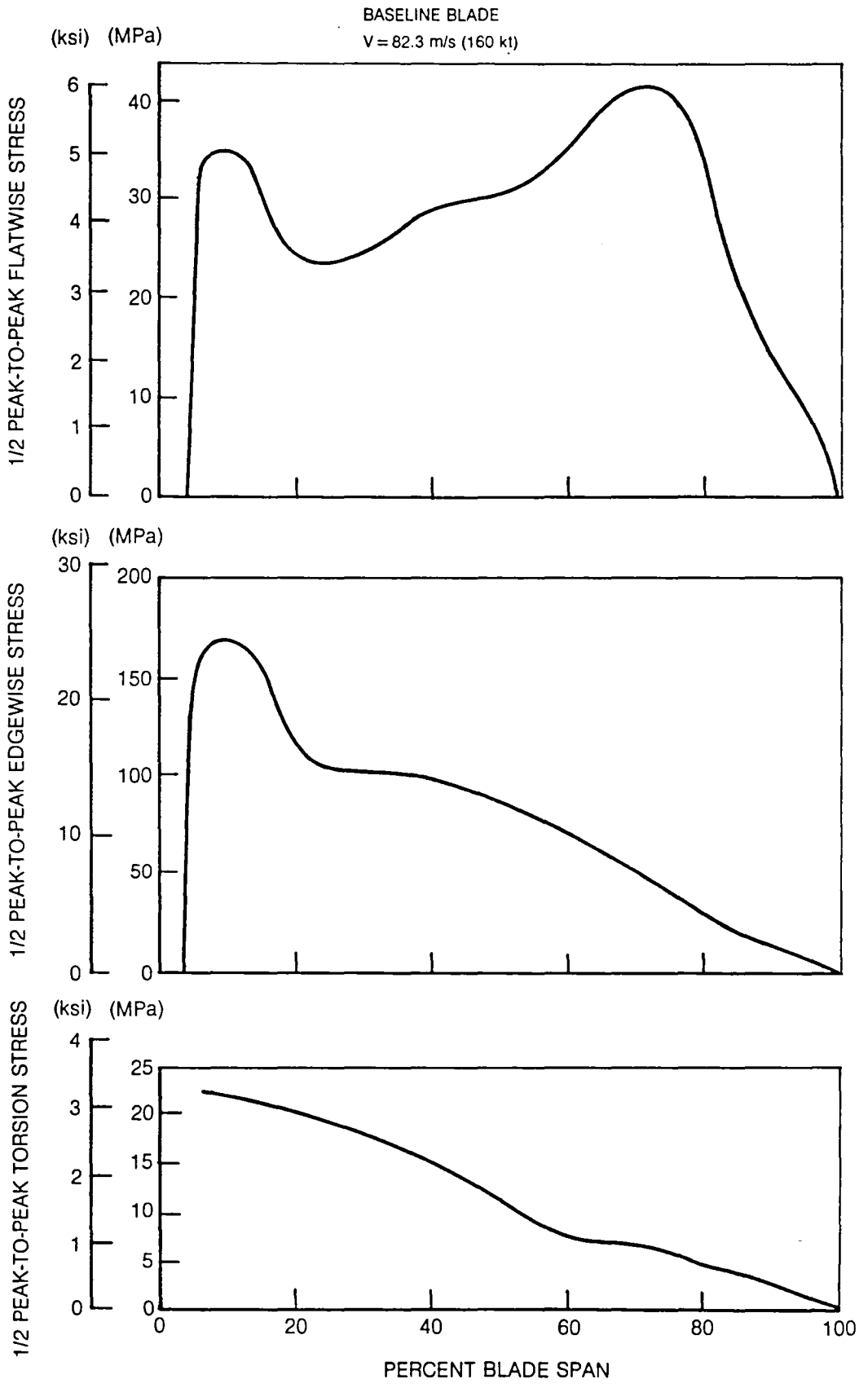

Figure 13. Predicted Peak-to-Peak Blade Stresses for the High Speed Flight Condition

82-11-15-36

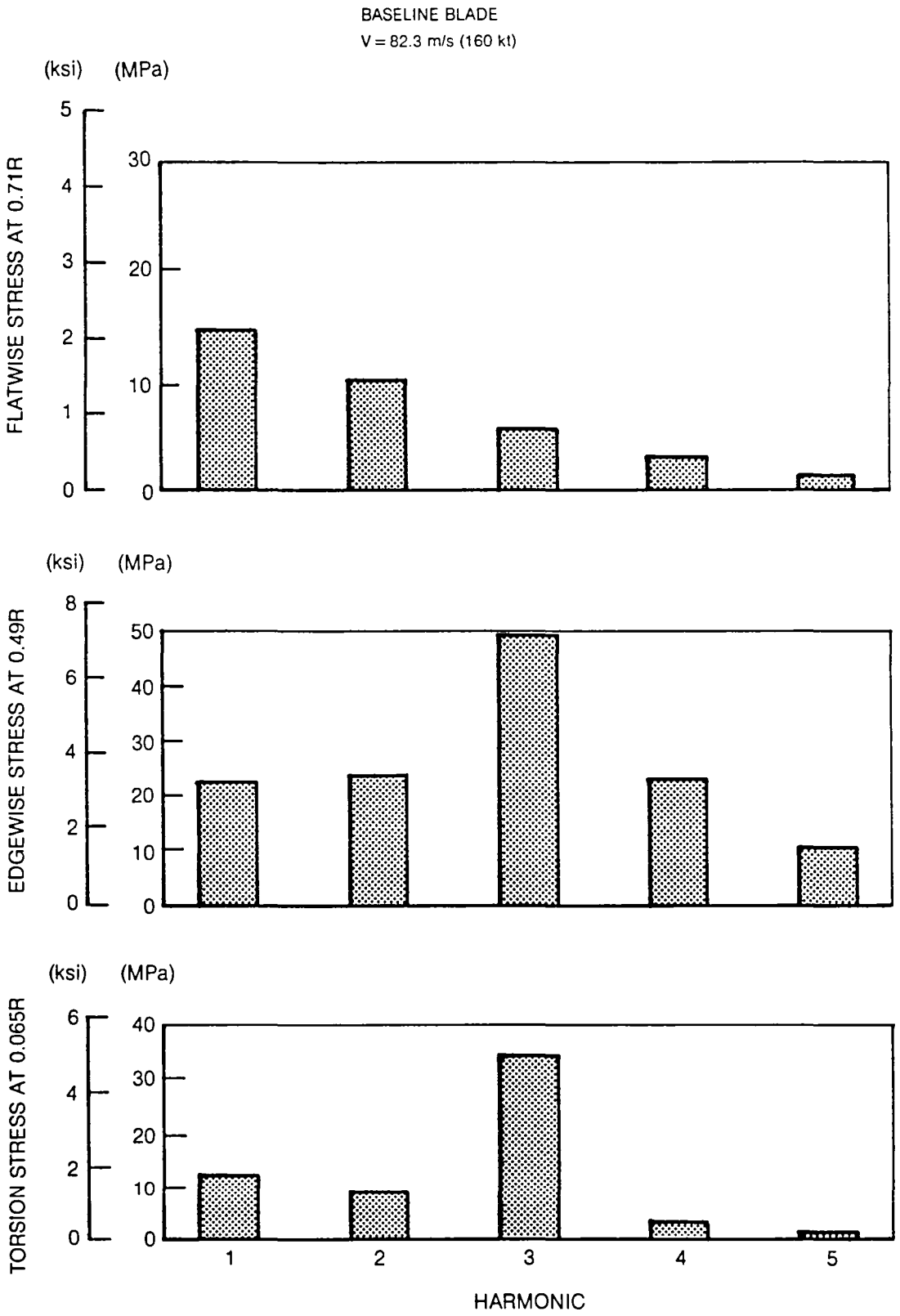

Figure 14. Predicted Amplitude of Harmonic Blade Stresses for the High Speed Flight Condition

82-11-15-35

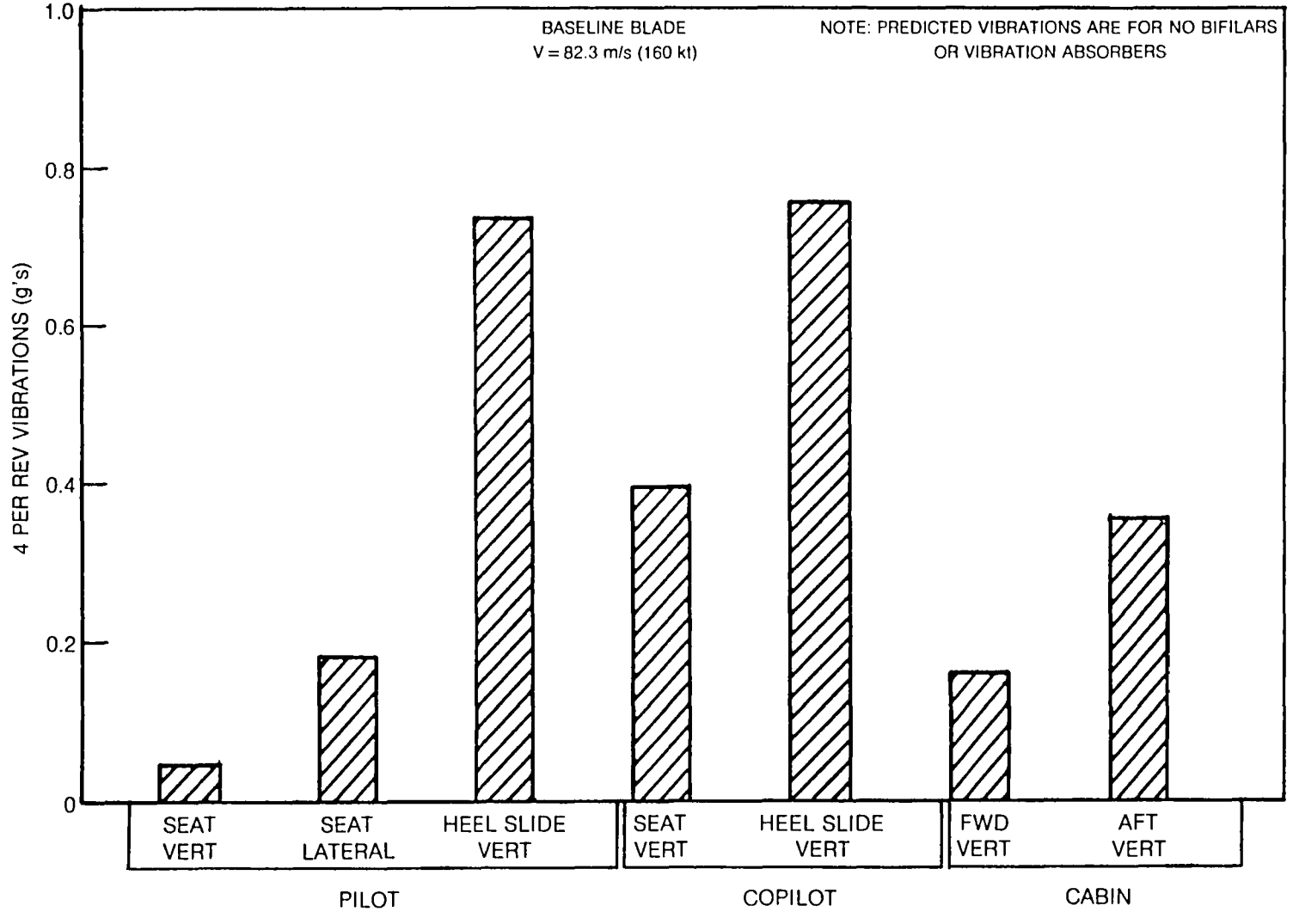

Figure 15. Predicted Fuselage 4 Per Rev Vibrations for the High Speed Flight Condition

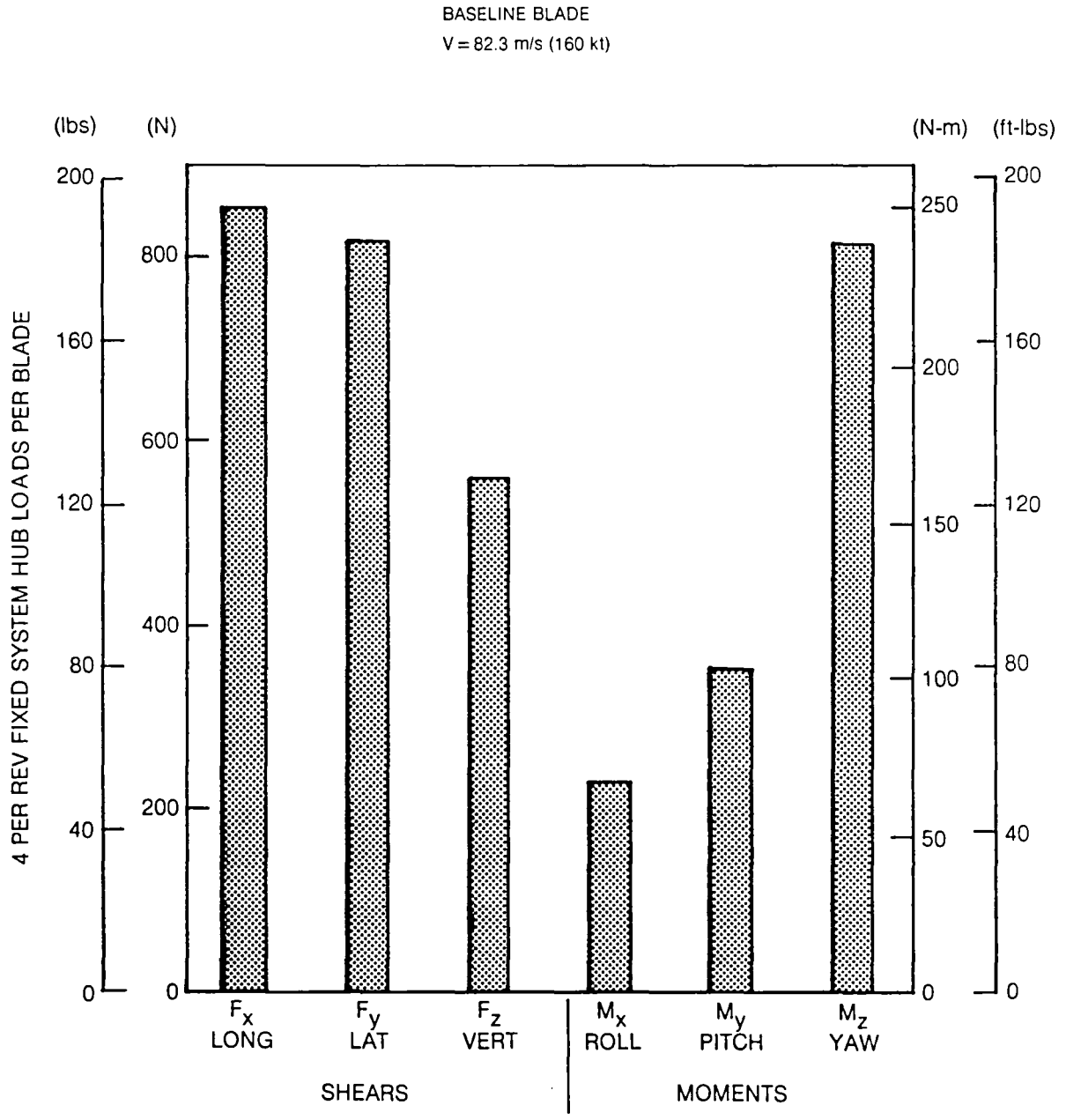

Figure 16. Predicted 4 Per Rev Fixed System Hub Loads for the High Speed Flight Condition

82-11-15-40

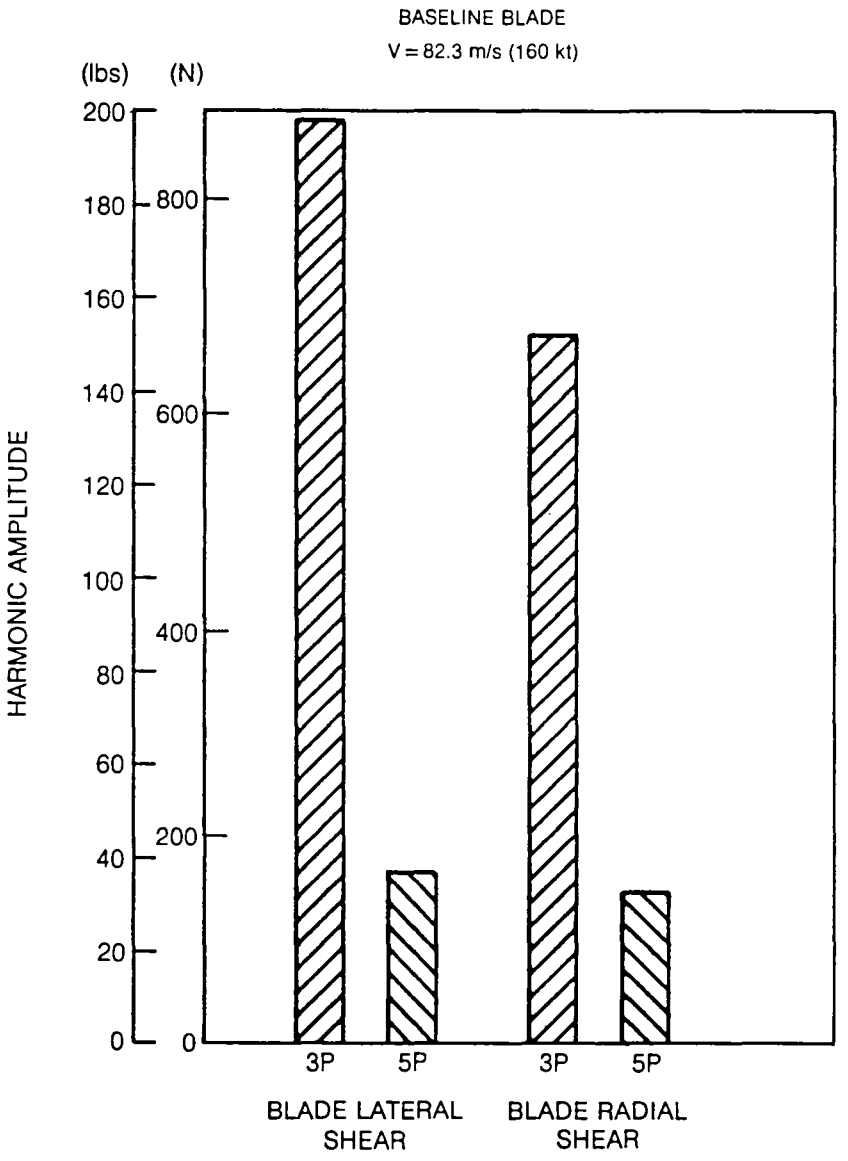

Figure 17. Predicted 3 and 5 Per Rev Rotating Blade Root Inplane Shears for the High Speed Flight Condition

83-6-38-25

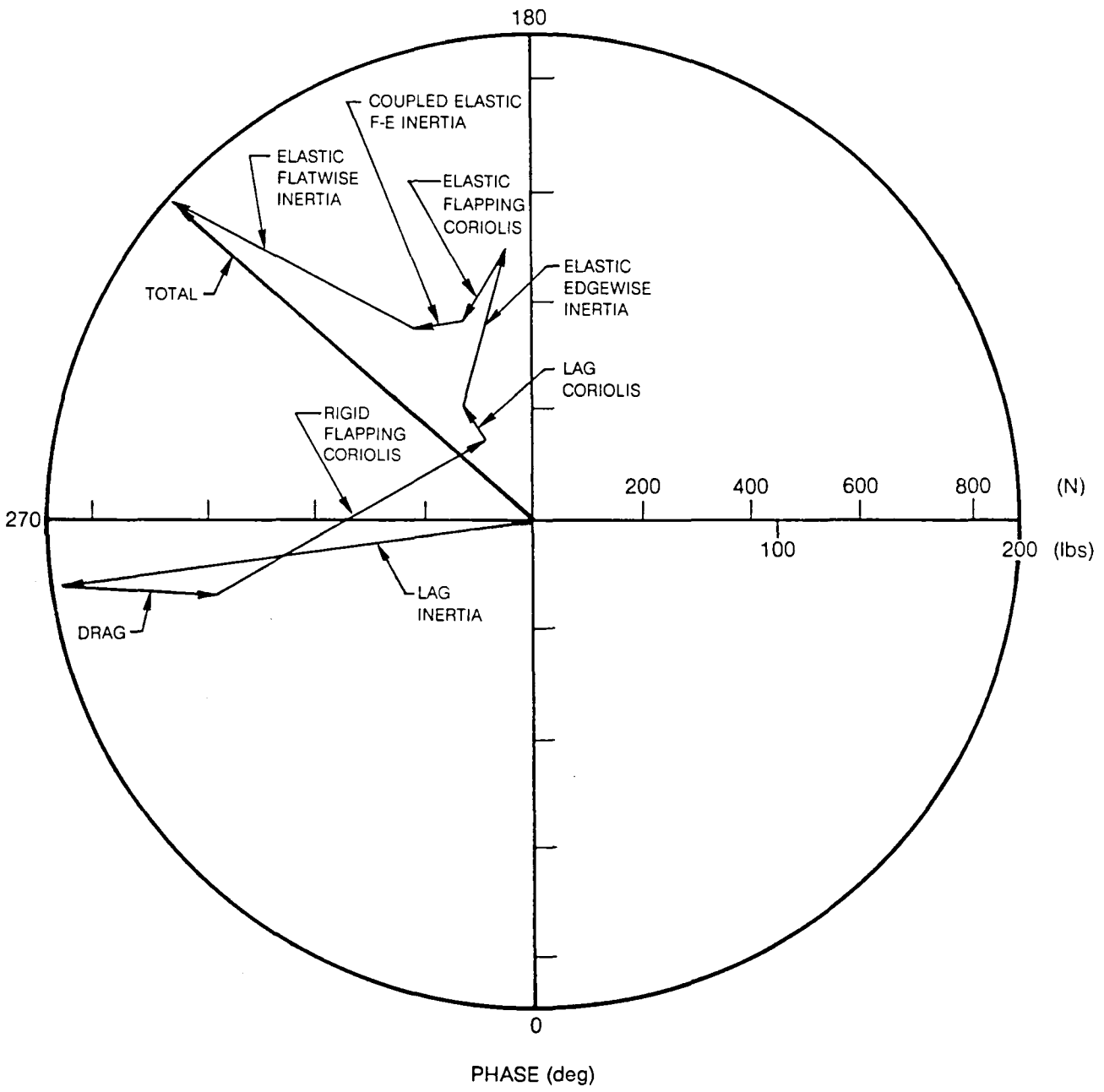

Figure 18. Predicted 3 Per Rev Rotating Blade Lateral Shear for the Baseline Blade at the High Speed Flight Condition

82-11-15-42

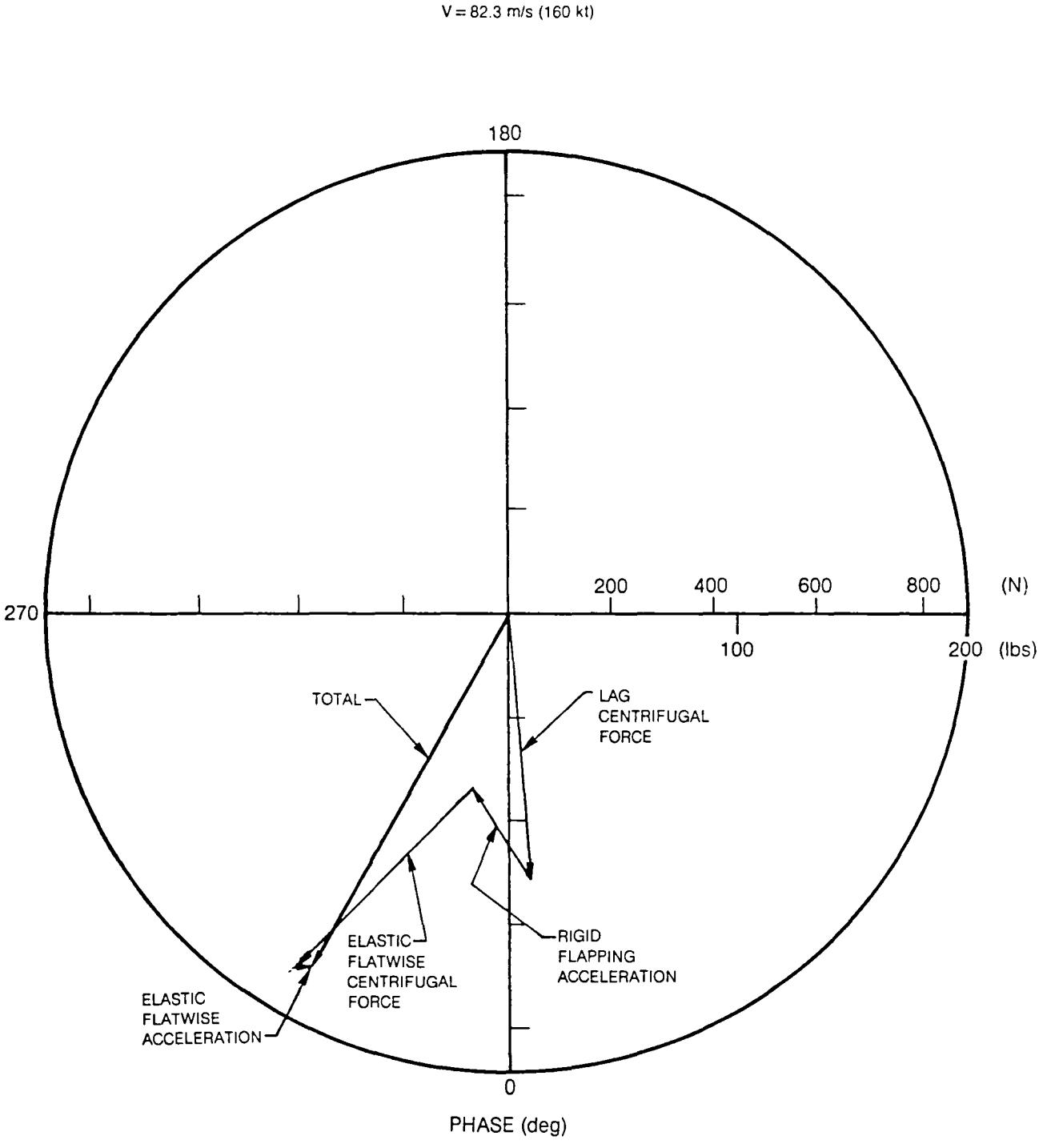

Figure 19. Predicted 3 Per Rev Rotating Blade Radial Shear for the Baseline Blade at the High Speed Flight Condition

82-11-15-43

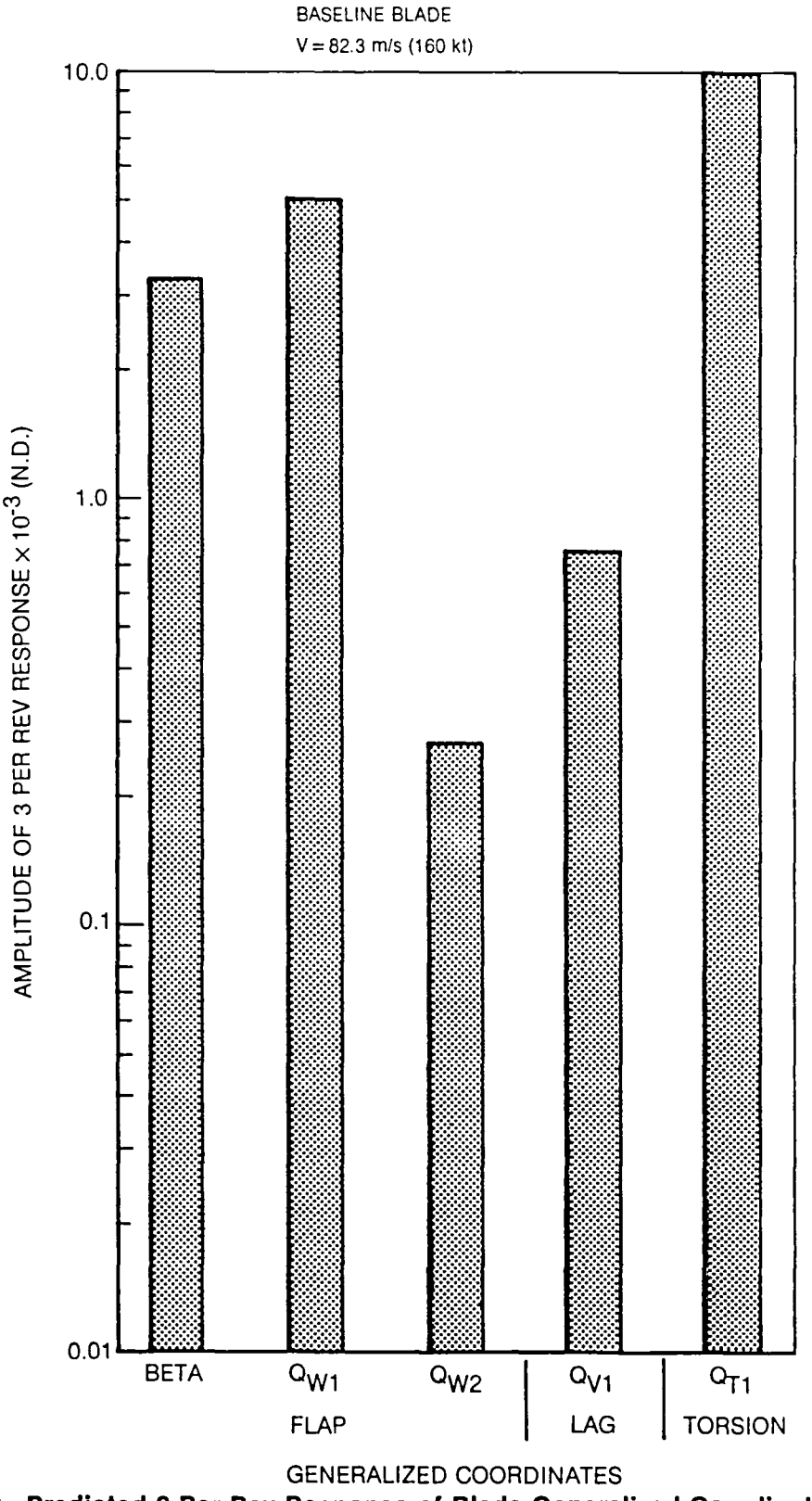

Figure 20. Predicted 3 Per Rev Response of Blade Generalized Coordinates for the High Speed Flight Condition

82-11-15-39

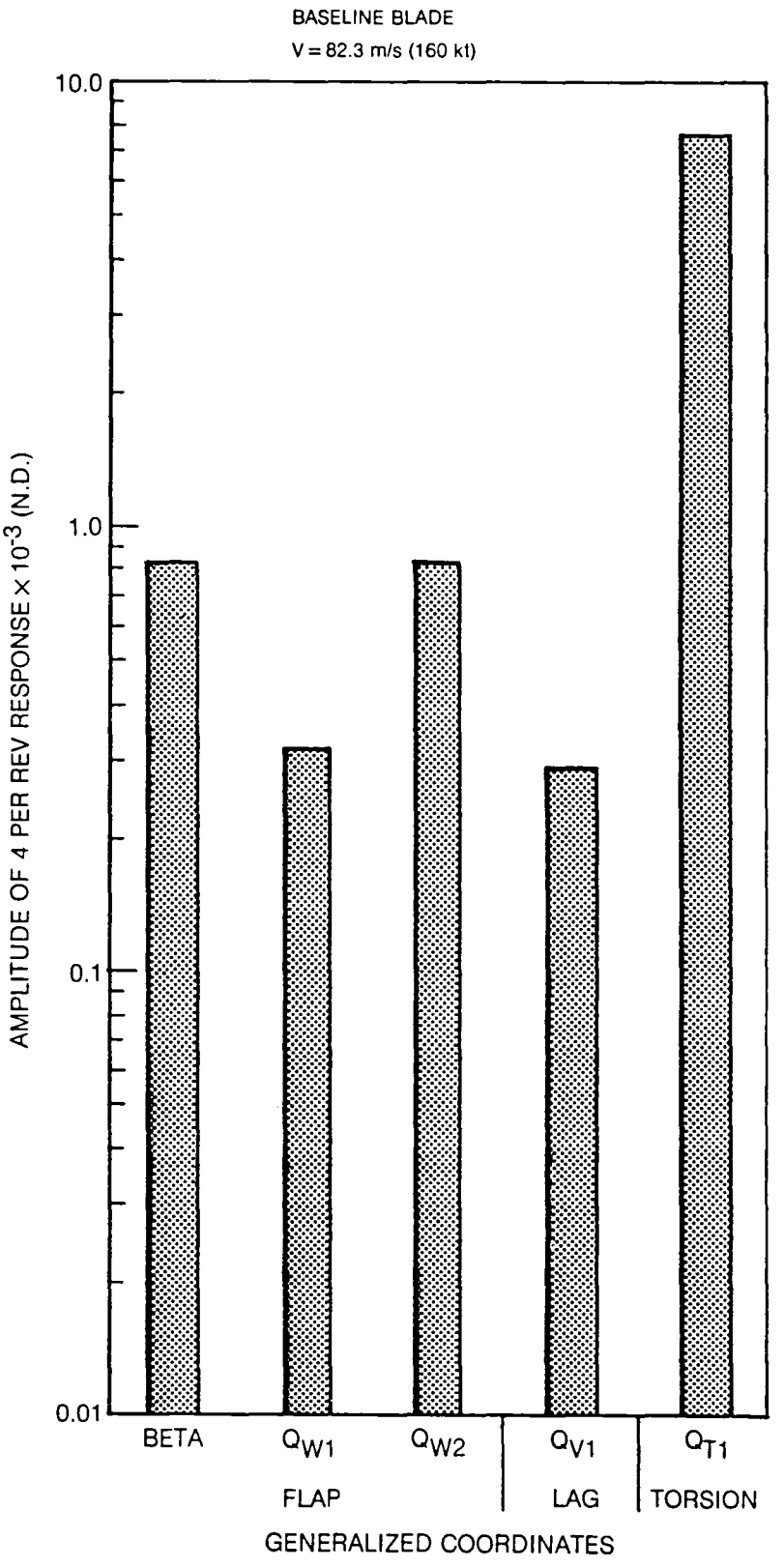

Figure 21. Predicted 4 Per Rev Response of Blade Generalized Coordinates for the High Speed Flight Condition

82-11-15-38

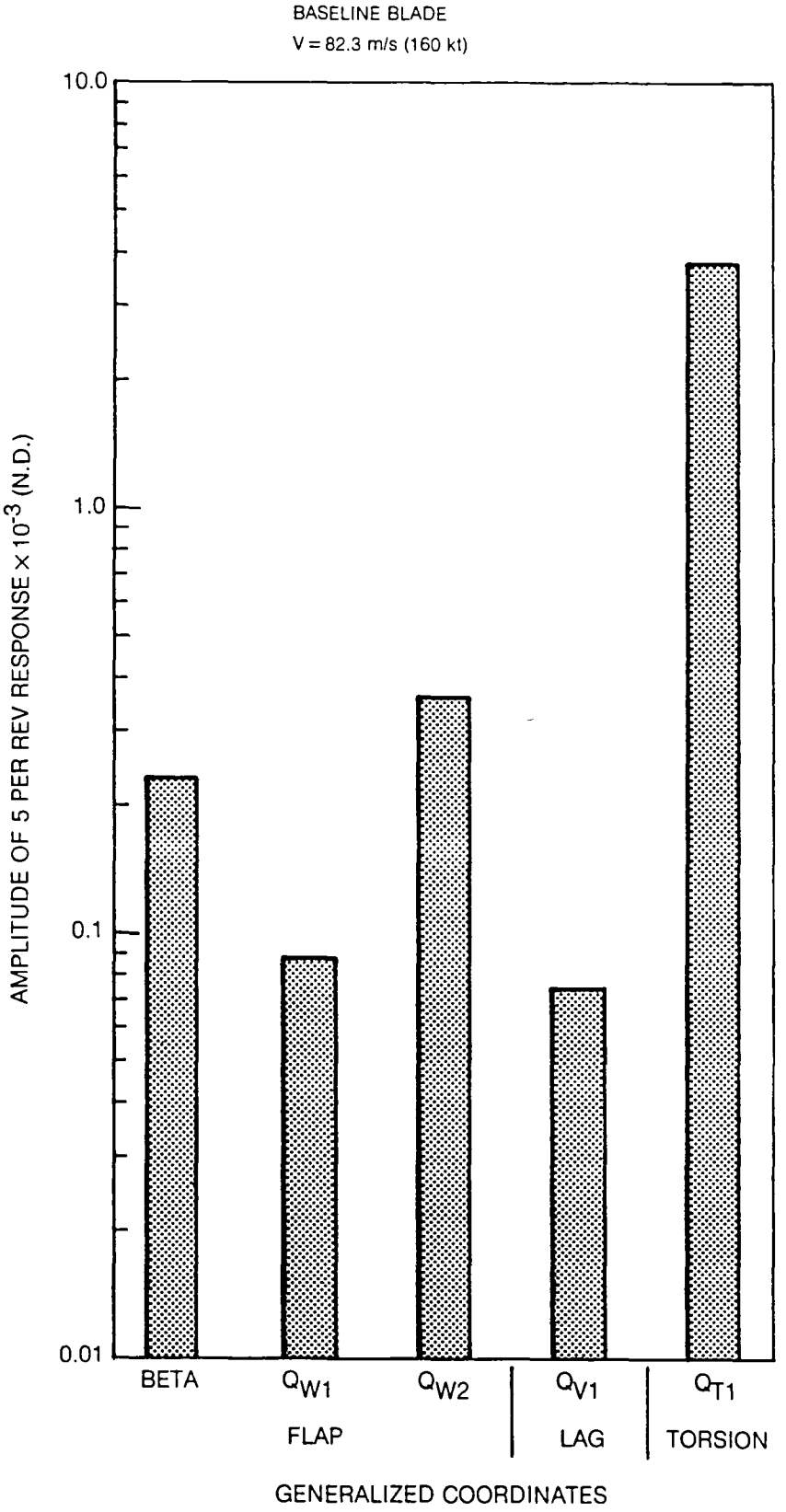

Figure 22. Predicted 5 Per Rev Response of Blade Generalized Coordinates for the High Speed Flight Condition

82-11-15-37

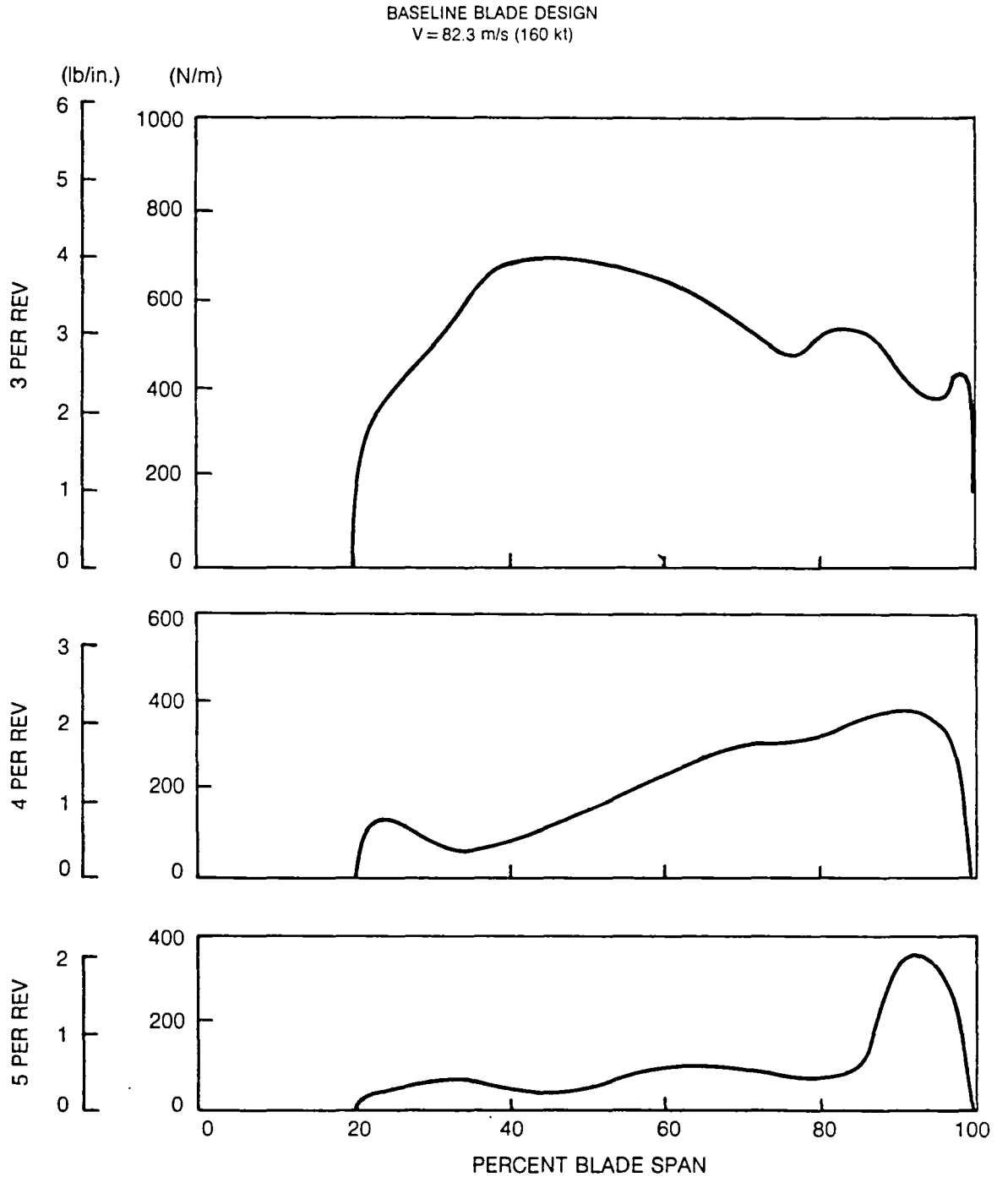

Figure 23. Predicted Amplitude of Vibratory Lift Airloads with Damping Airloads Due to Motion of the First Flexible Flatwise Mode Deleted for the High Speed Flight Condition

82-11-15-8

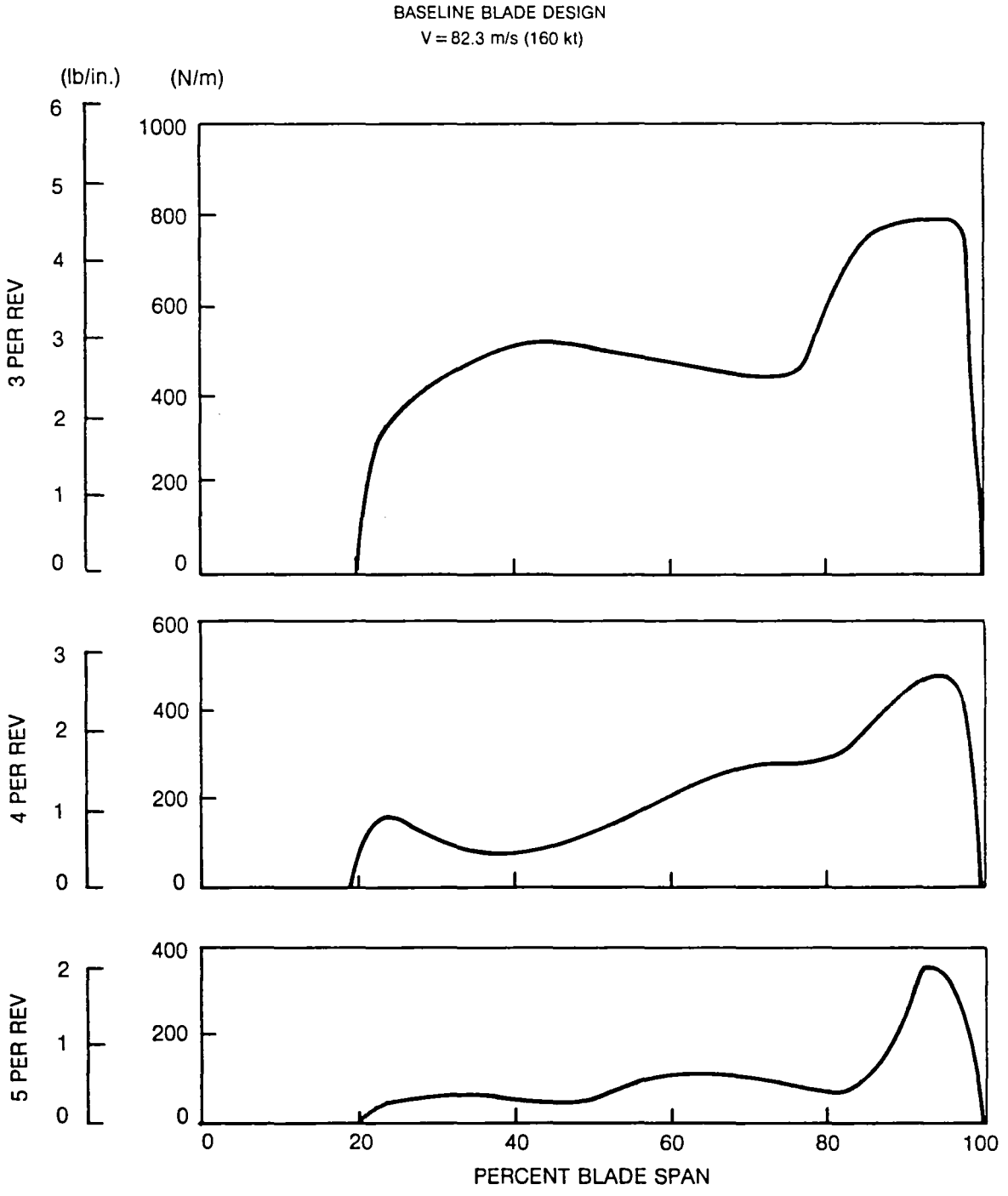

Figure 24. Predicted Amplitude of Vibratory Lift Airloads with Damping Airloads Due to Motion of the Second Flexible Flatwise Mode Deleted for the High Speed Flight Condition

82-11-15-9

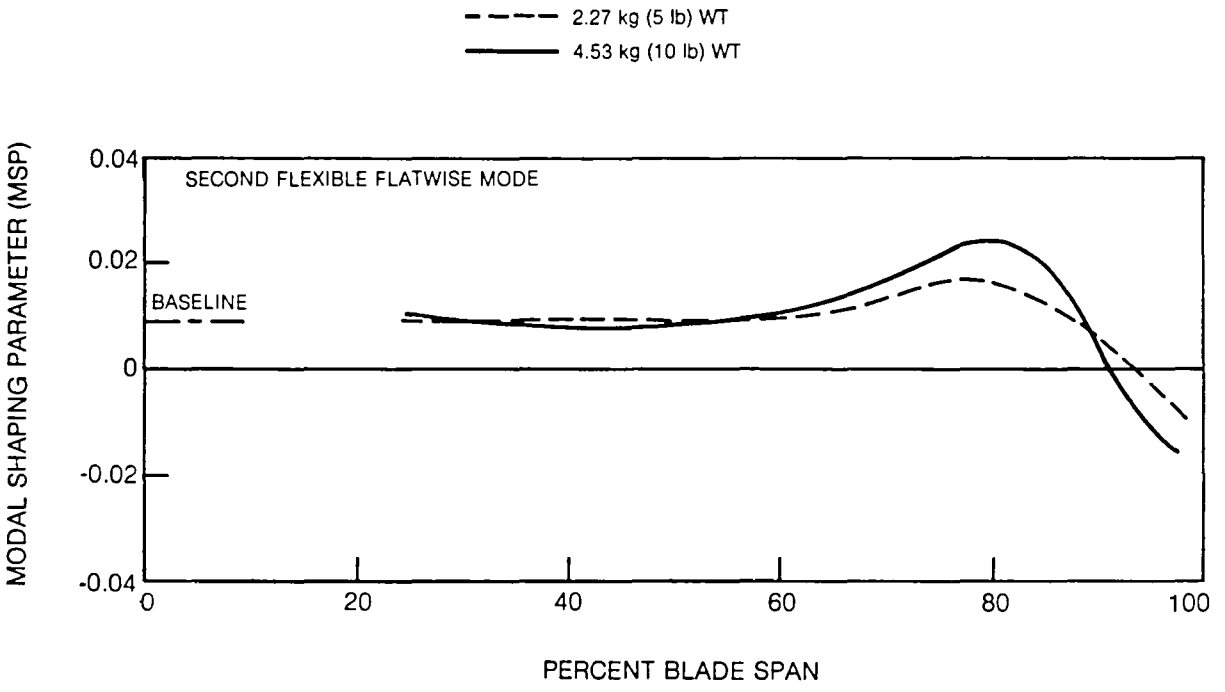

Figure 25. Predicted Effect of Location of Local Weight on Modal Shaping Parameter

83-6-38-24

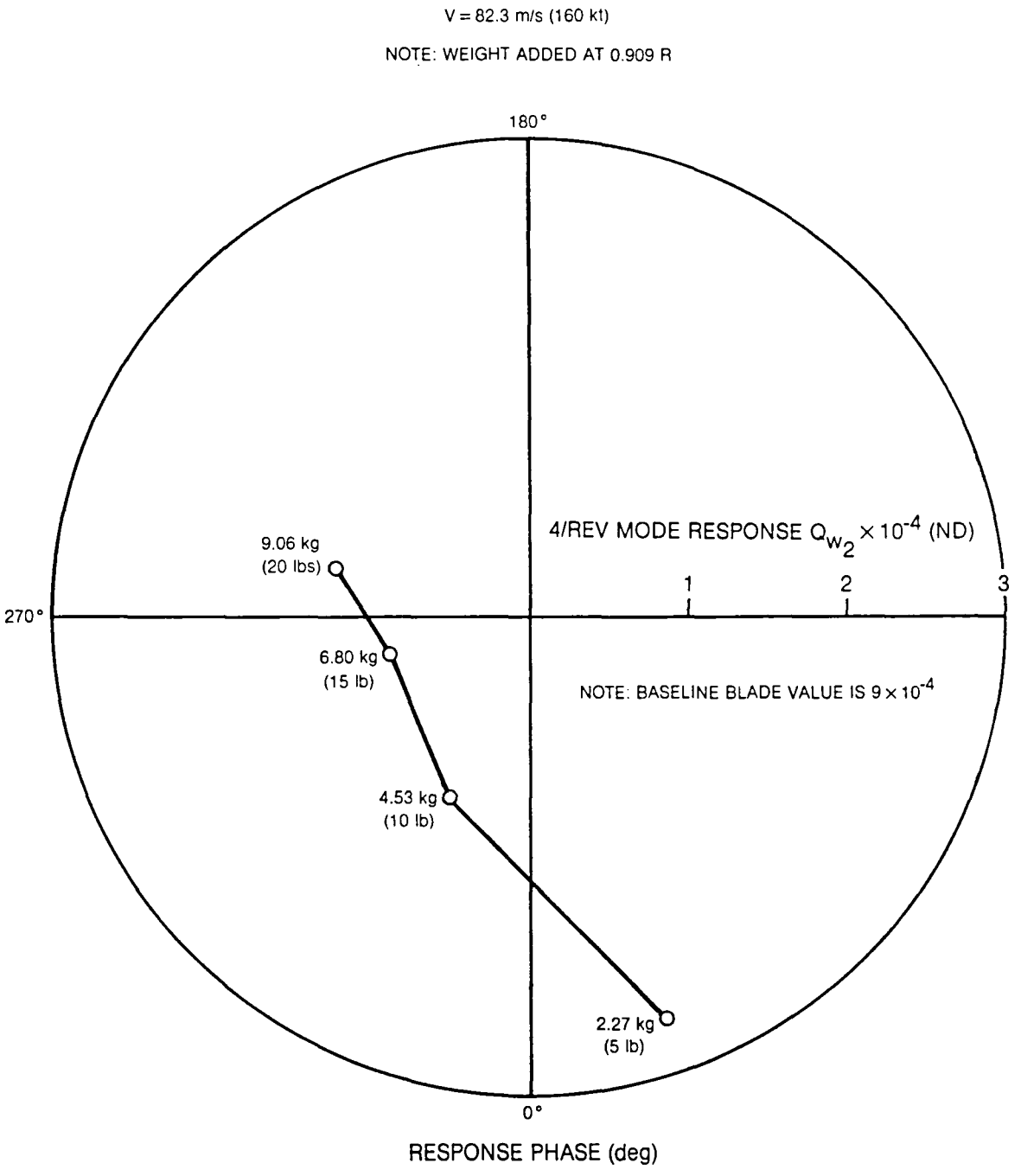

Figure 26. Predicted Effect of Added Tip Weight on 4 Per Rev Response of Second Flexible Flatwise Mode for the High Speed Flight Condition

82-11-15-32

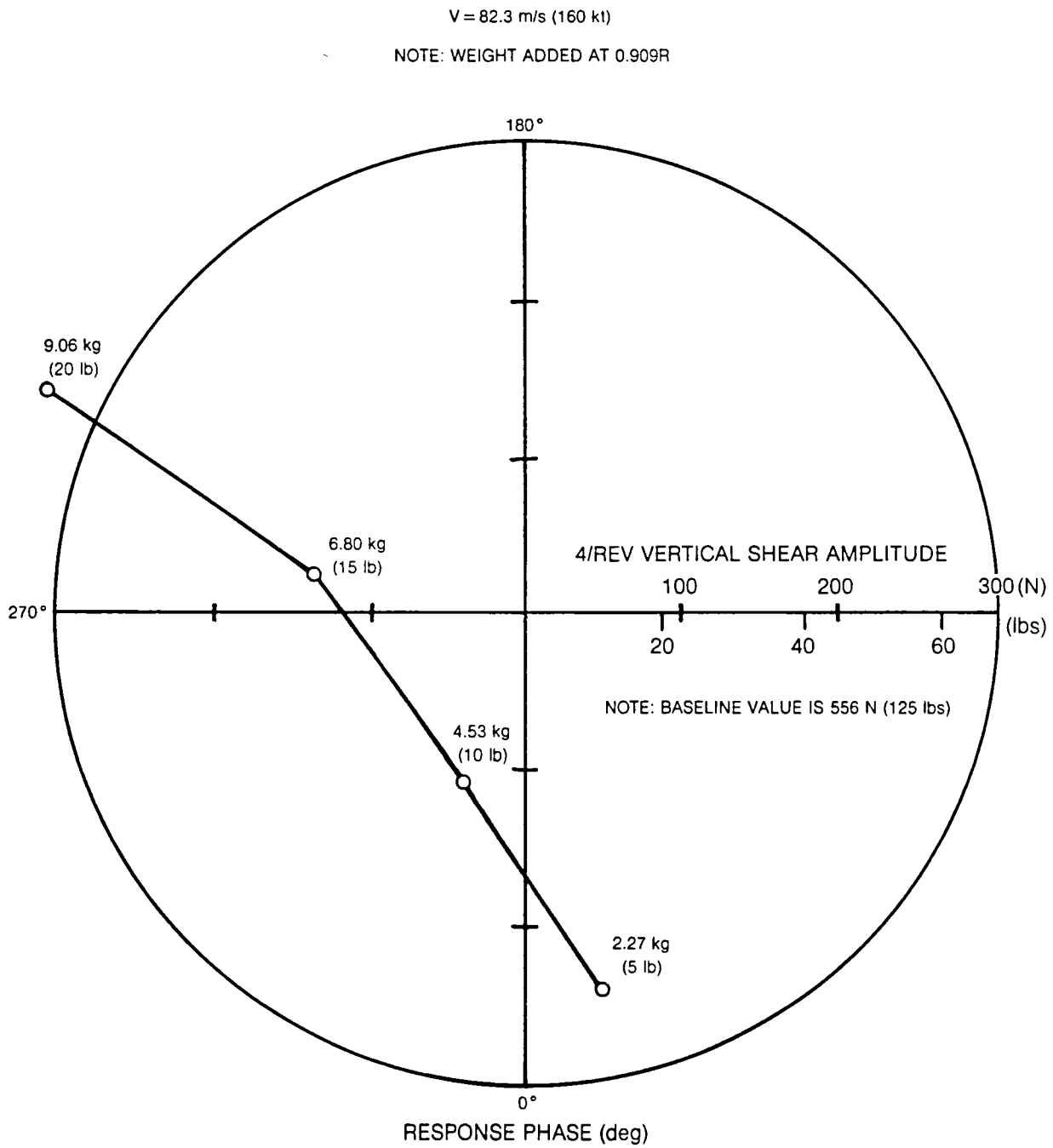

Figure 27. Predicted Effect of Added Tip Weight on 4 Per Blade Root Vertical Shear for the High Speed Flight Condition

82-11-15-31

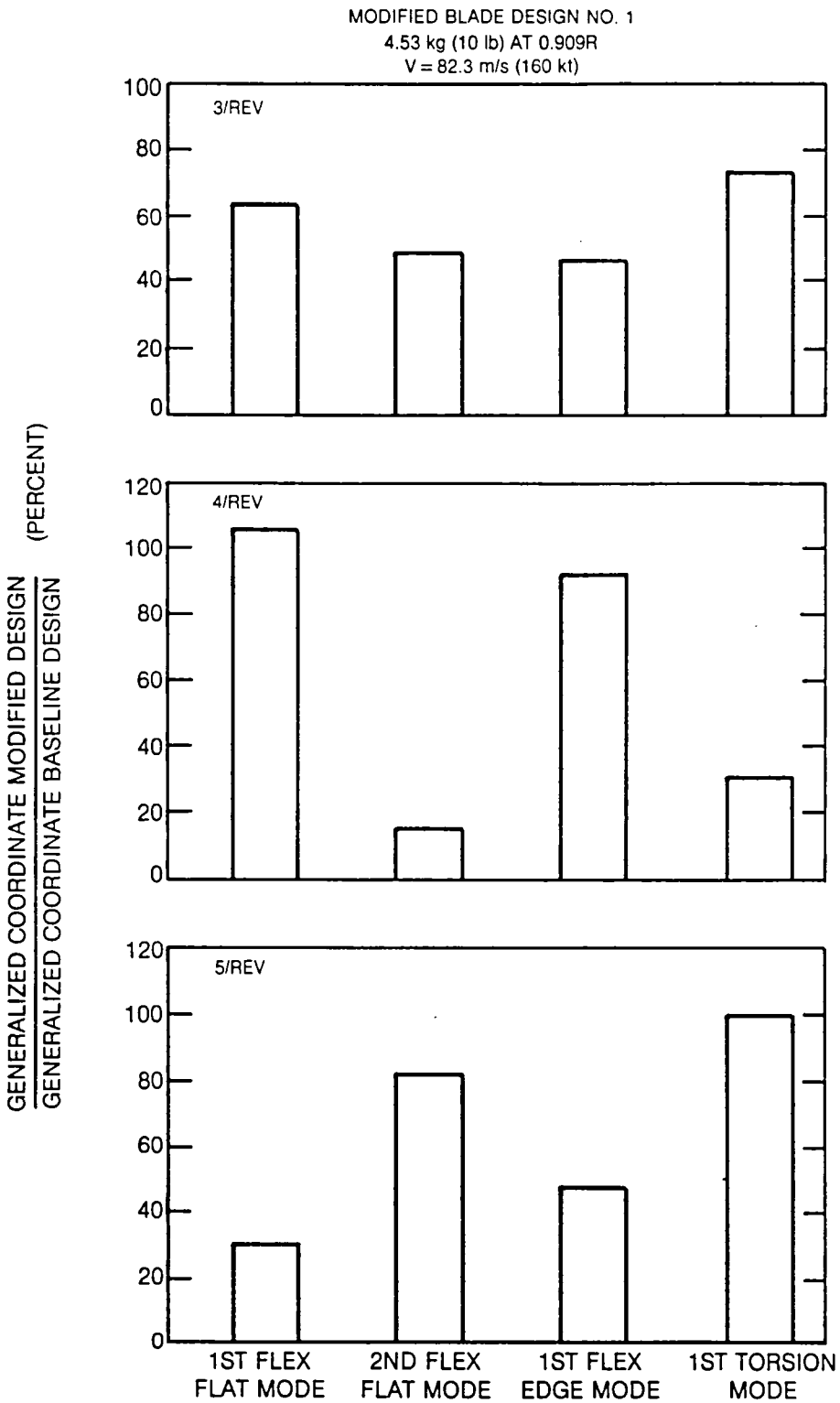

Figure 28. Predicted Change in Blade Mode Generalized Coordinates with Modified Blade Design for the High Speed Flight Condition

83-6-38-23

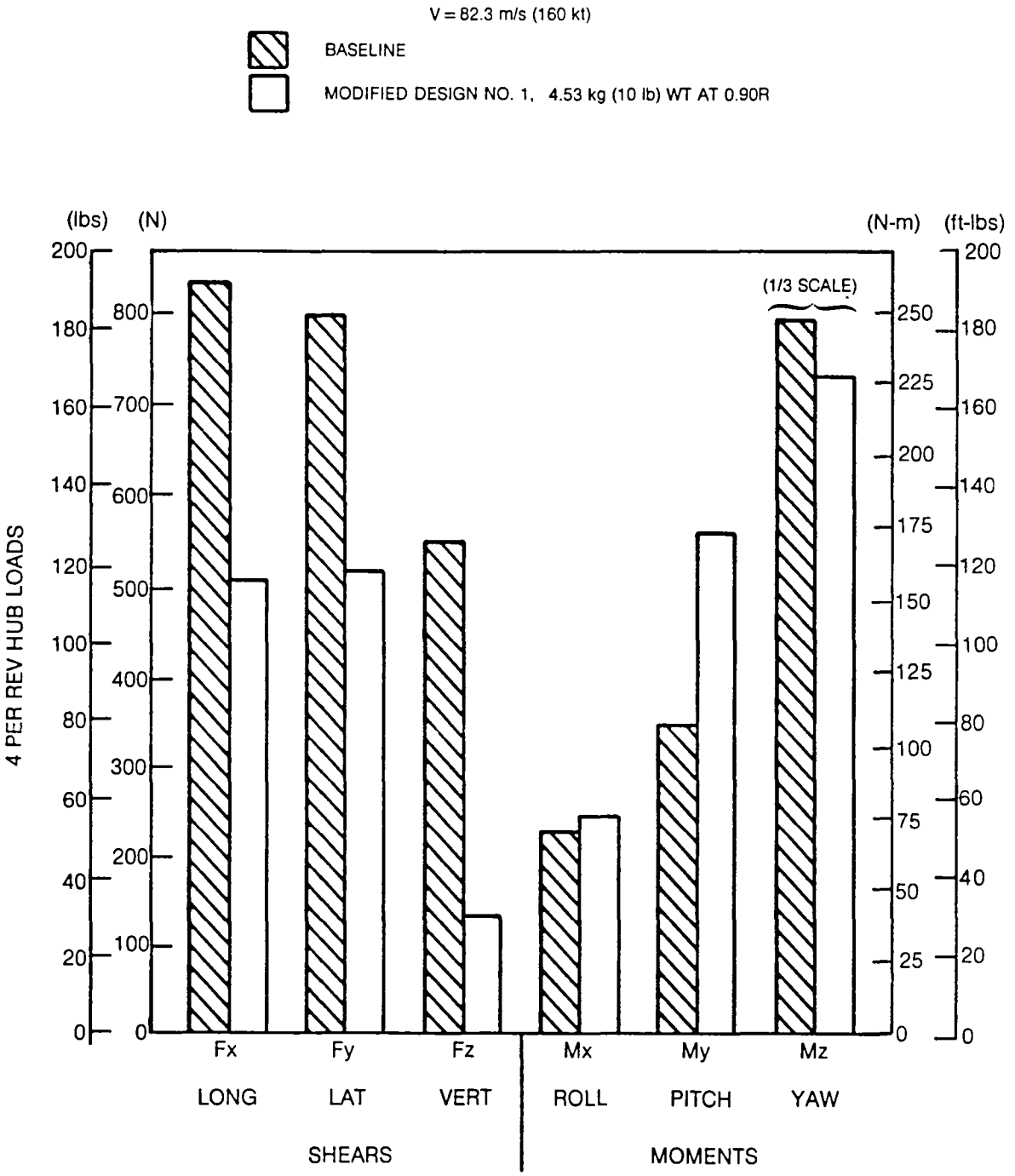

Figure 29. Comparison of Predicted Baseline and Modified Blade Vibratory Fixed System Hub Loads for the High Speed Flight Condition

83-6-38-8

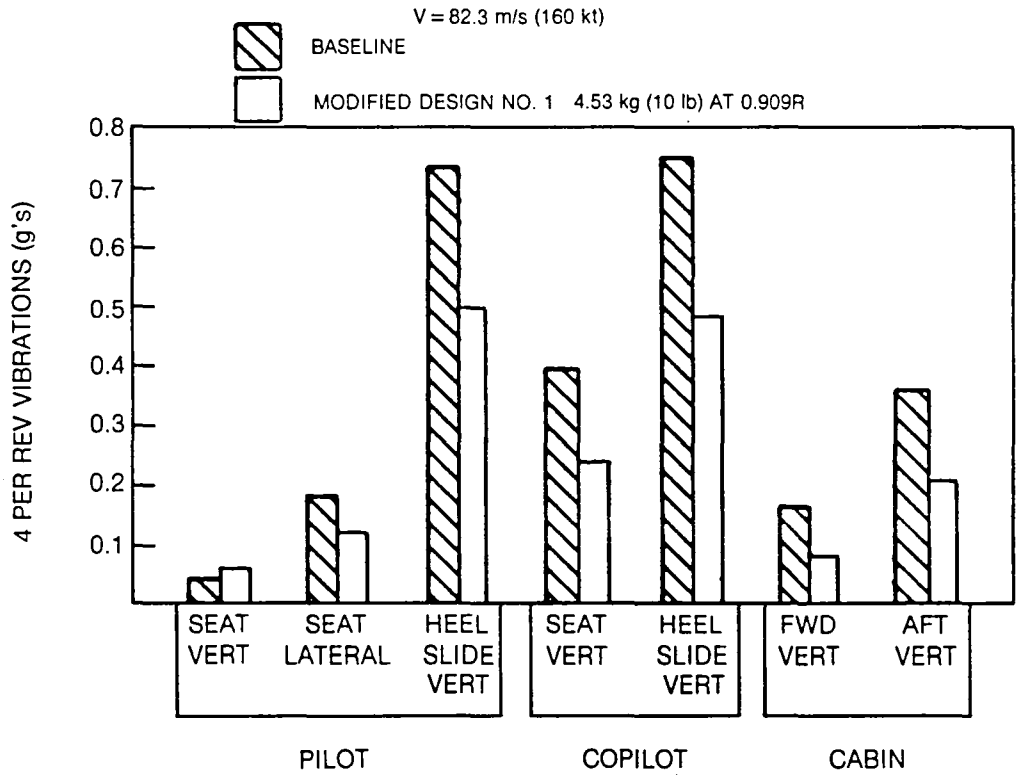

Figure 30. Predicted Fuselage 4 Per Rev Vibrations for Modified Blade Design No. 1 at the High Speed Flight Condition

83-6-38-21

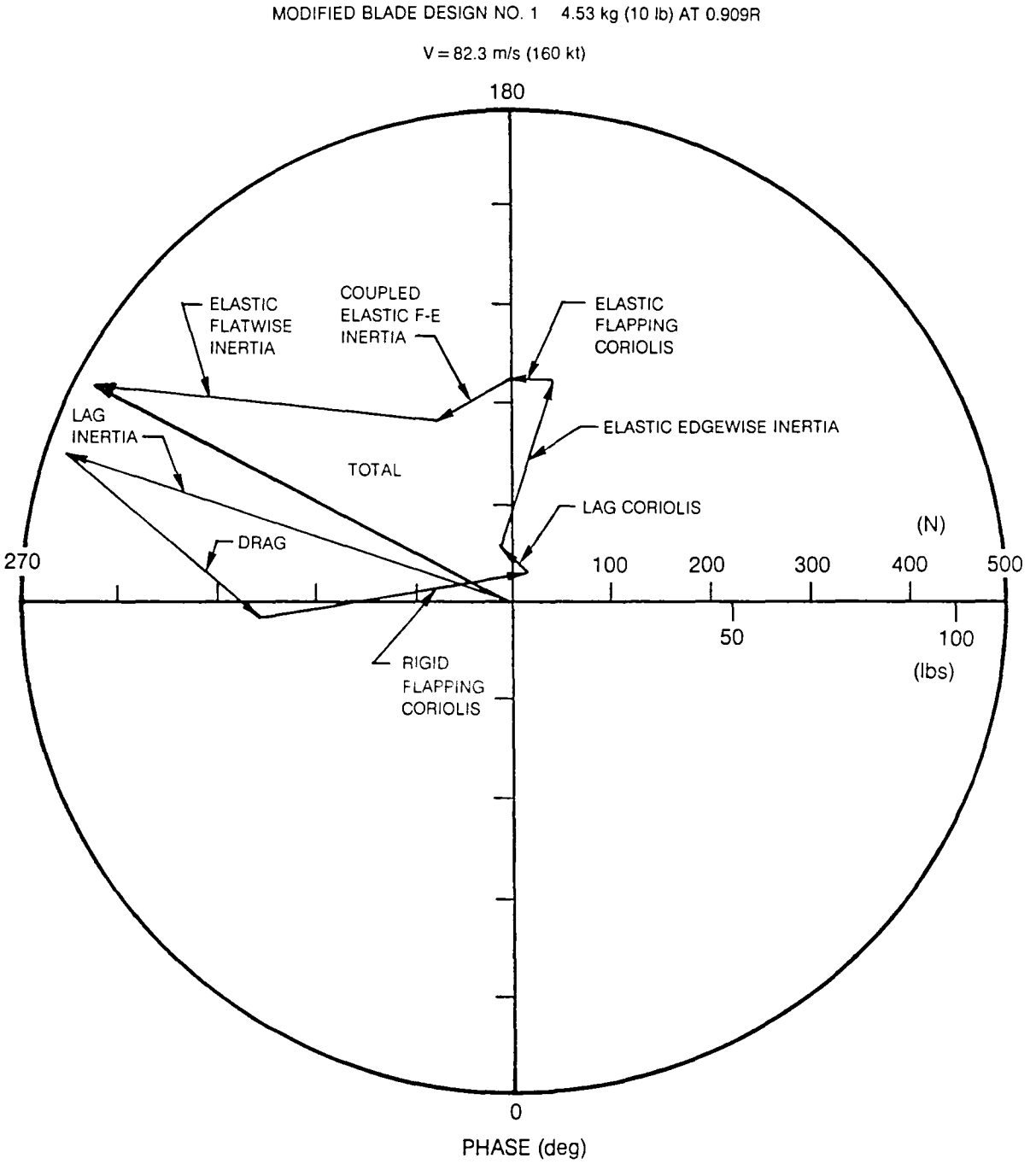

Figure 31. Predicted 3 Per Rev Rotating Blade Lateral Shear for Modified Blade Design No. 1 at the High Speed Flight Condition

82-11-15-44

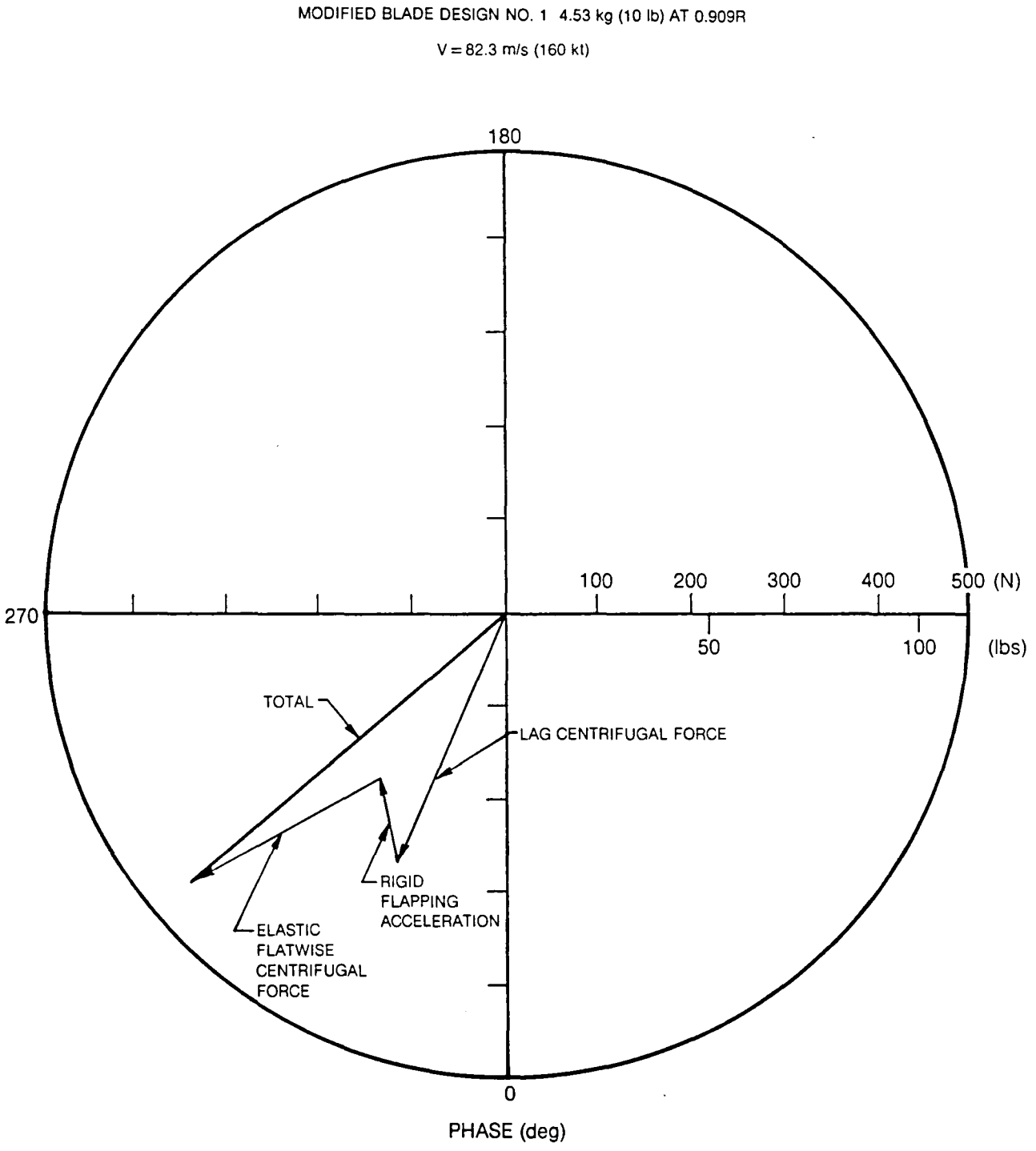

Figure 32. Predicted 3 Per Rev Rotating Blade Radial Shear for Modified Blade Design No. 1 at the High Speed Flight Condition

82-11-15-45

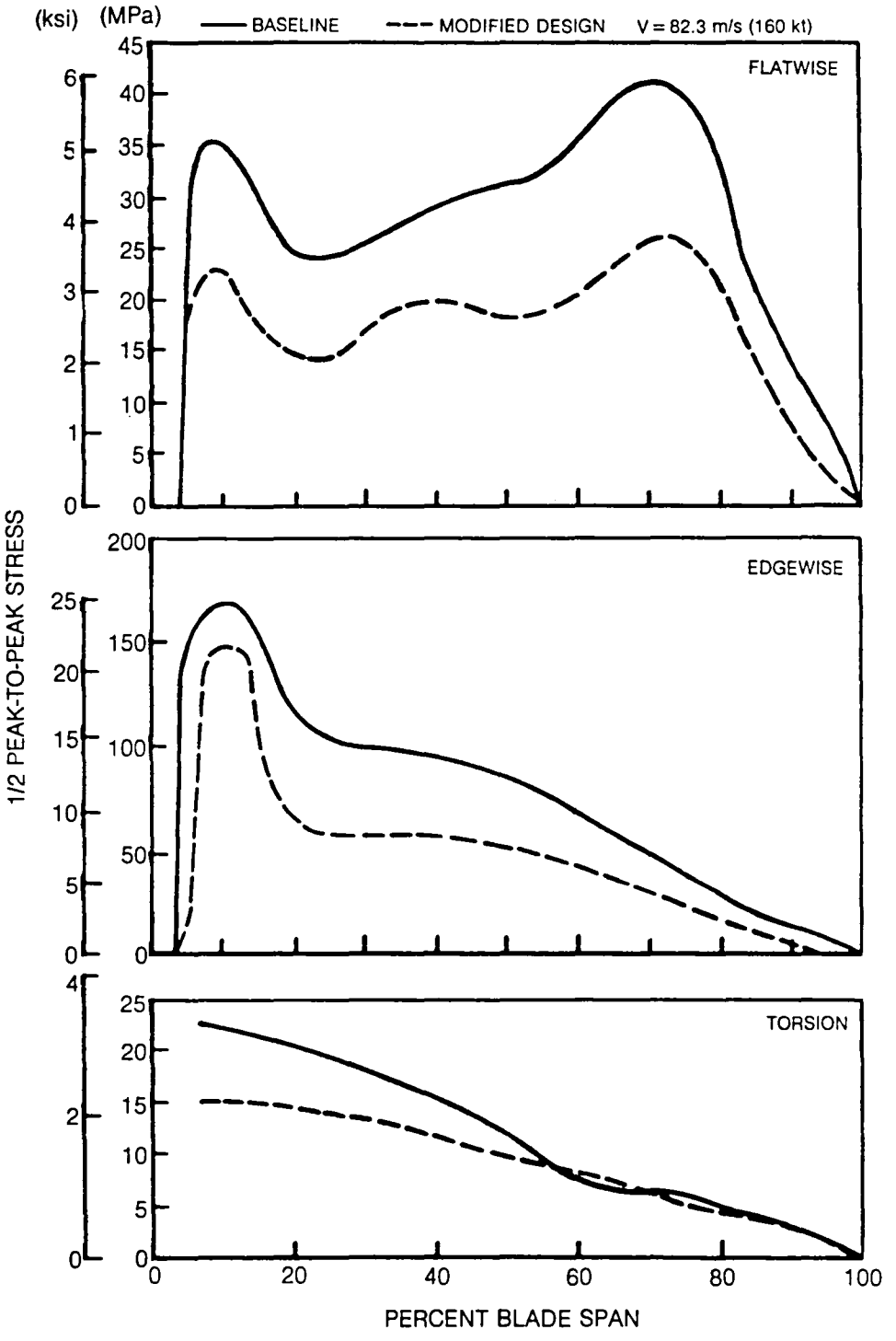

Figure 33. Predicted Change In Vibratory Stresses for Modified Blade Design No. 1 at the High Speed Flight Condition

83-6-38-7

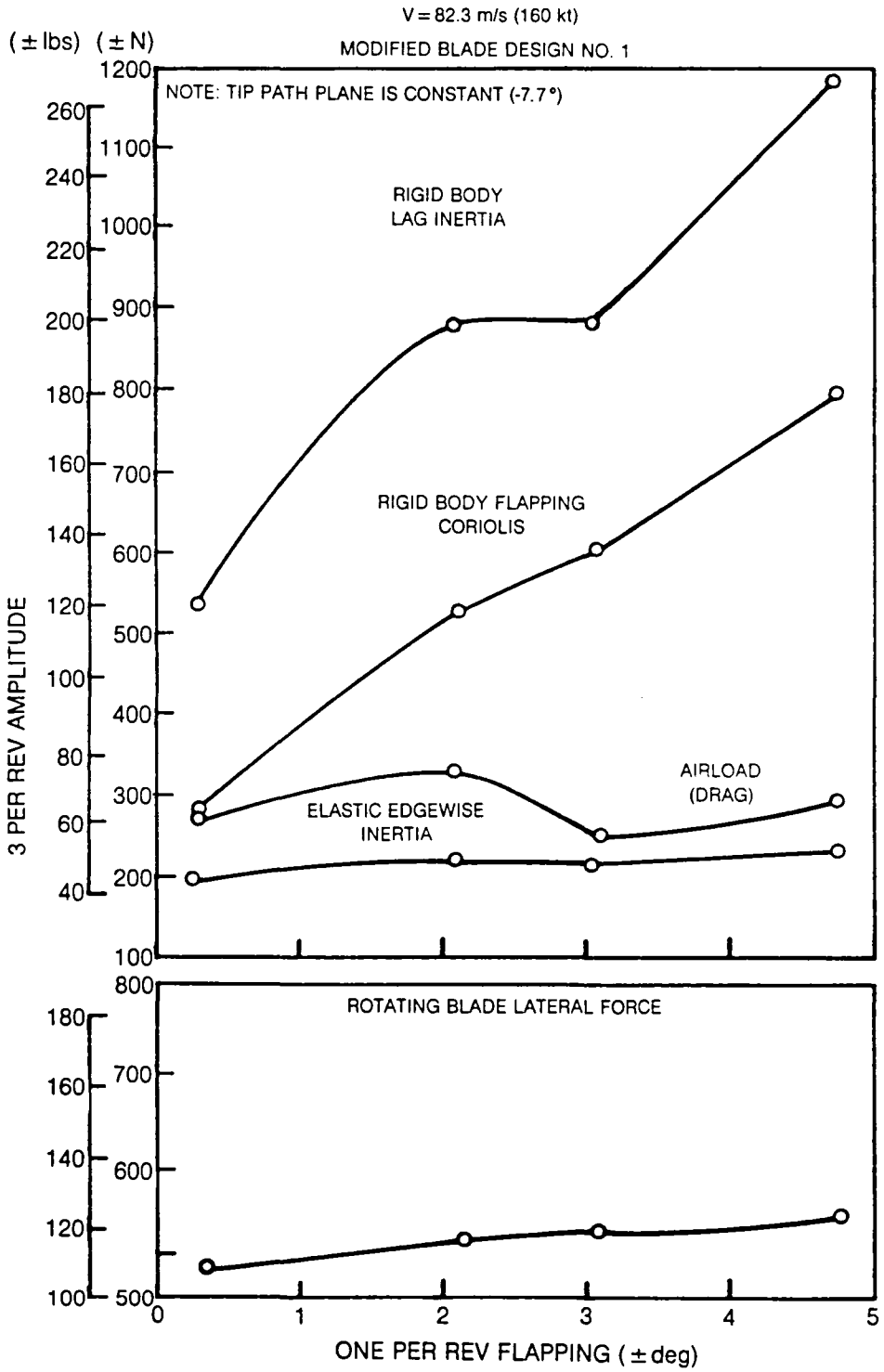

Figure 34. Predicted Effect of Blade Flapping on 3 Per Rev Lateral Force for the High Speed Flight Condition

83-6-38-6

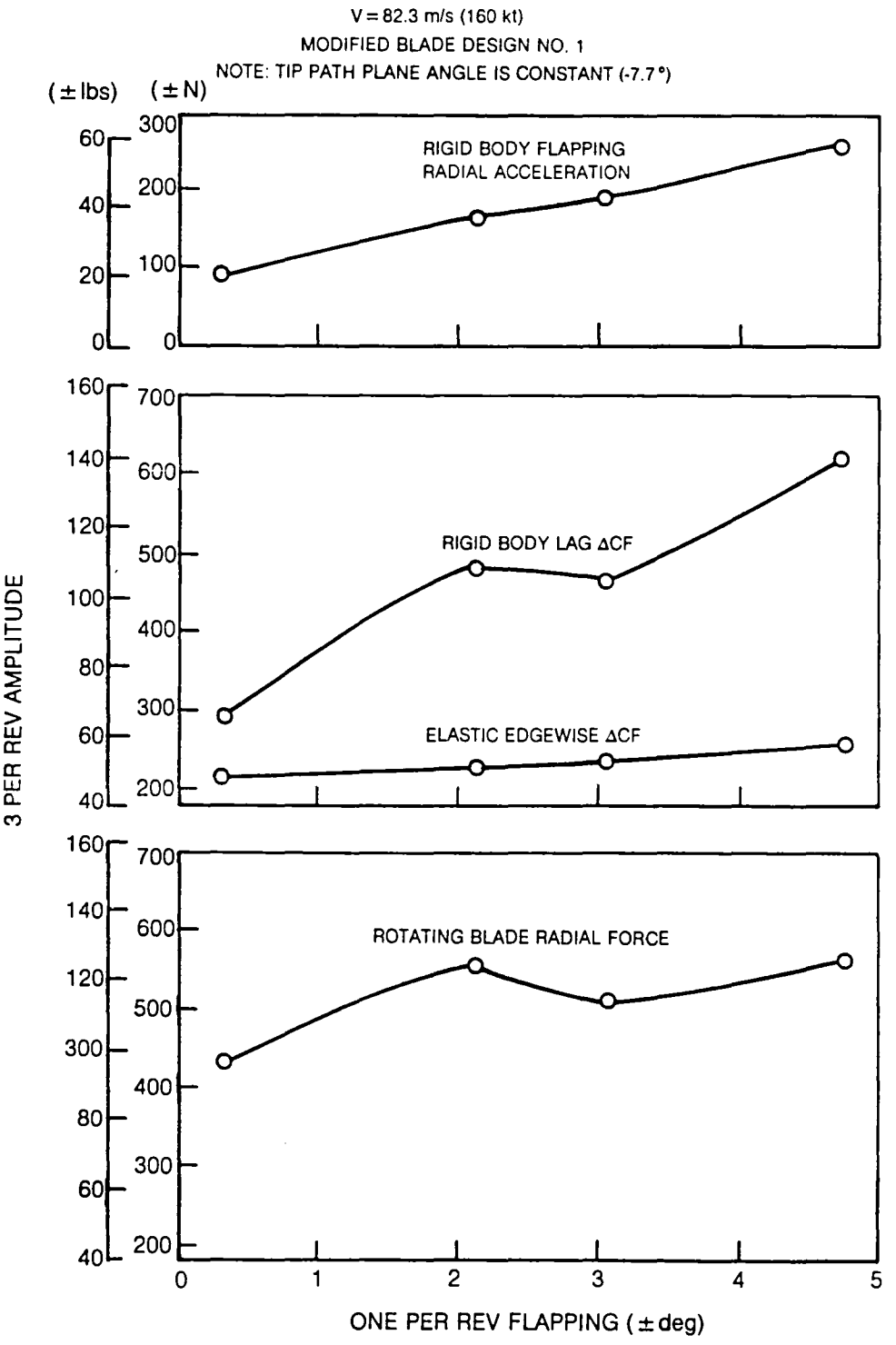

Figure 35. Predicted Effect of Blade Flapping on 3 Per Rev Radial Force for the High Speed Flight Condition

83-6-38-5

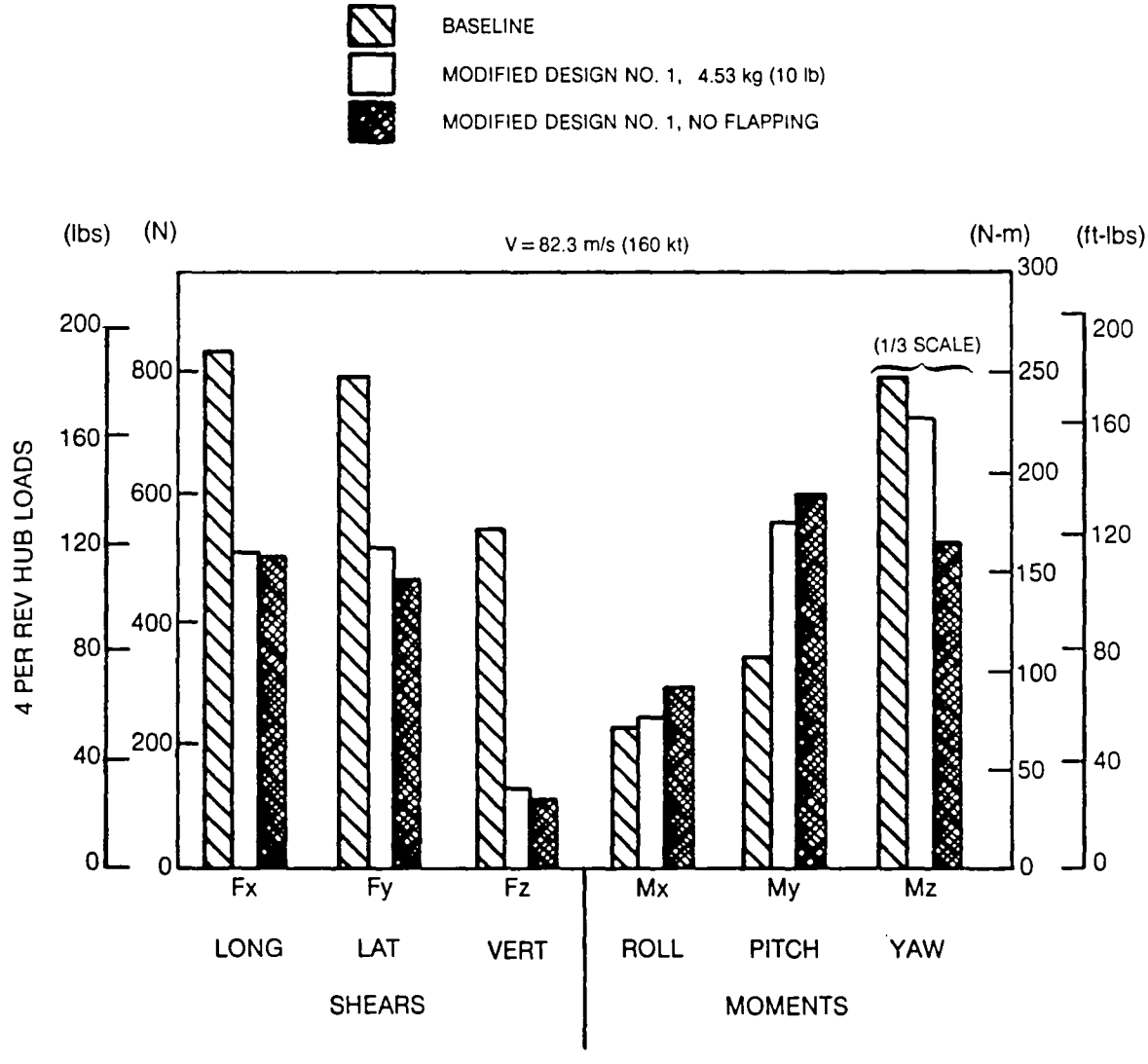

Figure 36. Comparison of Predicted Baseline and Modified Blade Vibratory Fixed System Hub Loads for the High Speed Flight Condition

83-6-38-4

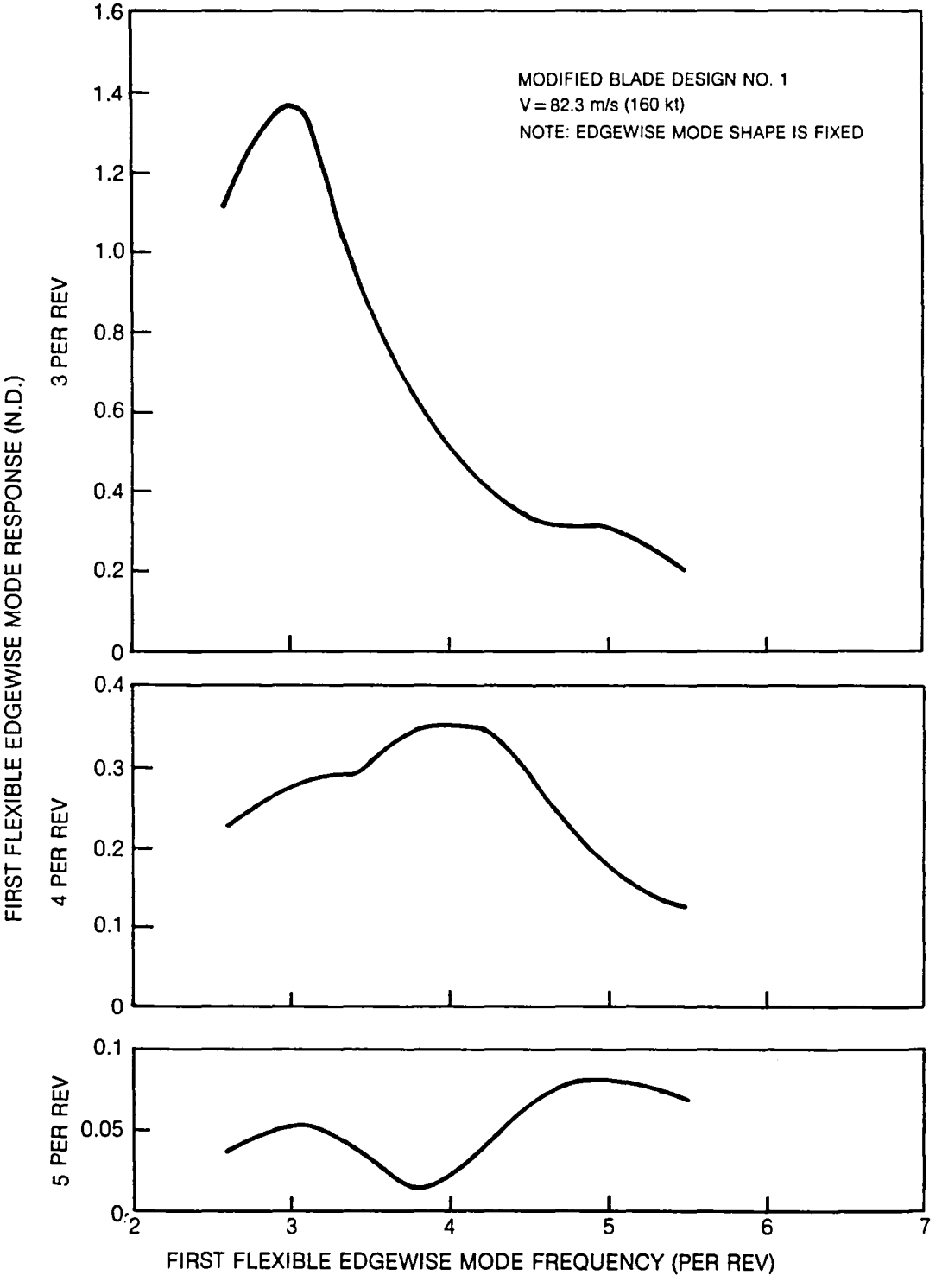

Figure 37. Predicted Effect of Edgewise Frequency on Vibratory Edgewise Mode Response for the High Speed Flight Condition

82-11-15-25

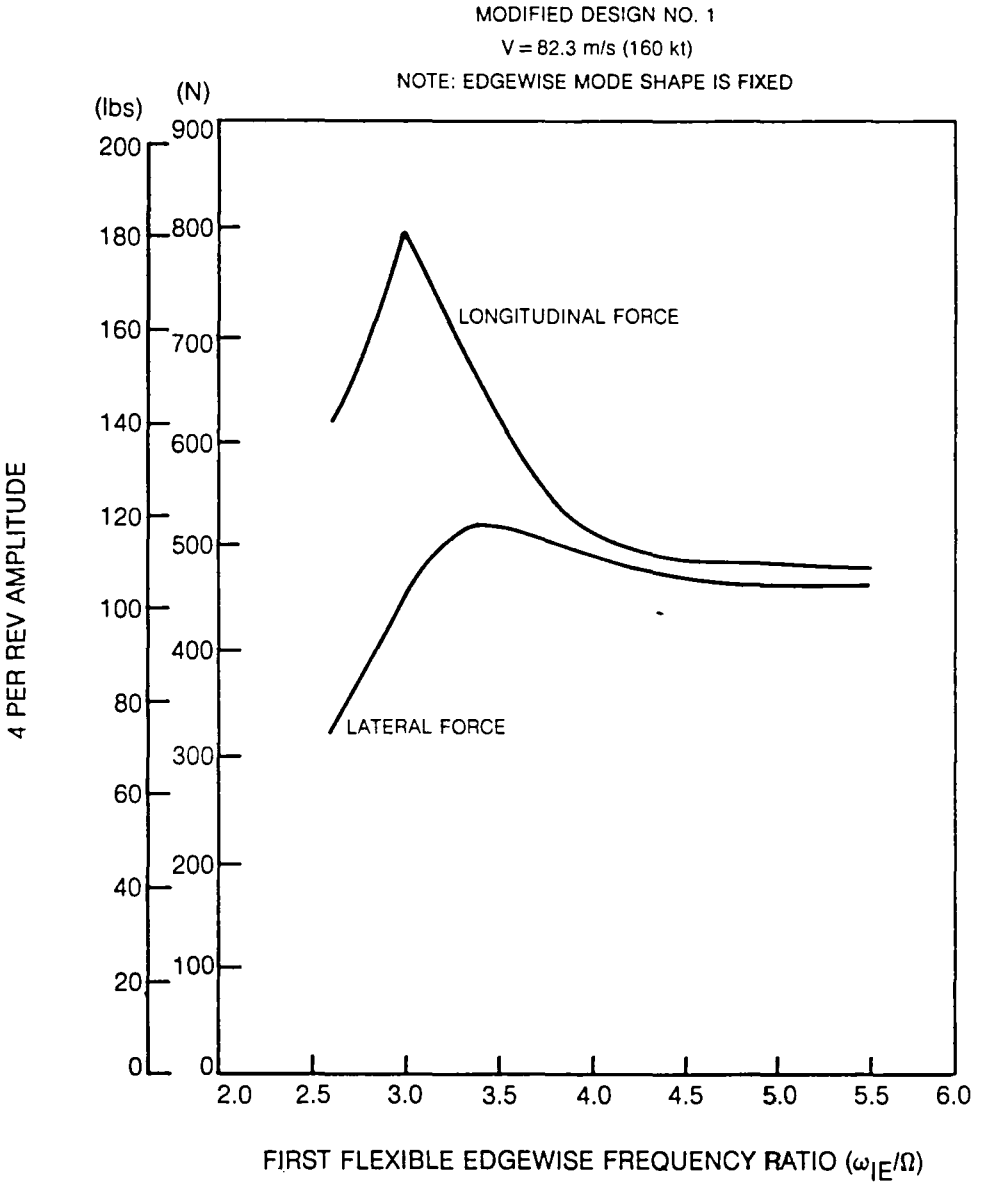

Figure 38. Predicted Effect of Edgewise Frequency on 4 Per Rev Fixed System Hub Inplane Forces for the High Speed Flight Condition

83-6-38-22

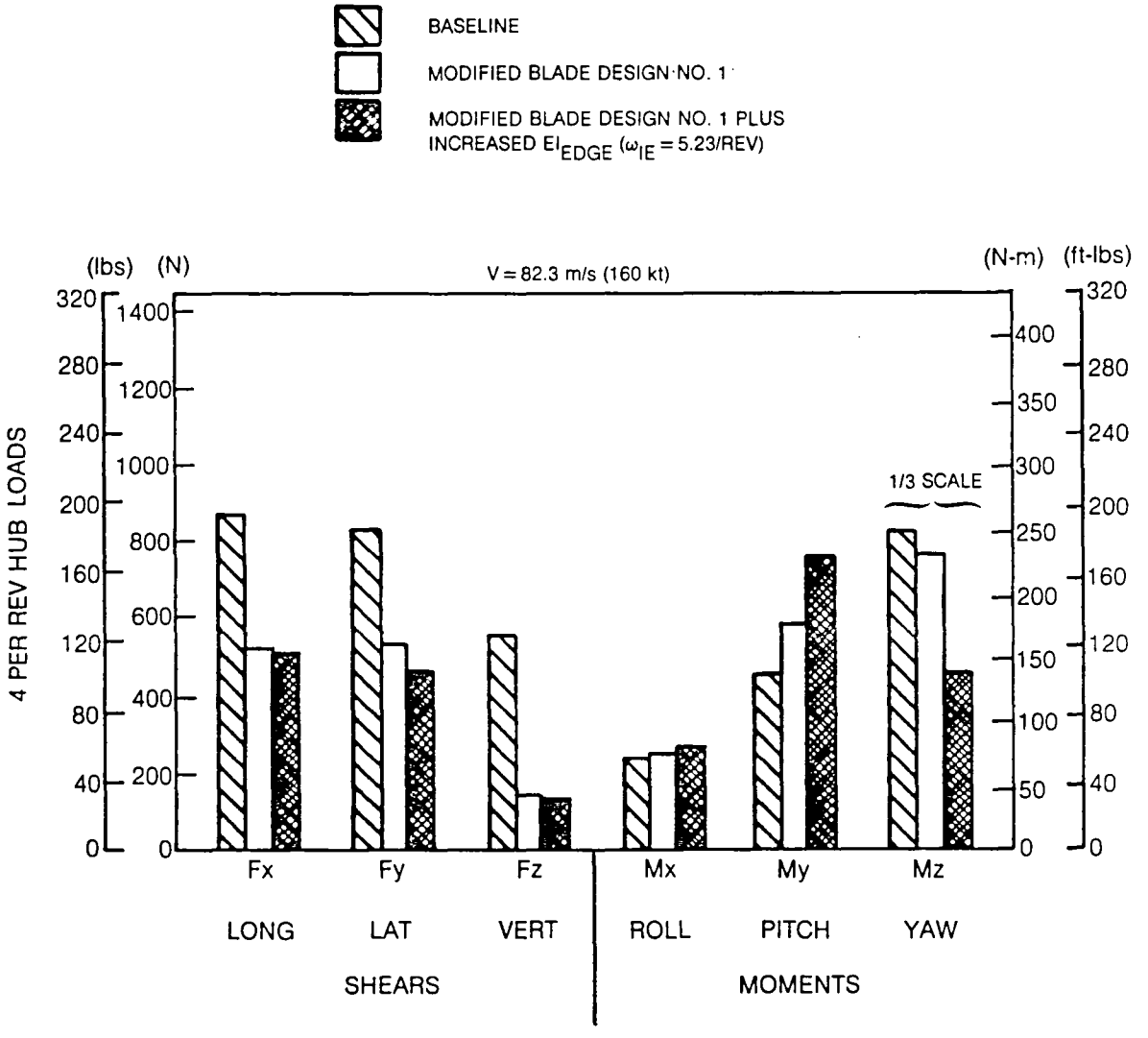

Figure 39. Comparison of Predicted Baseline and Modified Blade Vibratory Fixed System Hub Loads for the High Speed Flight Condition

82-11-12-2

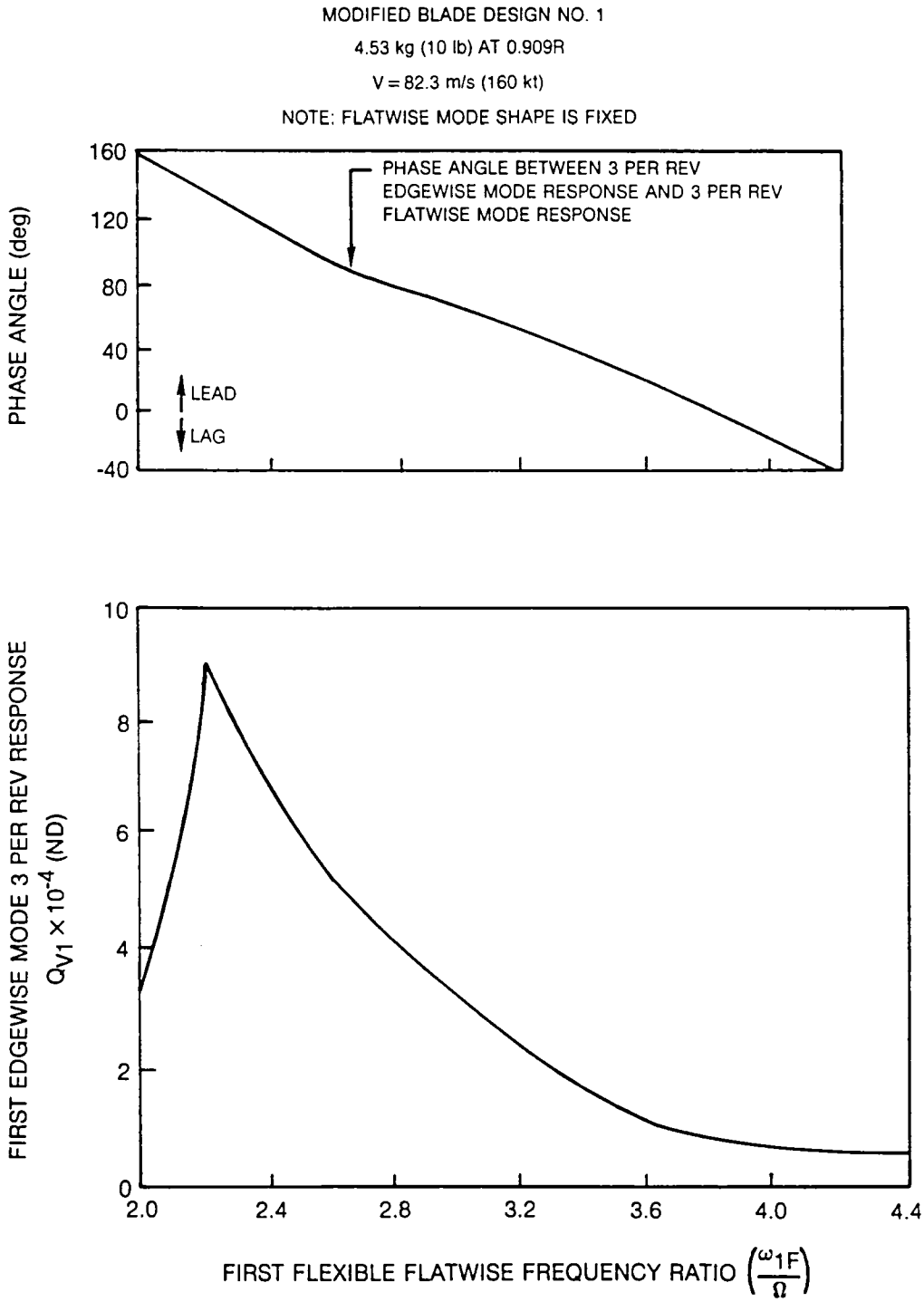

Figure 40. Predicted Effect of Flatwise Frequency on 3 Per Rev Response of First Flexible Edgewise Mode for the High Speed Flight Condition

82-11-15-29

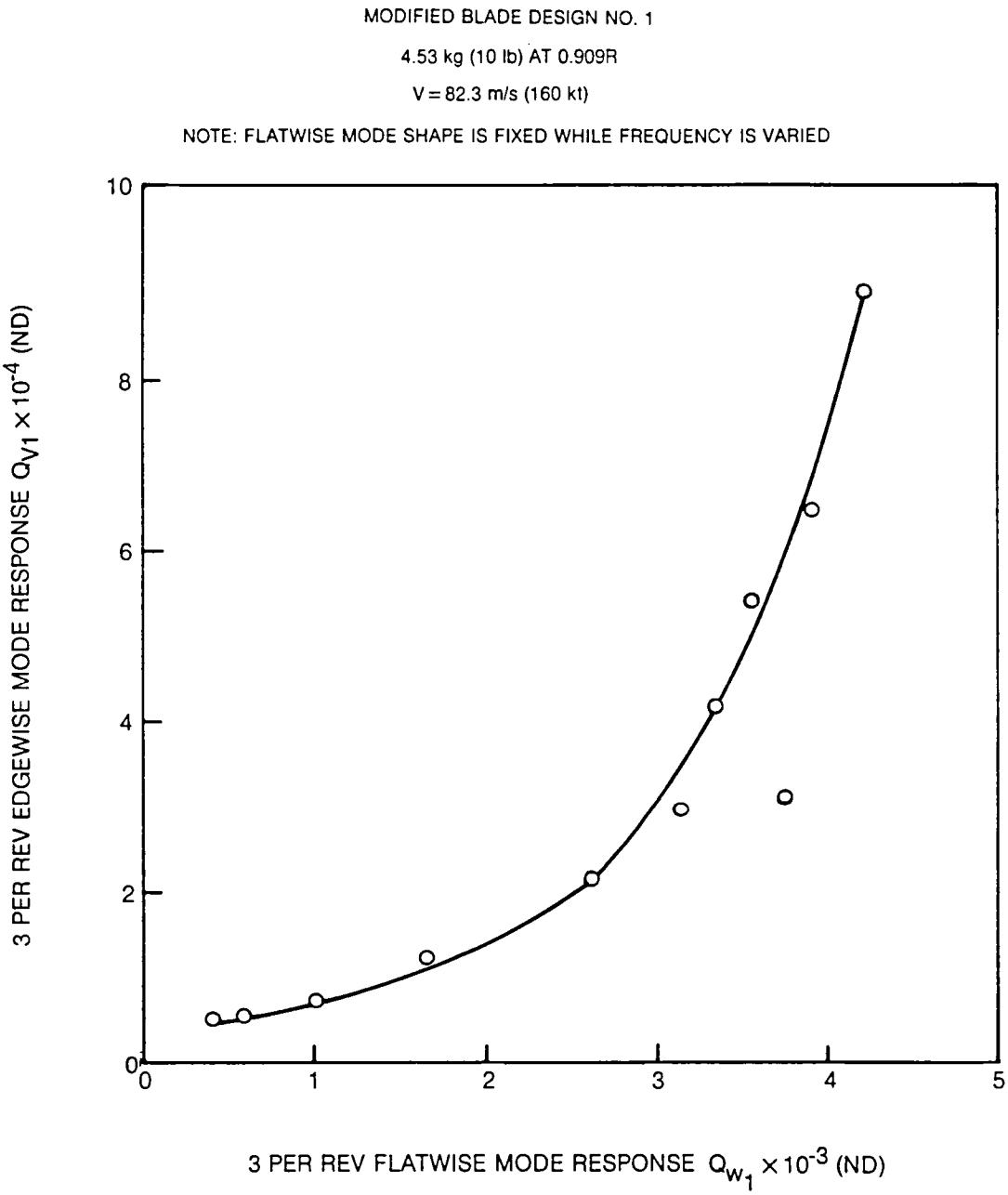

Figure 41. Predicted Relationship Between Flatwise and Edgewise Mode Response for the High Speed Flight Condition

82-11-15-28

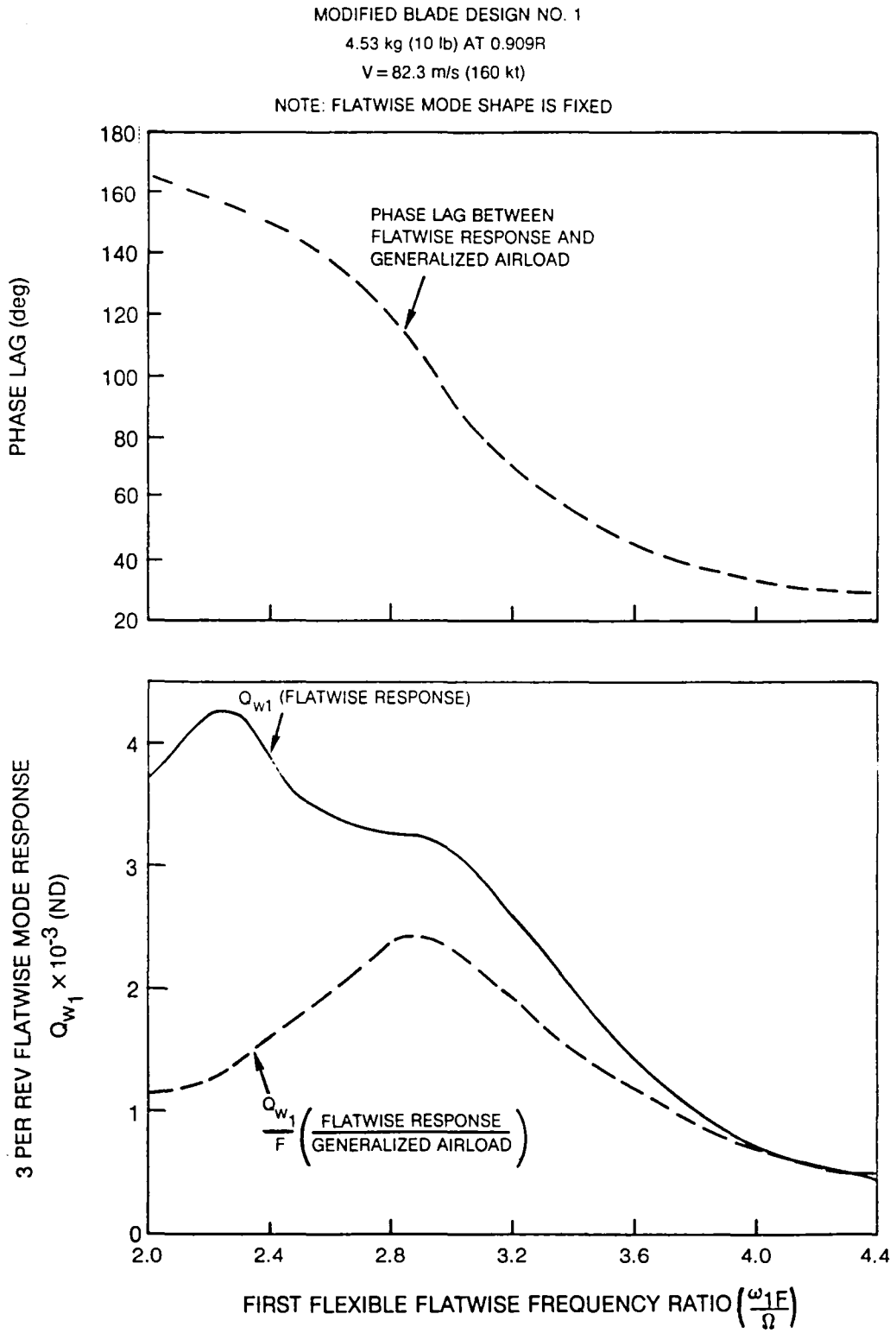

Figure 42. Predicted Effect of Flatwise Frequency on 3 Per Rev Response of First Flexible Flatwise Mode for the High Speed Flight Condition

82–11–15–30

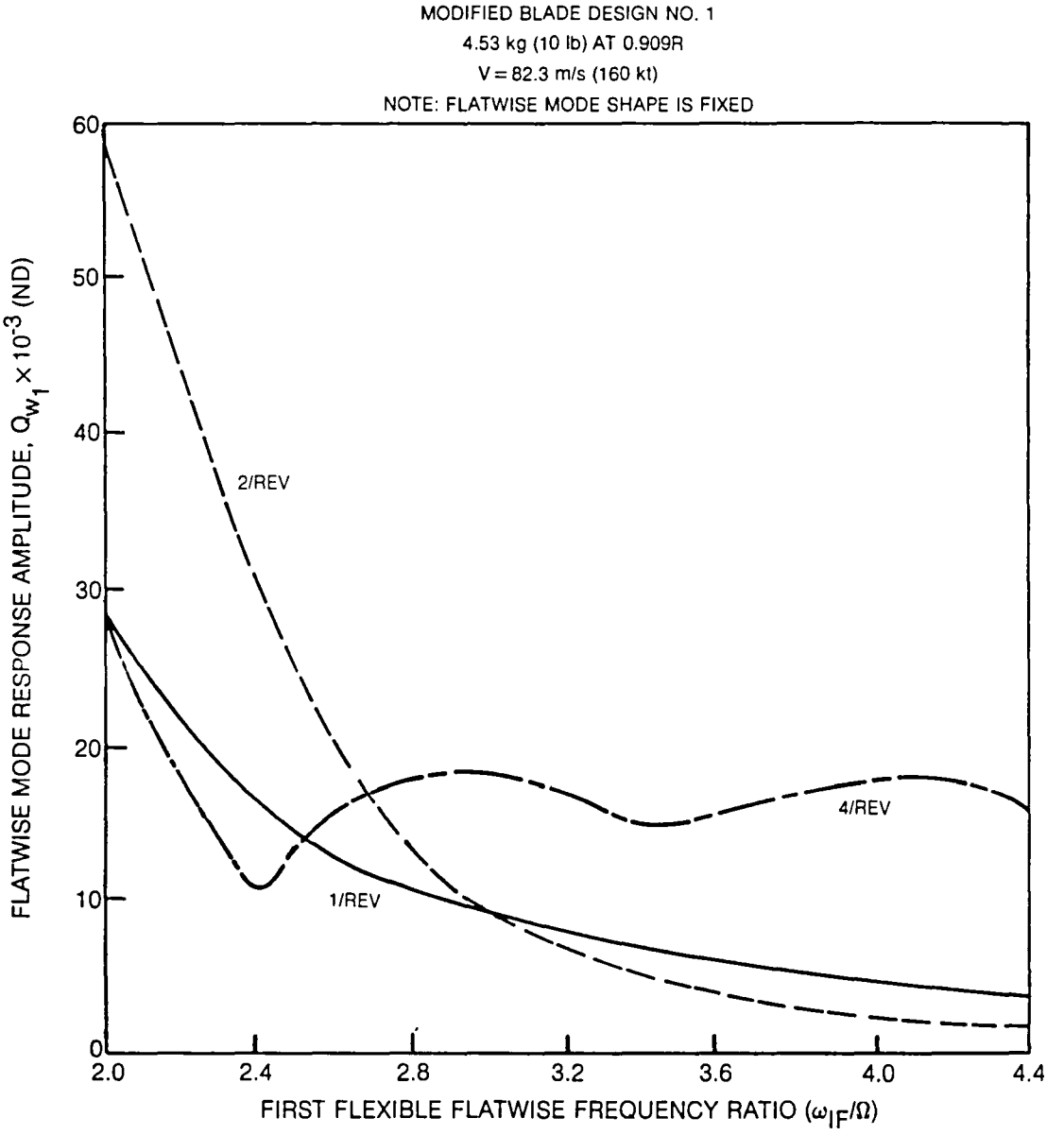

Figure 43. Predicted Effect of Flatwise Frequency on 1, 2 and 4 Per Rev Response of First Flexible Flatwise Mode for the High Speed Flight Condition

83-6-38-14

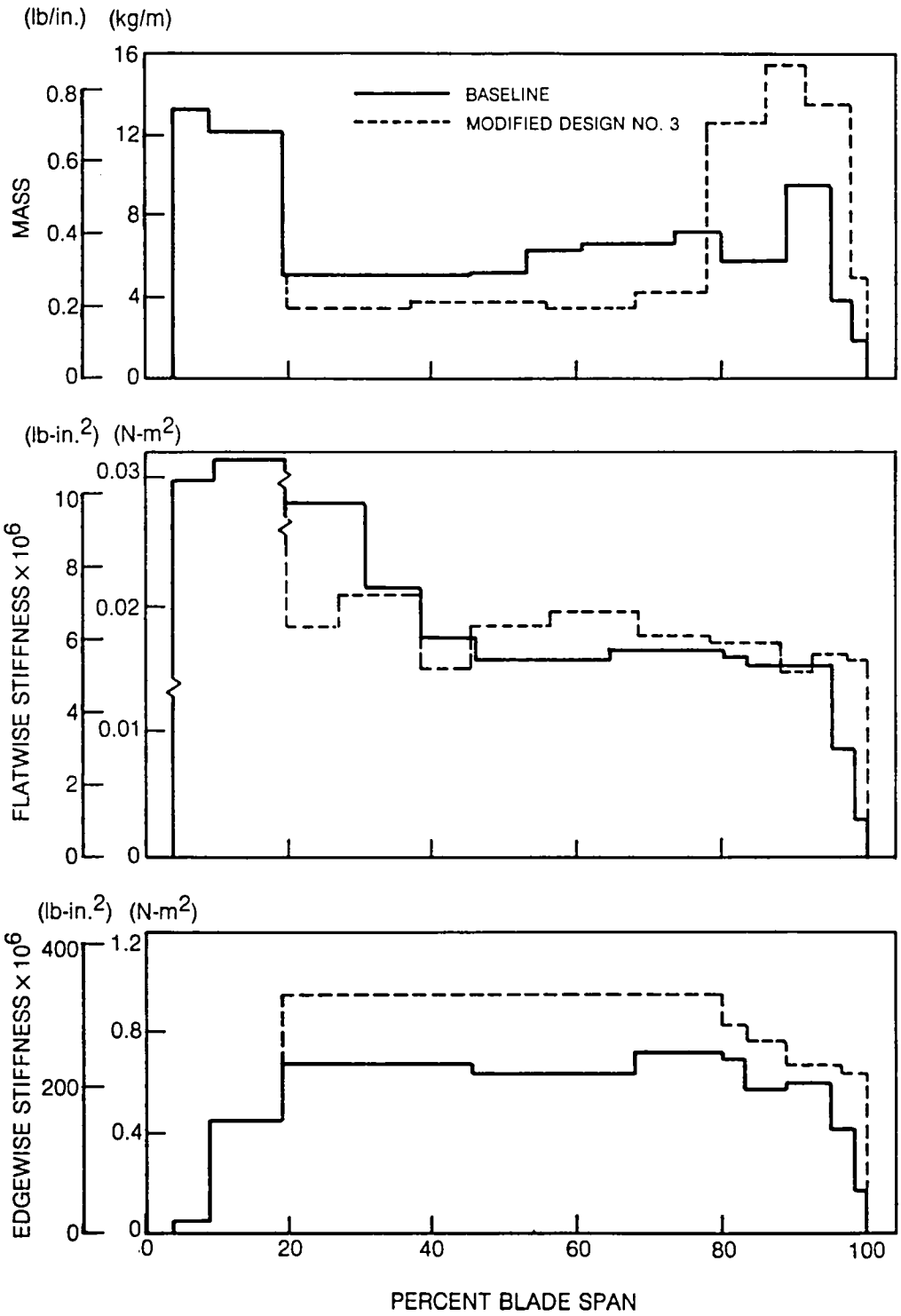

Figure 44. Spanwise Mass and Elastic Bending Stiffness for Modified Design No. 3

83-6-38-26

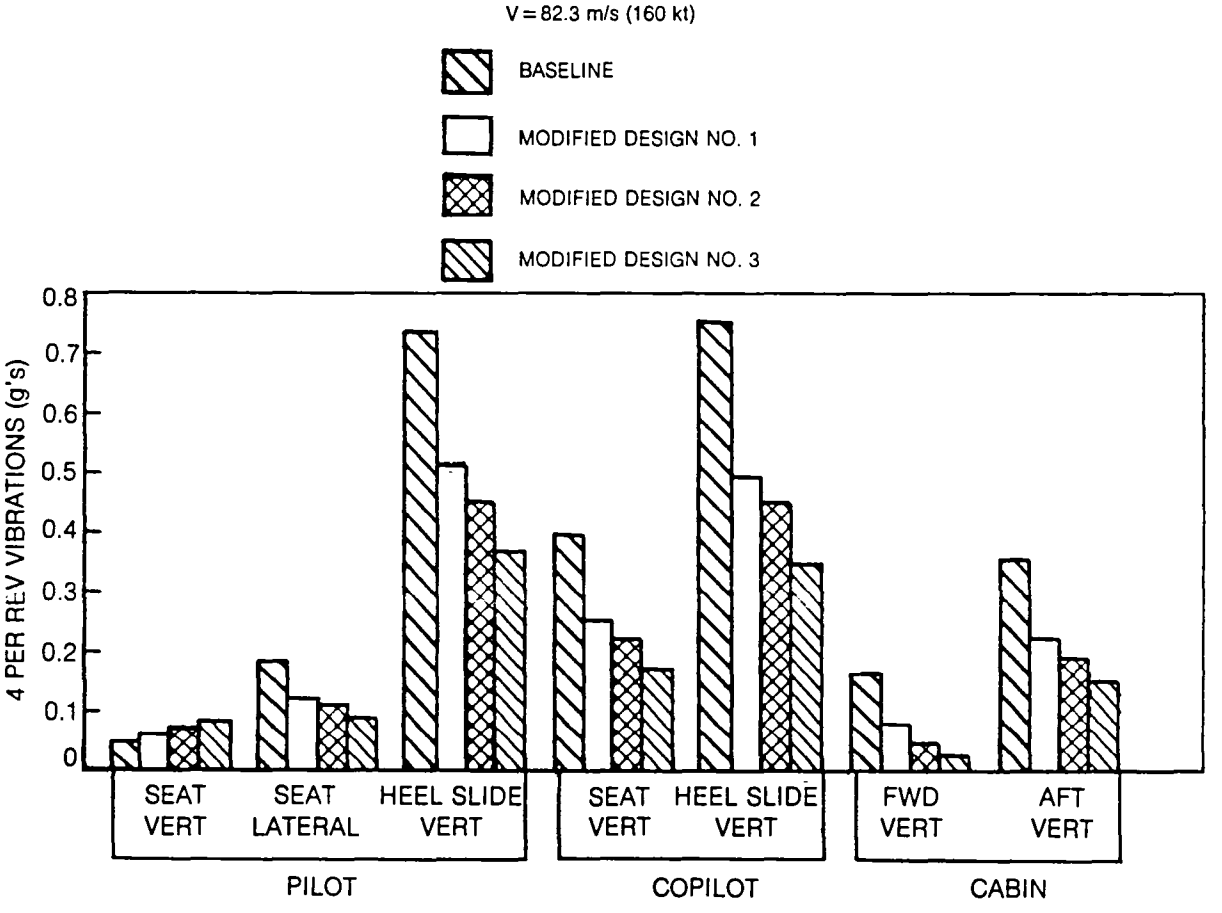

Figure 45. Predicted 4 Per Rev Fuselage Vibrations for the Modified Blade Designs at the High Speed Flight Condition

83-6-38-32

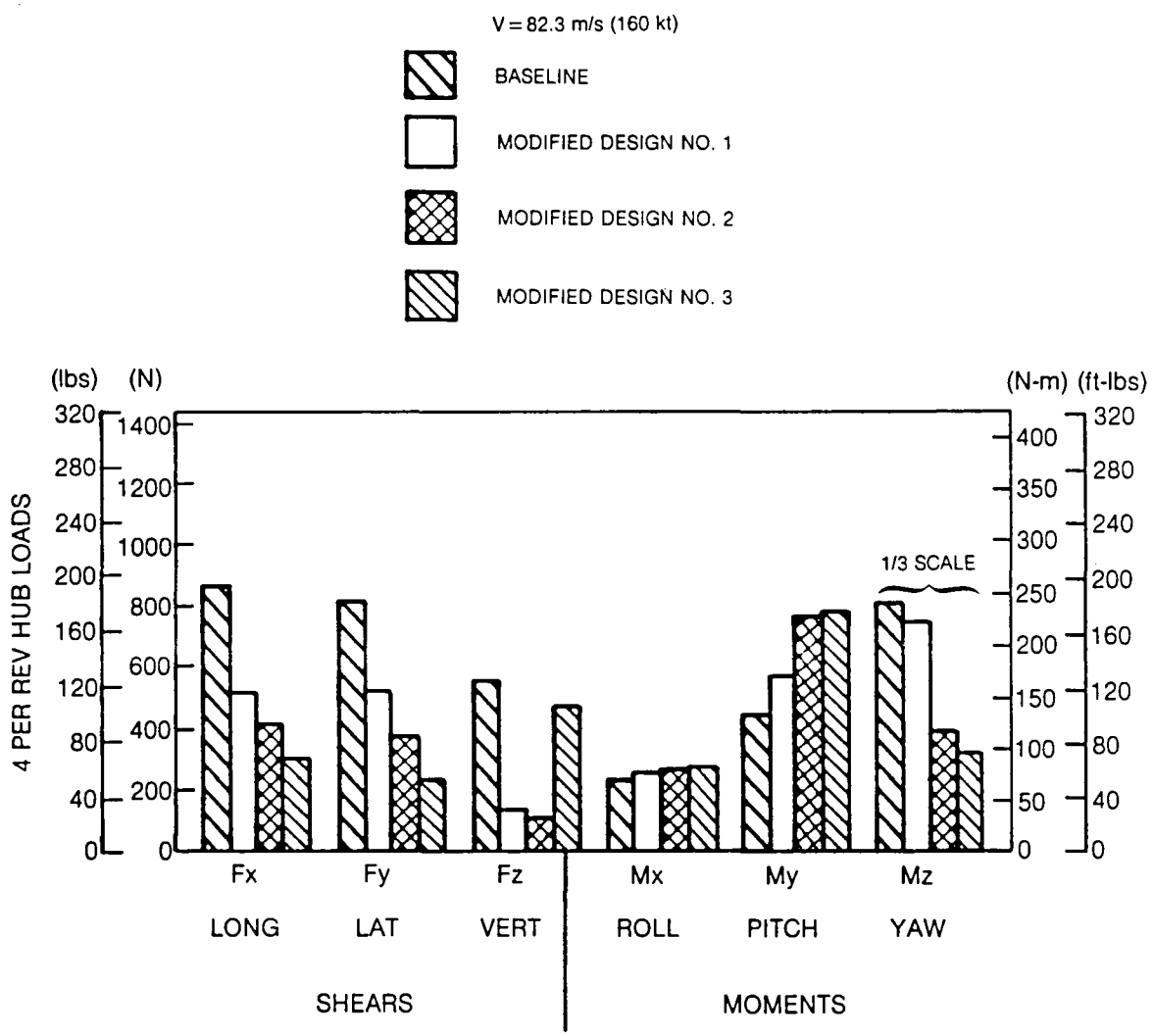

Figure 46. Comparison of Predicted Baseline and Modified Blade Vibratory Fixed System Hub Loads for the High Speed Flight Condition

82-12-99-1

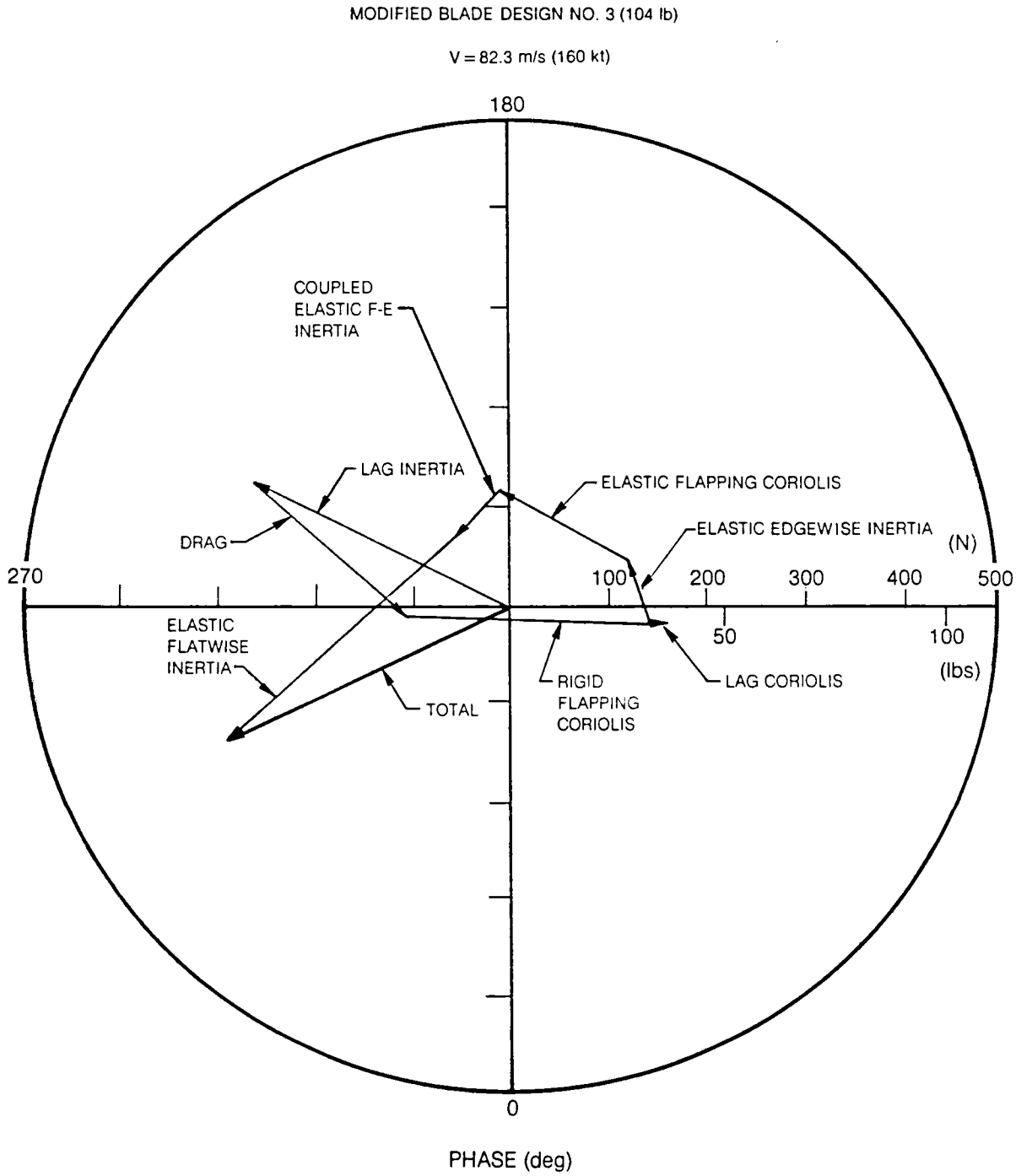

Figure 47. Predicted 3 Per Rev Rotating Blade Lateral Shear for Modified Blade Design No. 3 at the High Speed Flight Condition

82-11-15-46

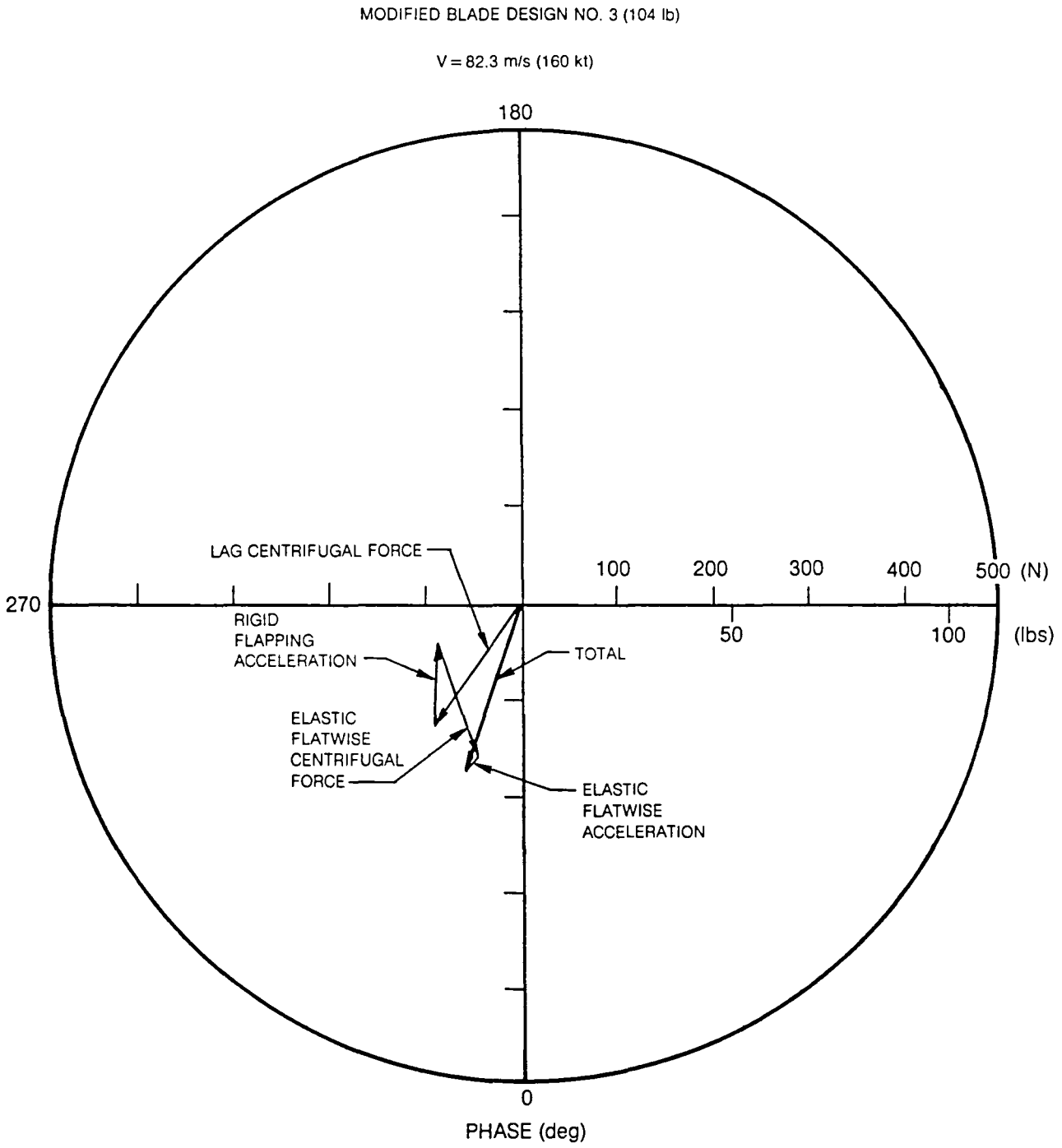

Figure 48. Predicted 3 Per Rev Rotating Blade Radial Shear for Modified Blade Design No. 3 at the High Speed Flight Condition

82-11-15-47

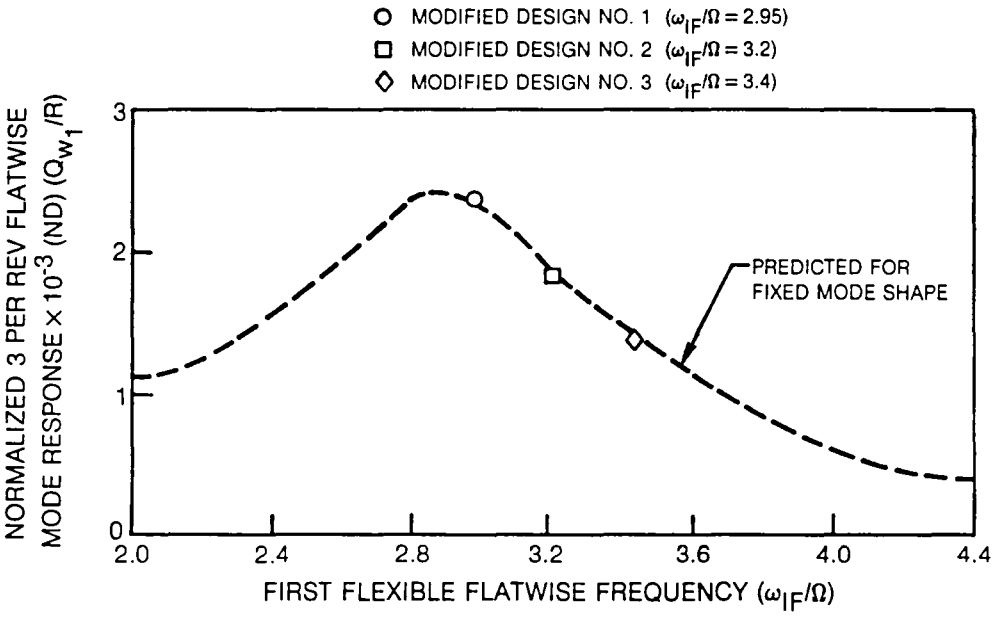

Figure 49. Predicted 3 Per Rev Normalized Flatwise Mode Response for the High Speed Flight Condition

83-6-38-15

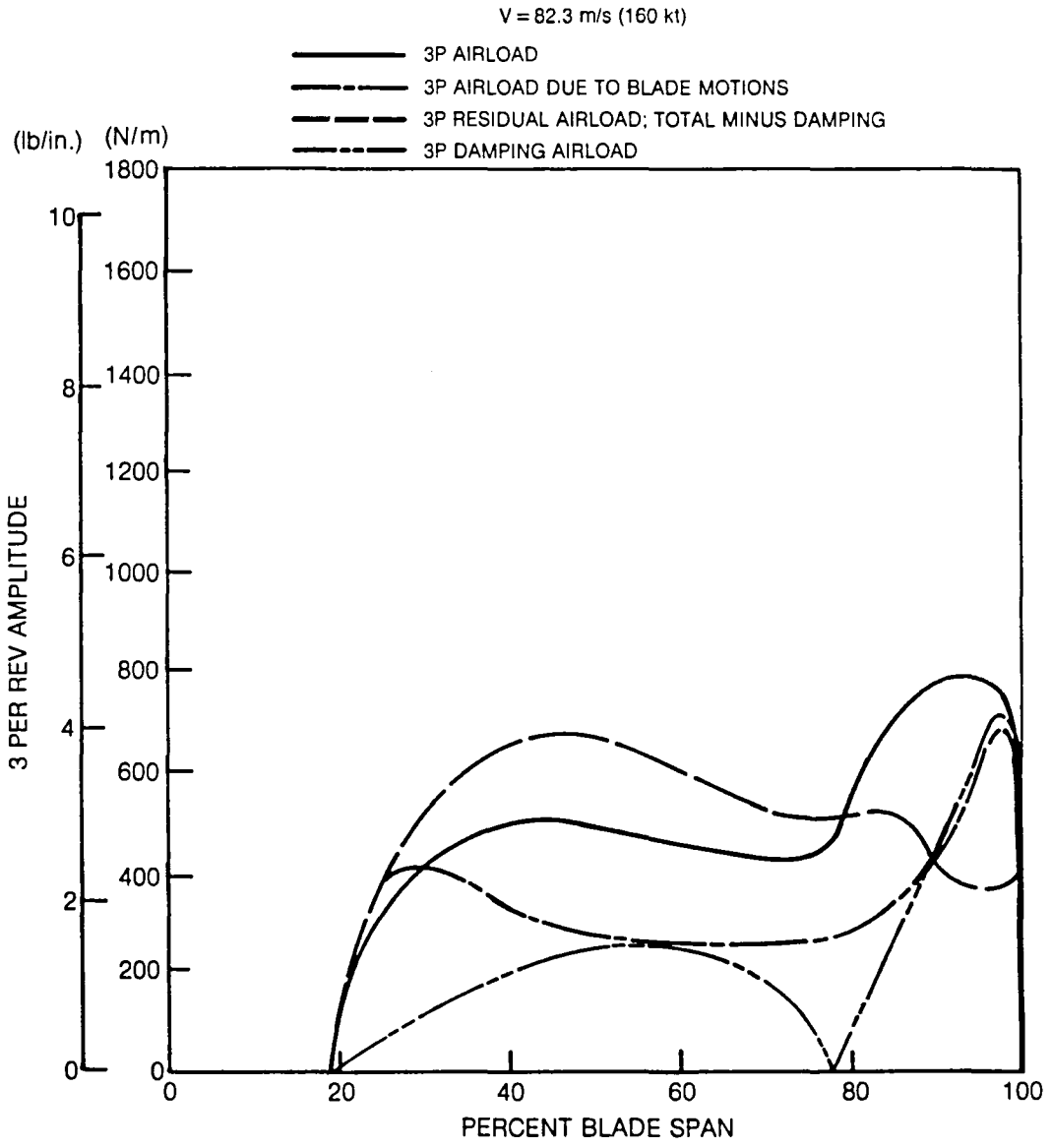

Figure 50. Predicted Amplitude of 3 Per Rev Lift Airload for the Baseline Blade at the High Speed Flight Condition

83-6-38-27

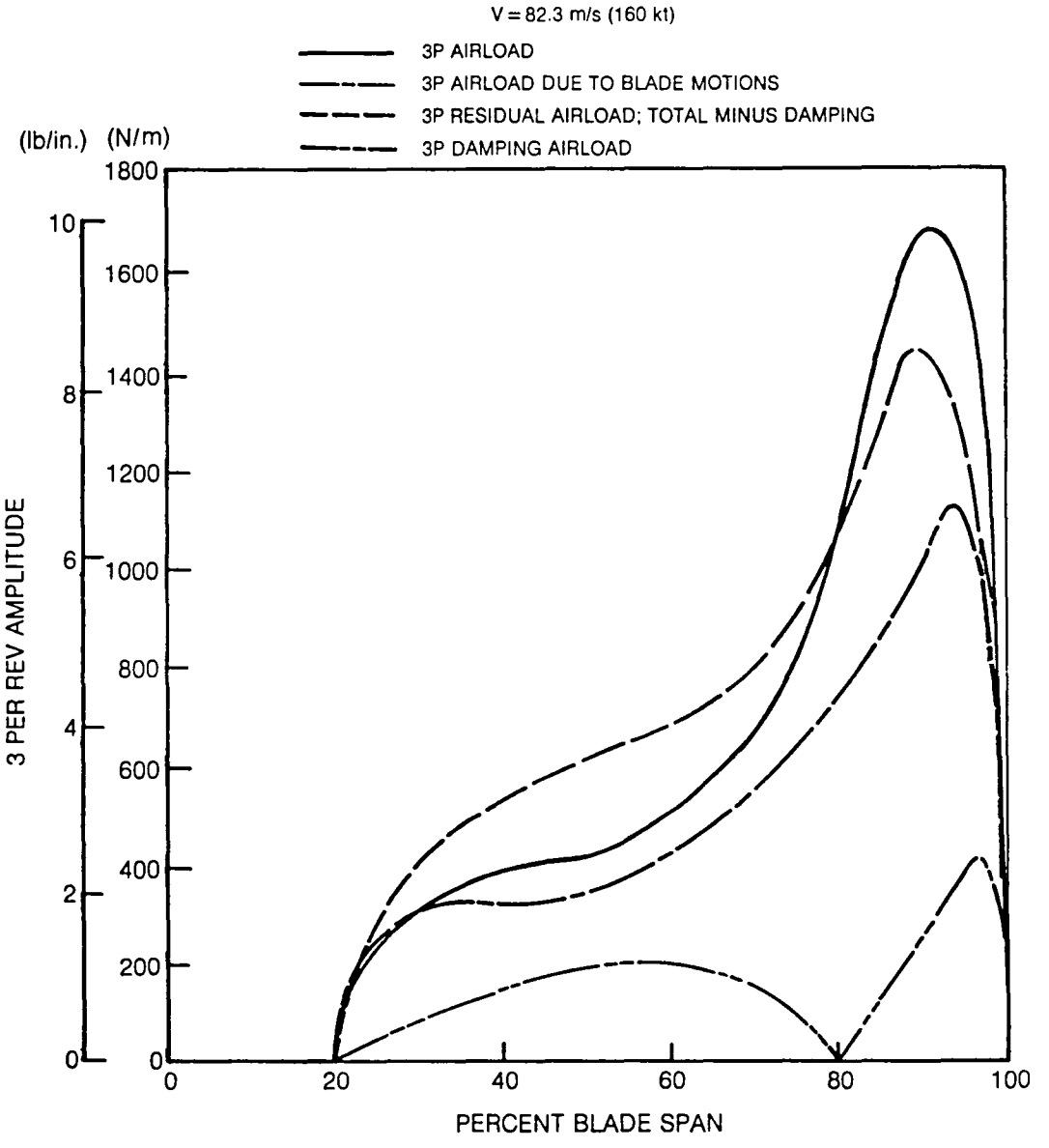

Figure 51. Predicted Amplitude of 3 Per Rev Lift Airload for Modified Design No. 1 at the High Speed Flight Condition

83-6-38-28

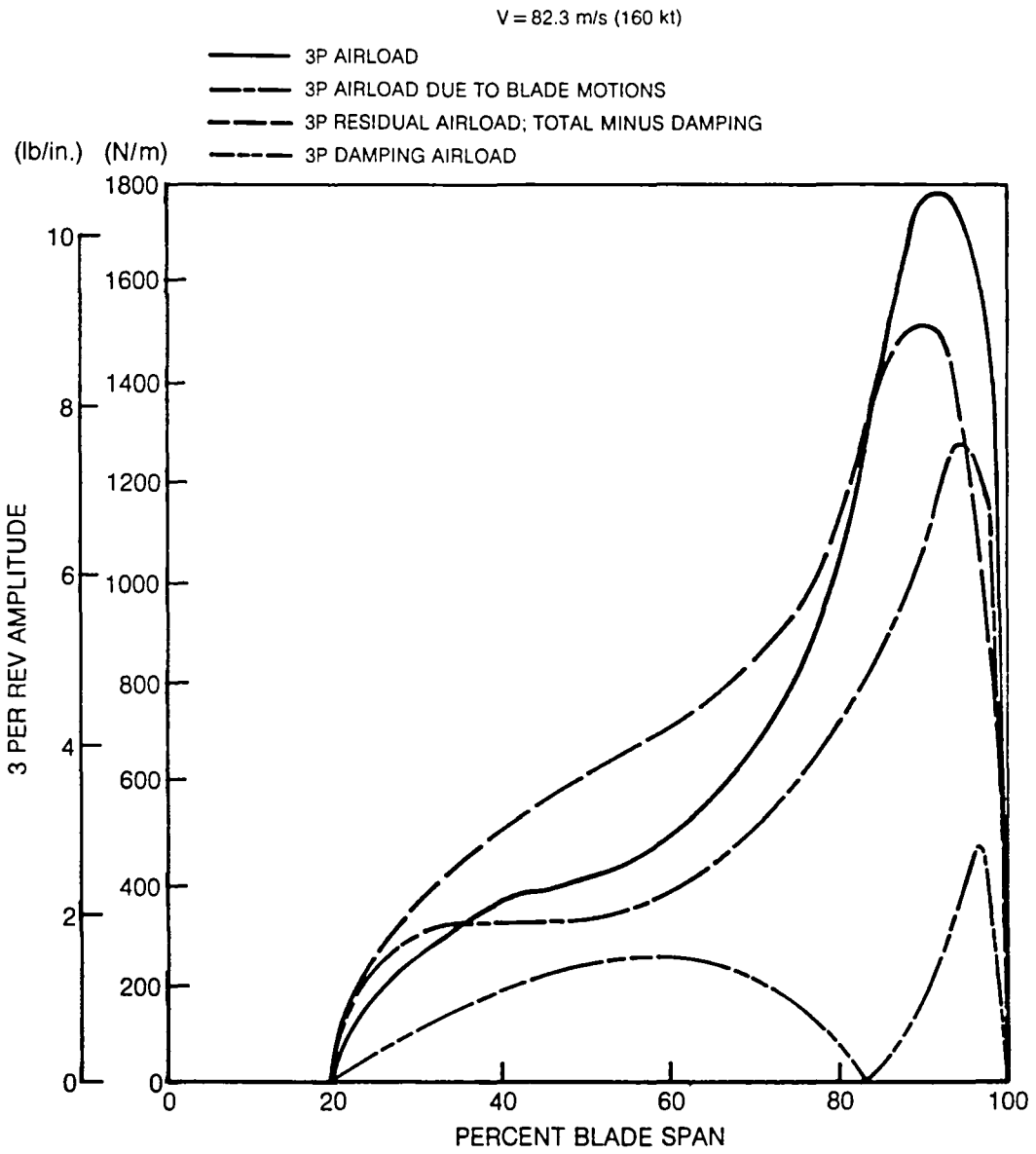

Figure 52. Predicted Amplitude of 3 Per Rev Lift Airload for Modified Design No. 3 at the High Speed Flight Condition

83-6-38-29

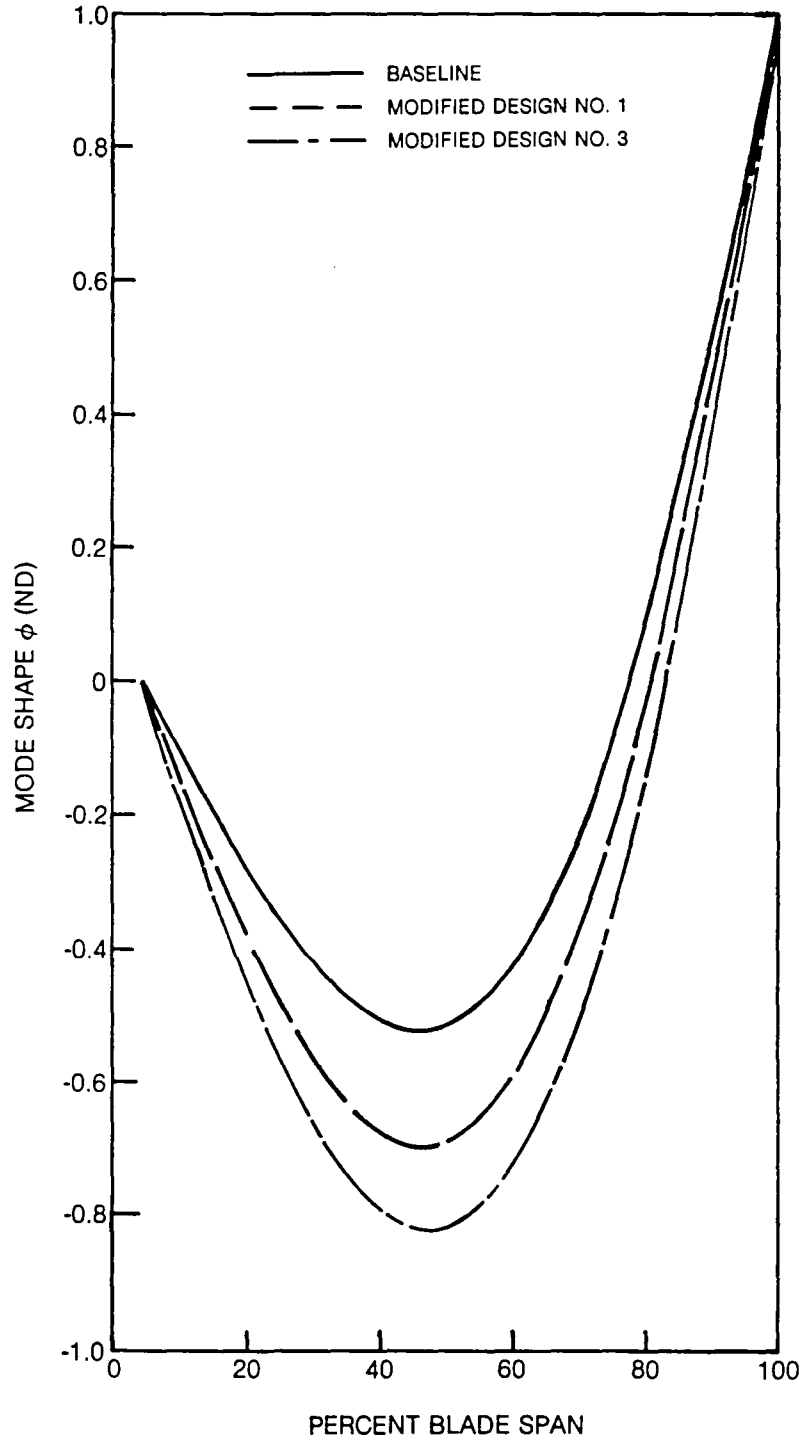

Figure 53. Predicted Mode Shapes for the First Elastic Flatwise Mode

83-6-38-16

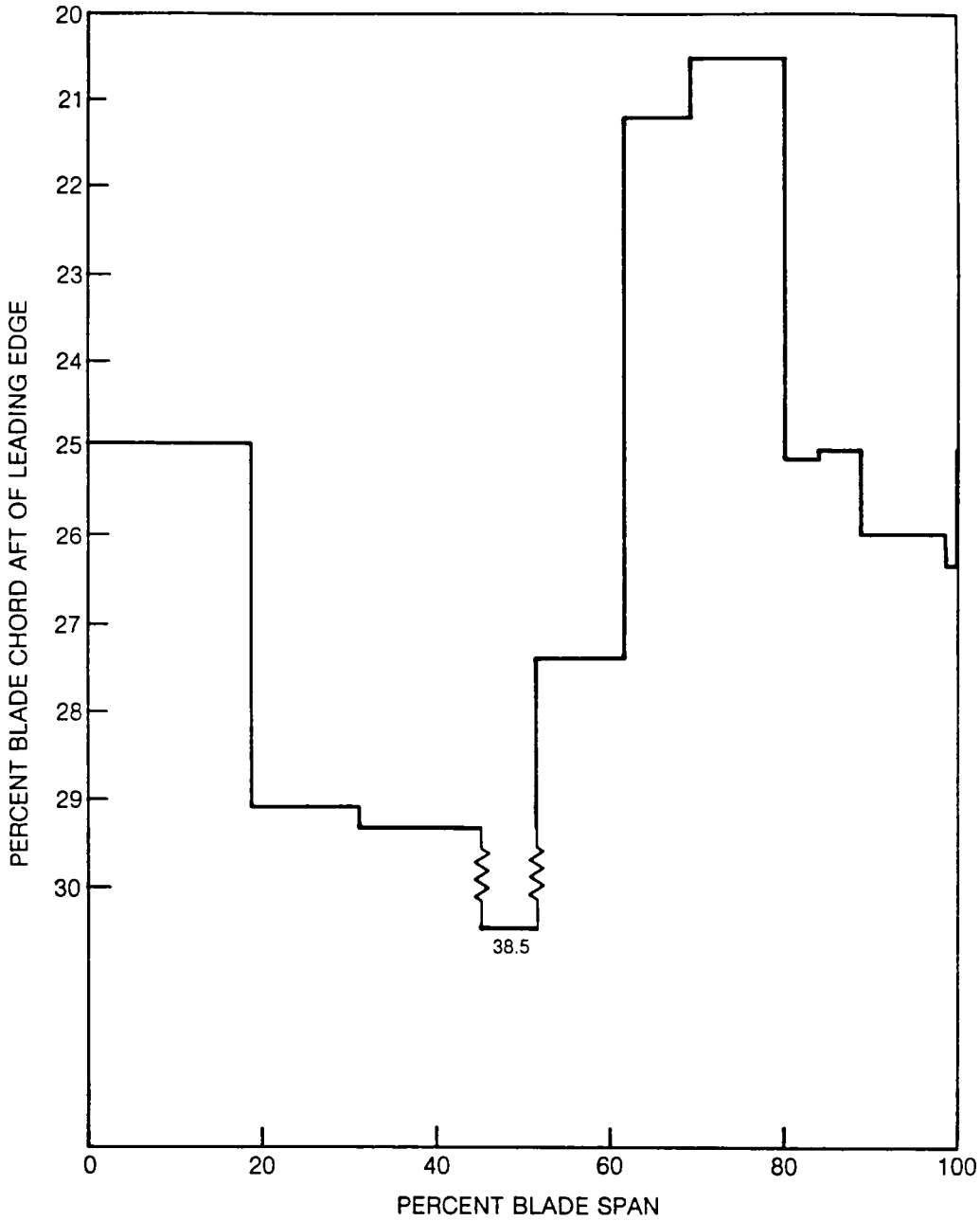

Figure 54. Chordwise CG Location for Modified Blade Design No. 3

83-6-38-18

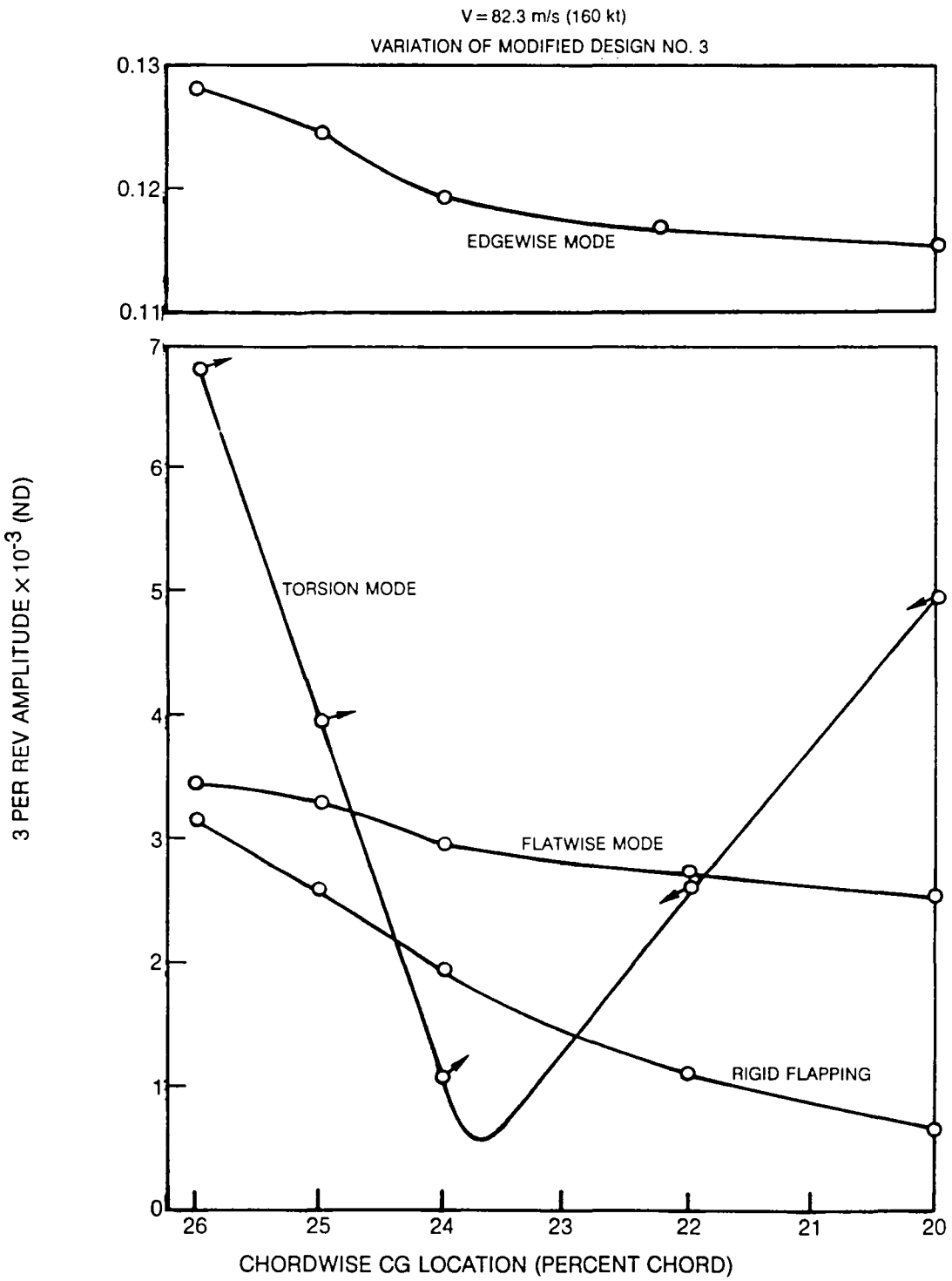

Figure 55. Predicted Effect of Outboard Blade CG Location on 3 Per Rev Modal Response for the High Speed Flight Condition

83-6-38-17

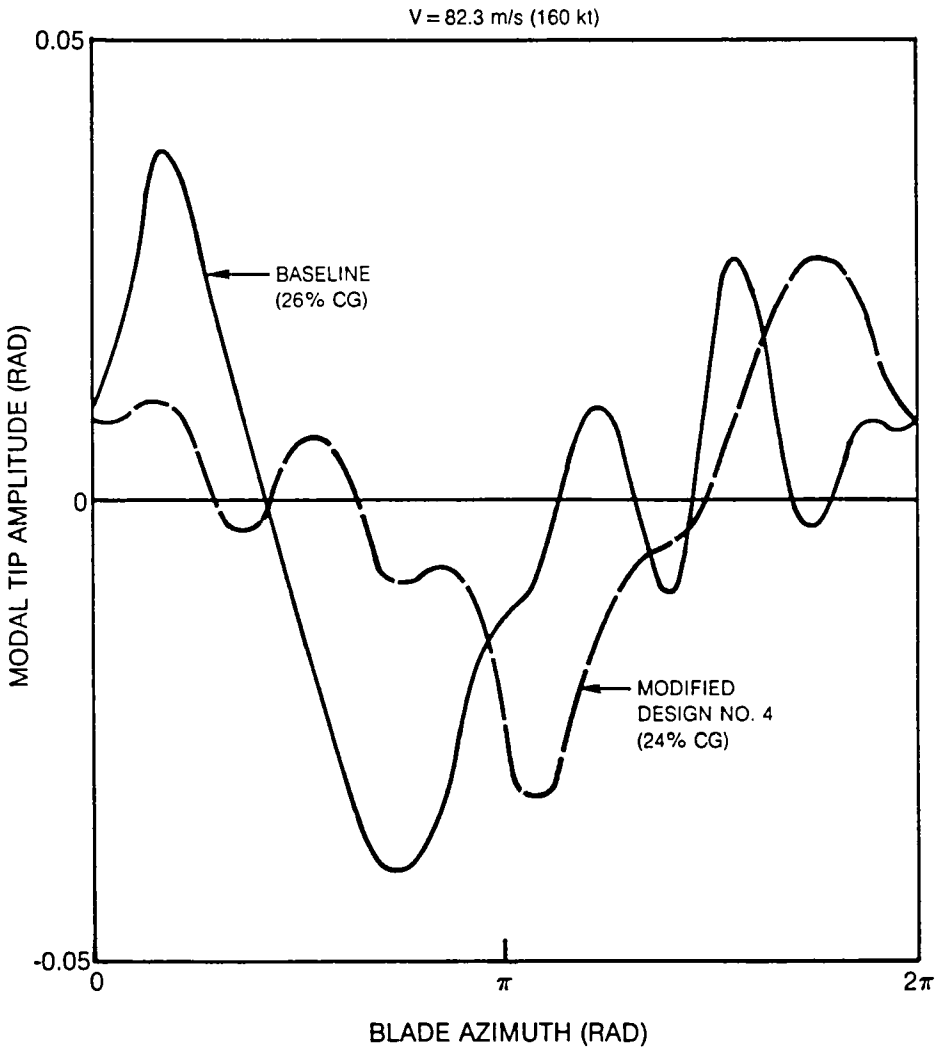

Figure 56. Predicted Blade Torsion Mode Response for the High Speed Flight Condition

83-6-38-19

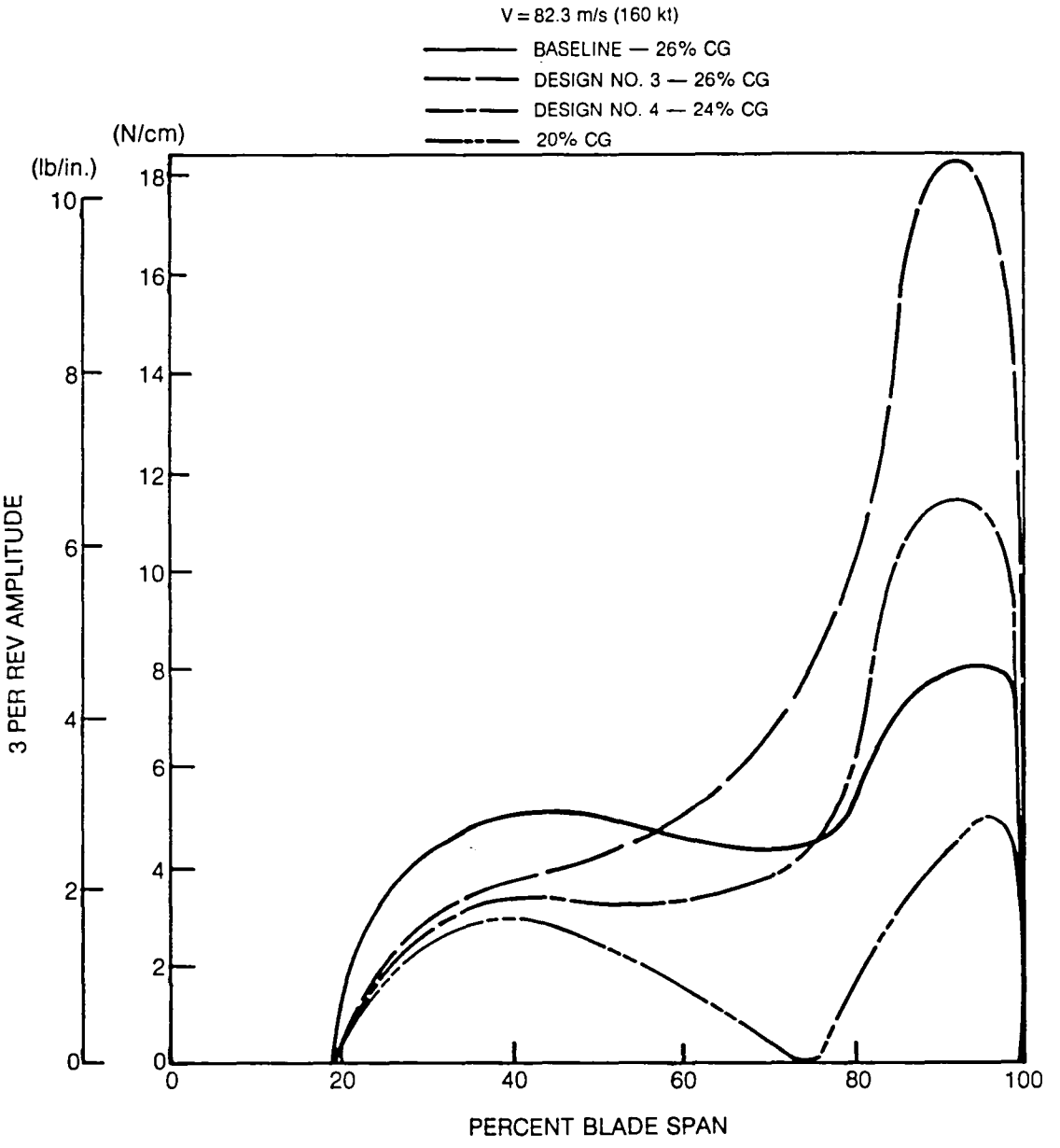

Figure 57. Predicted Amplitude of 3 Per Rev Lift Airload at the High Speed Flight Condition

83-6-38-20

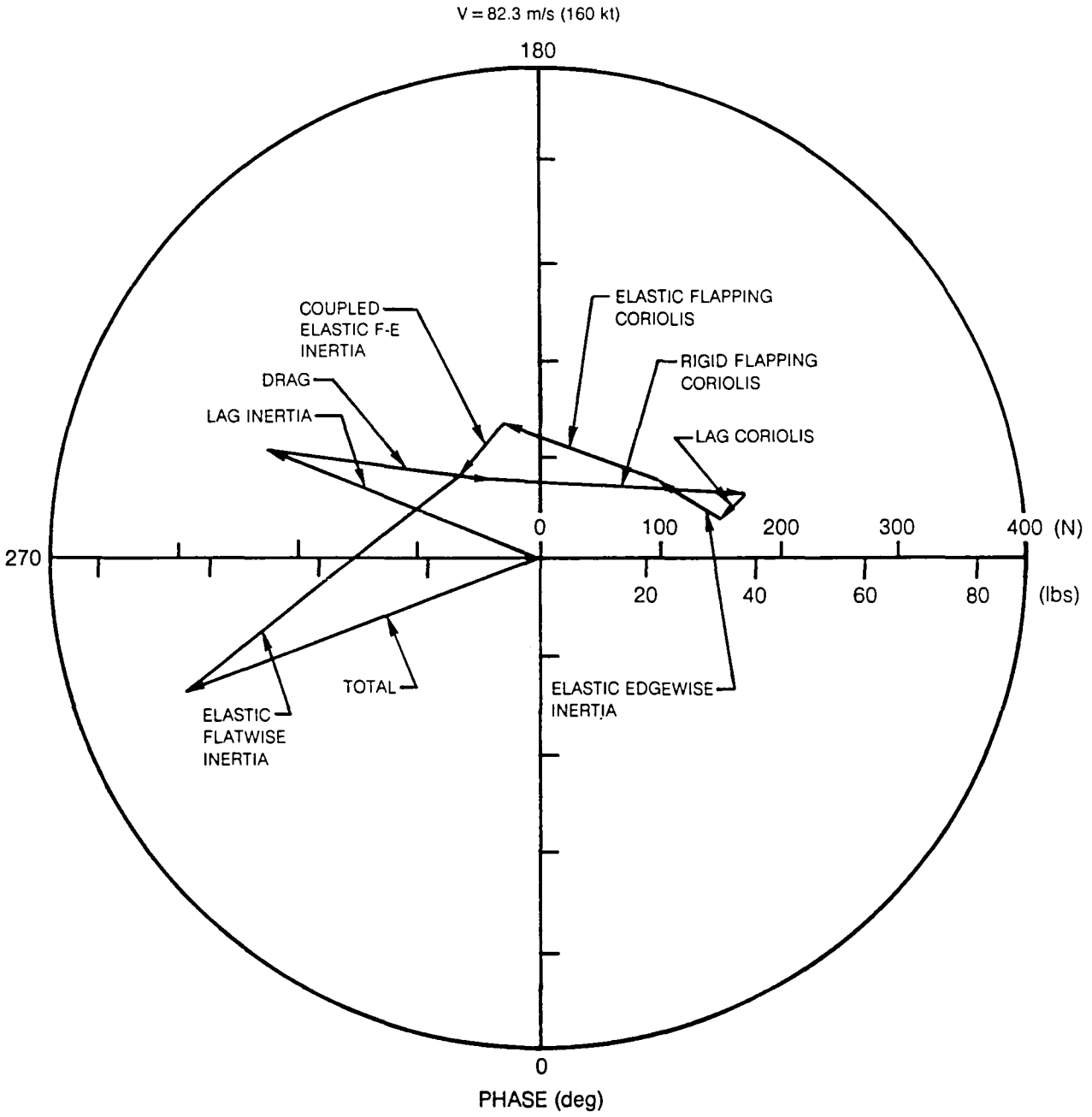

Figure 58. Predicted 3 Per Rev Rotating Blade Lateral Shear for Modified Blade Design No. 4 at the High Speed Flight Condition

83-6-38-12

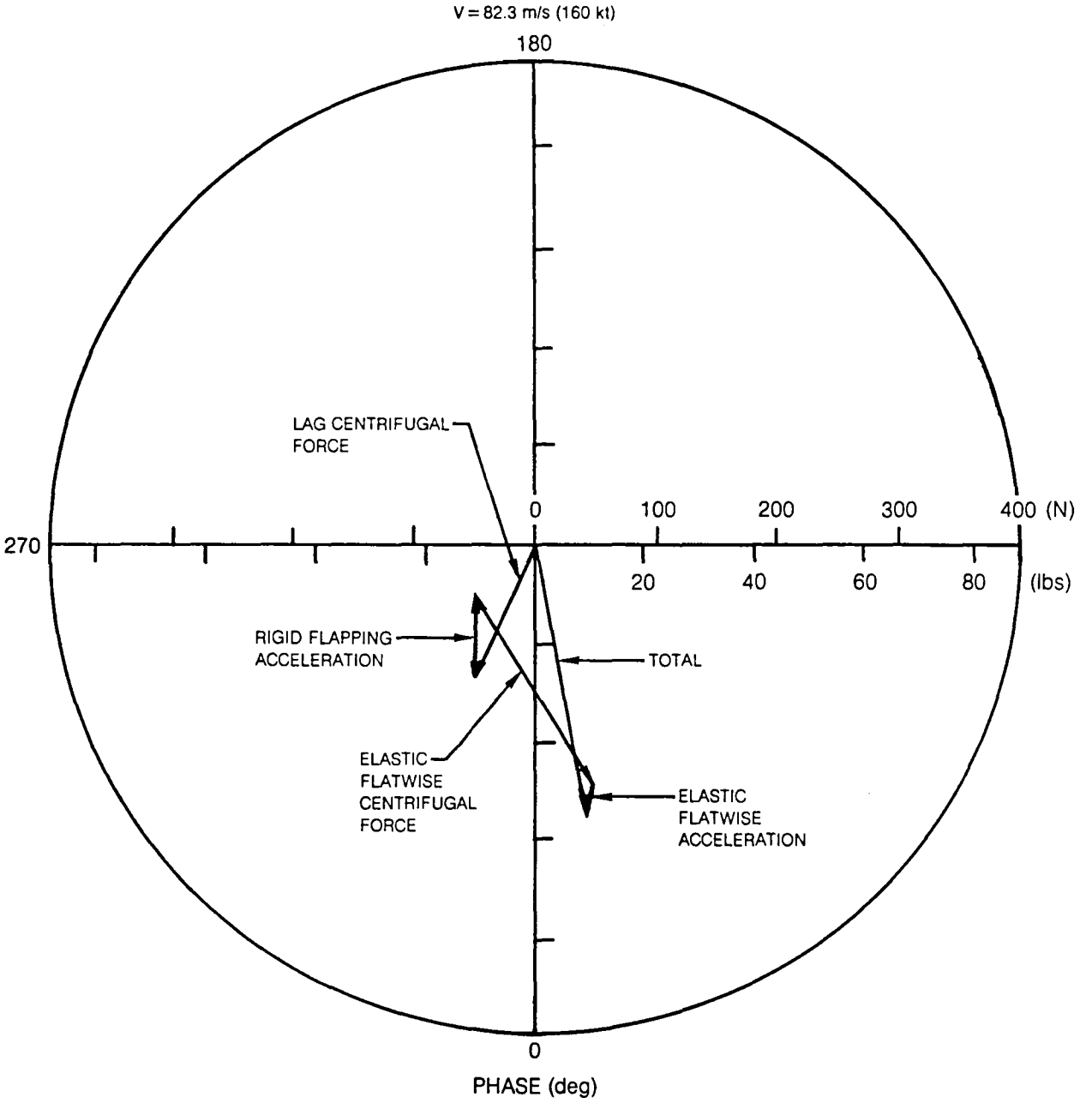

Figure 59. Predicted 3 Per Rev Rotating Blade Radial Shear for Modified Blade Design No. 4 at the High Speed Flight Condition

83-6-38-13

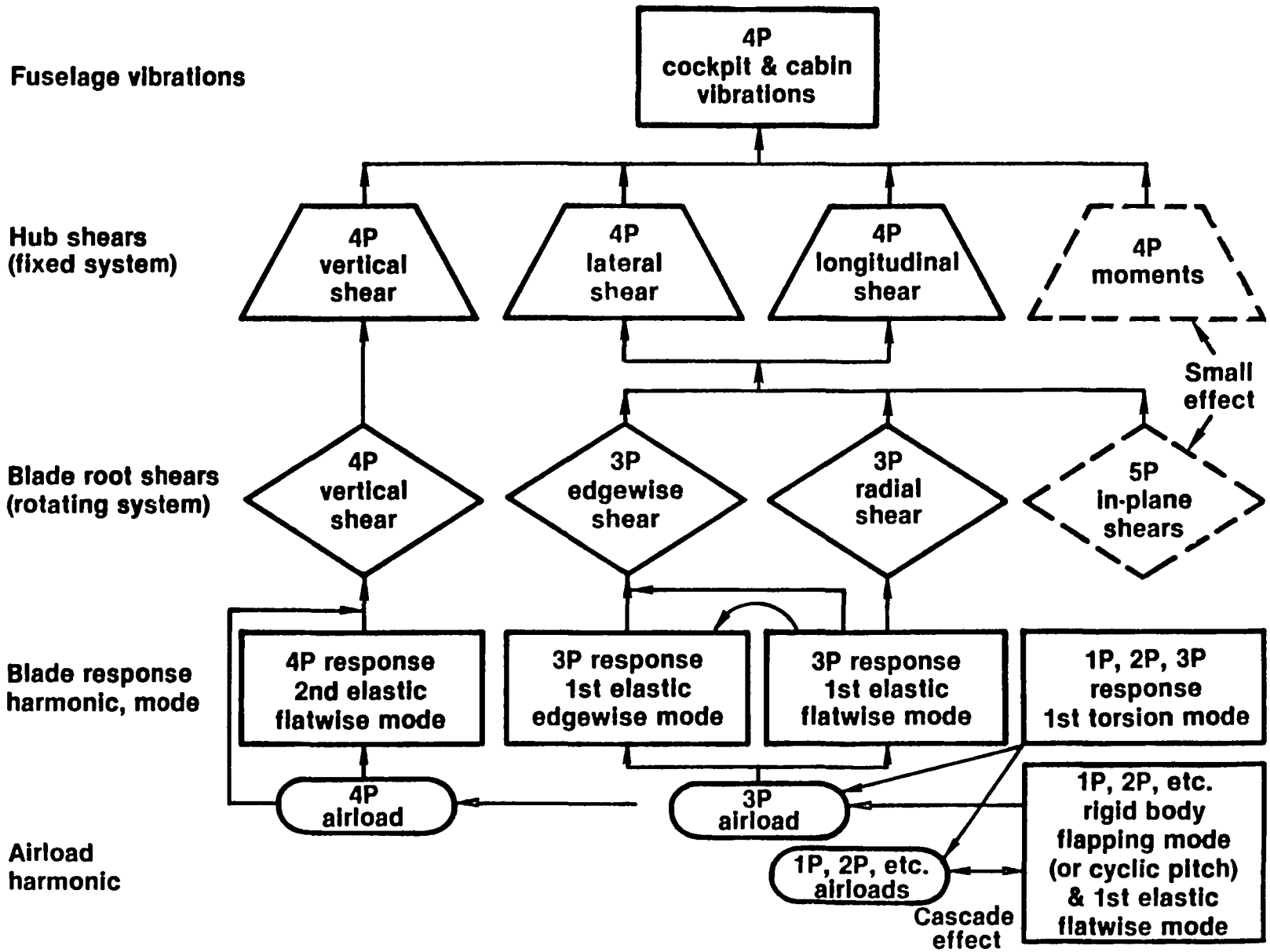

Figure 60. Primary Contributors to Helicopter Vibrations (4-Bladed Articulated Rotor, High Speed Flight)

83-11-24-1

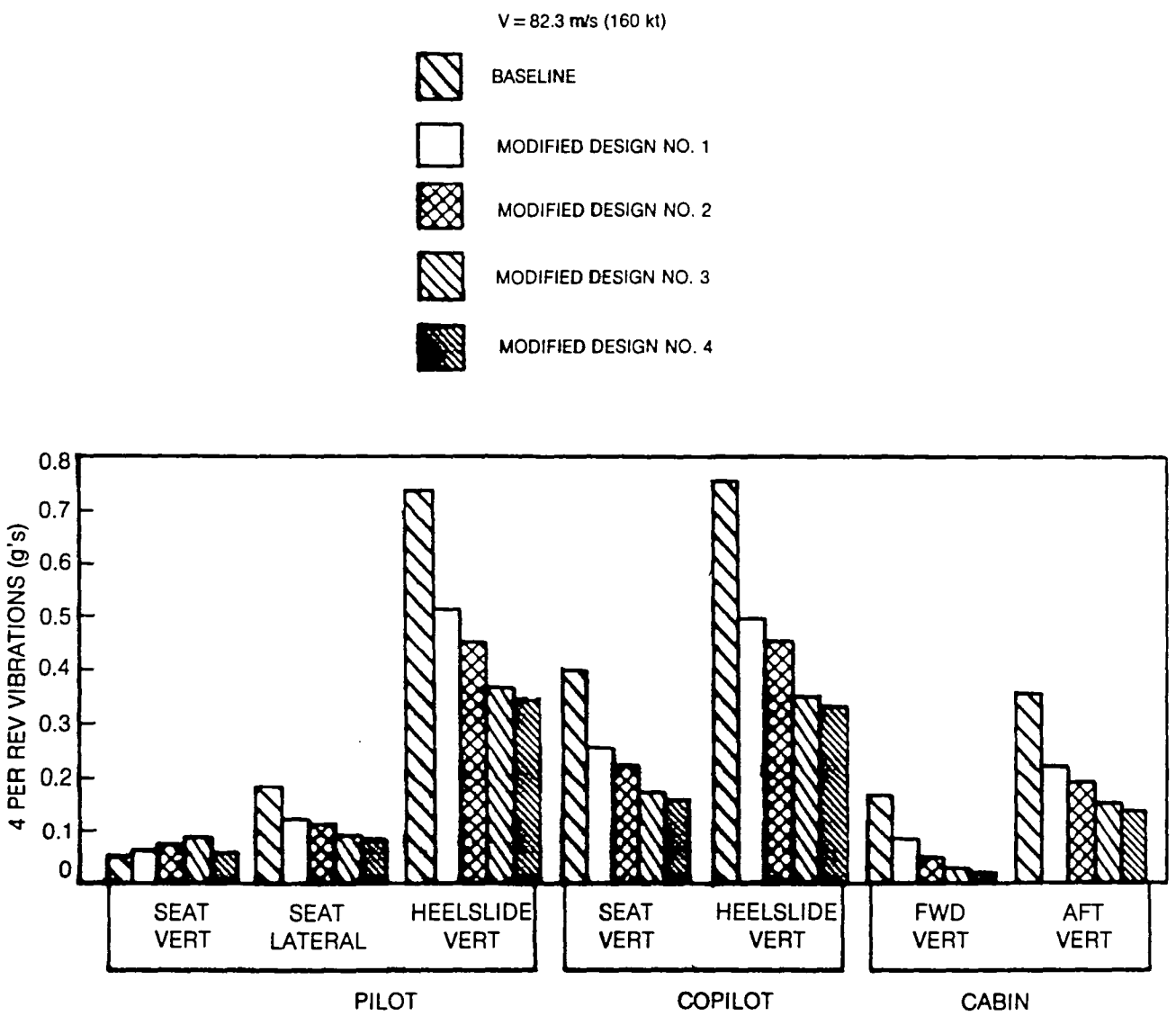

Figure 61. Predicted 4 Per Rev Fuselage Vibrations for the Modified Blade Designs at the High Speed Flight Condition

83-6-38-33

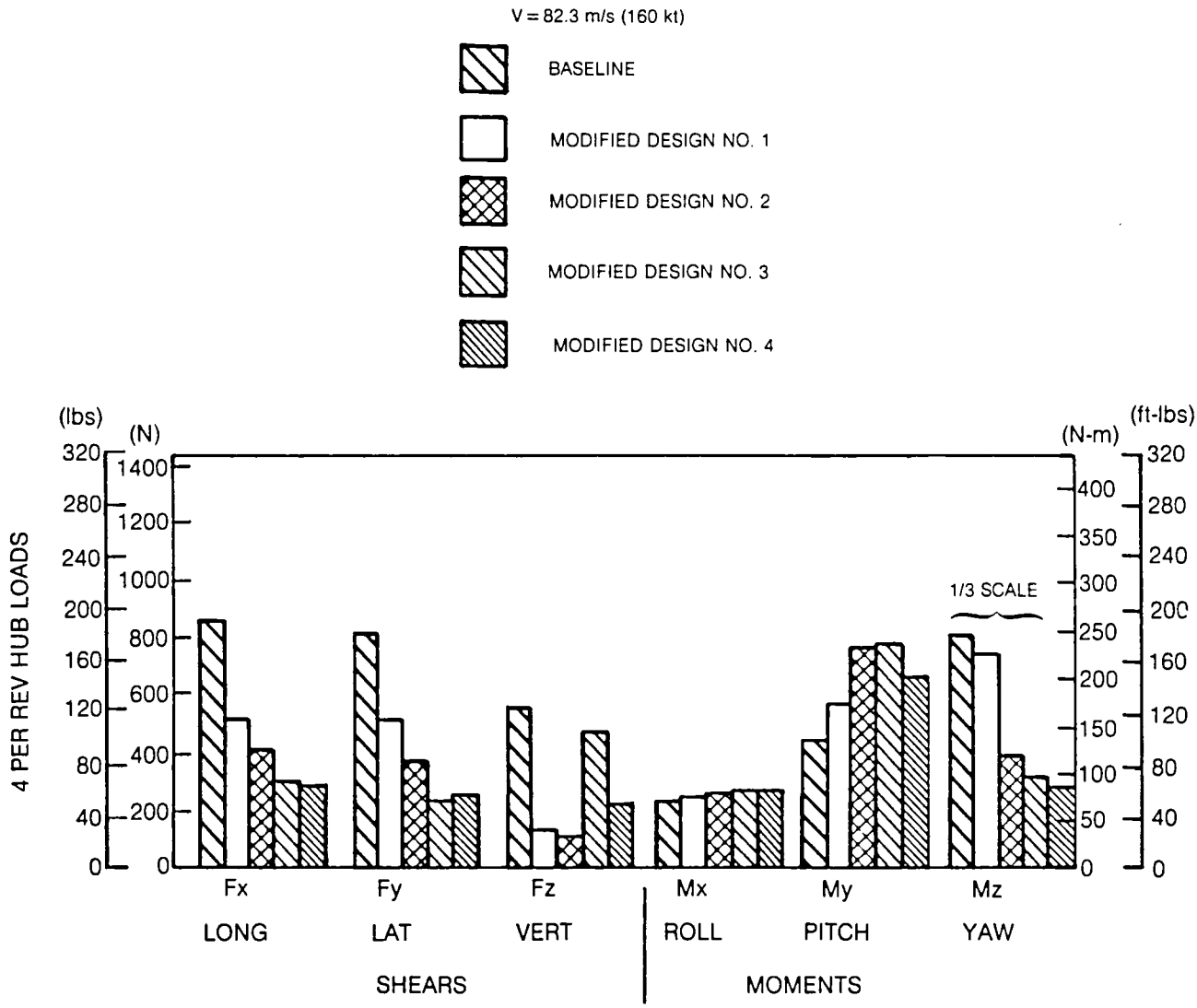

Figure 62. Summary of Predicted Baseline and Modified Blade Vibratory Fixed System Hub Loads for the High Speed Flight Condition

83-6-38-30

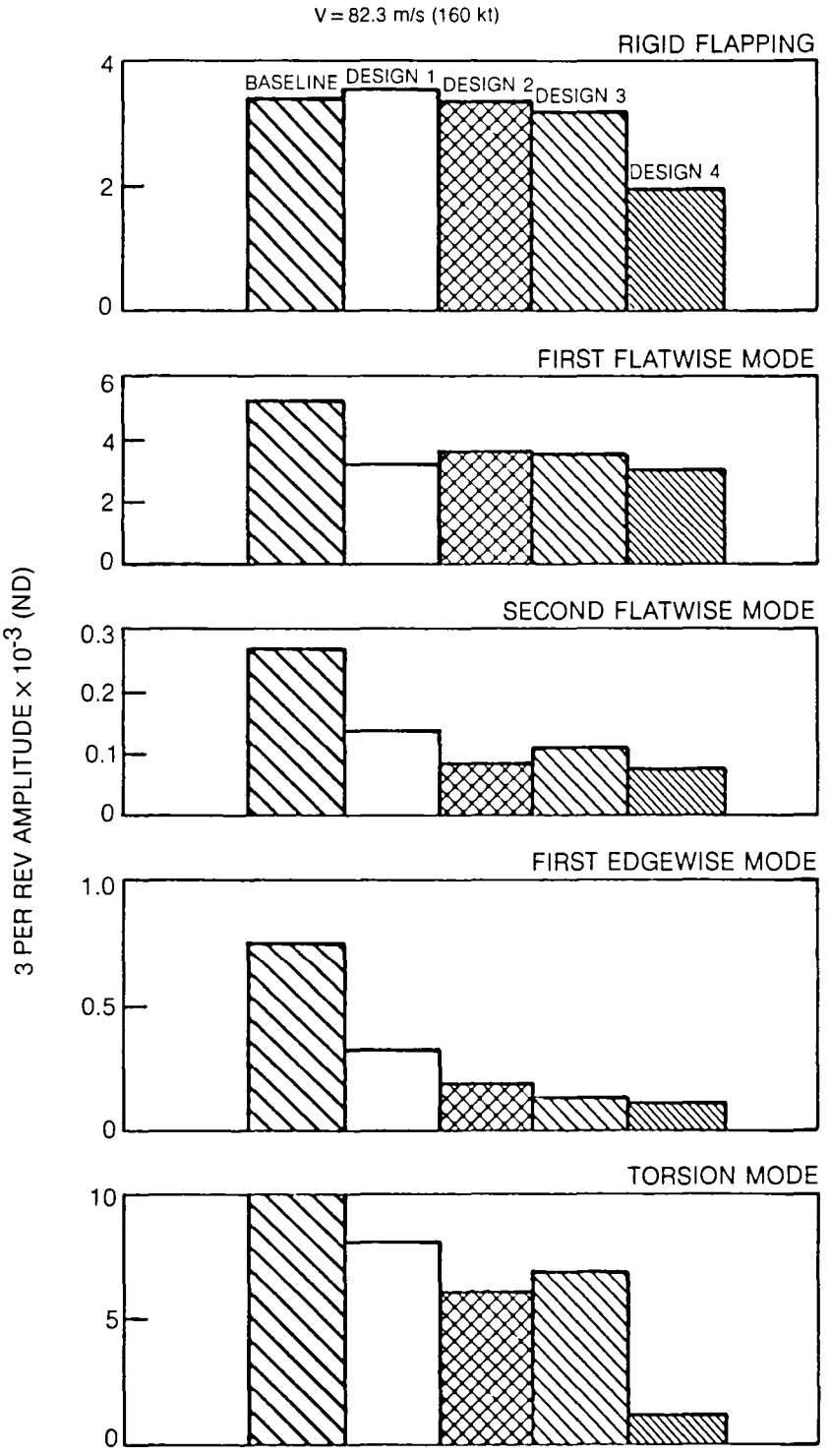

Figure 63. Summary of Predicted 3 Per Rev Modal Response for the High Speed Flight Condition

83-6-38-11

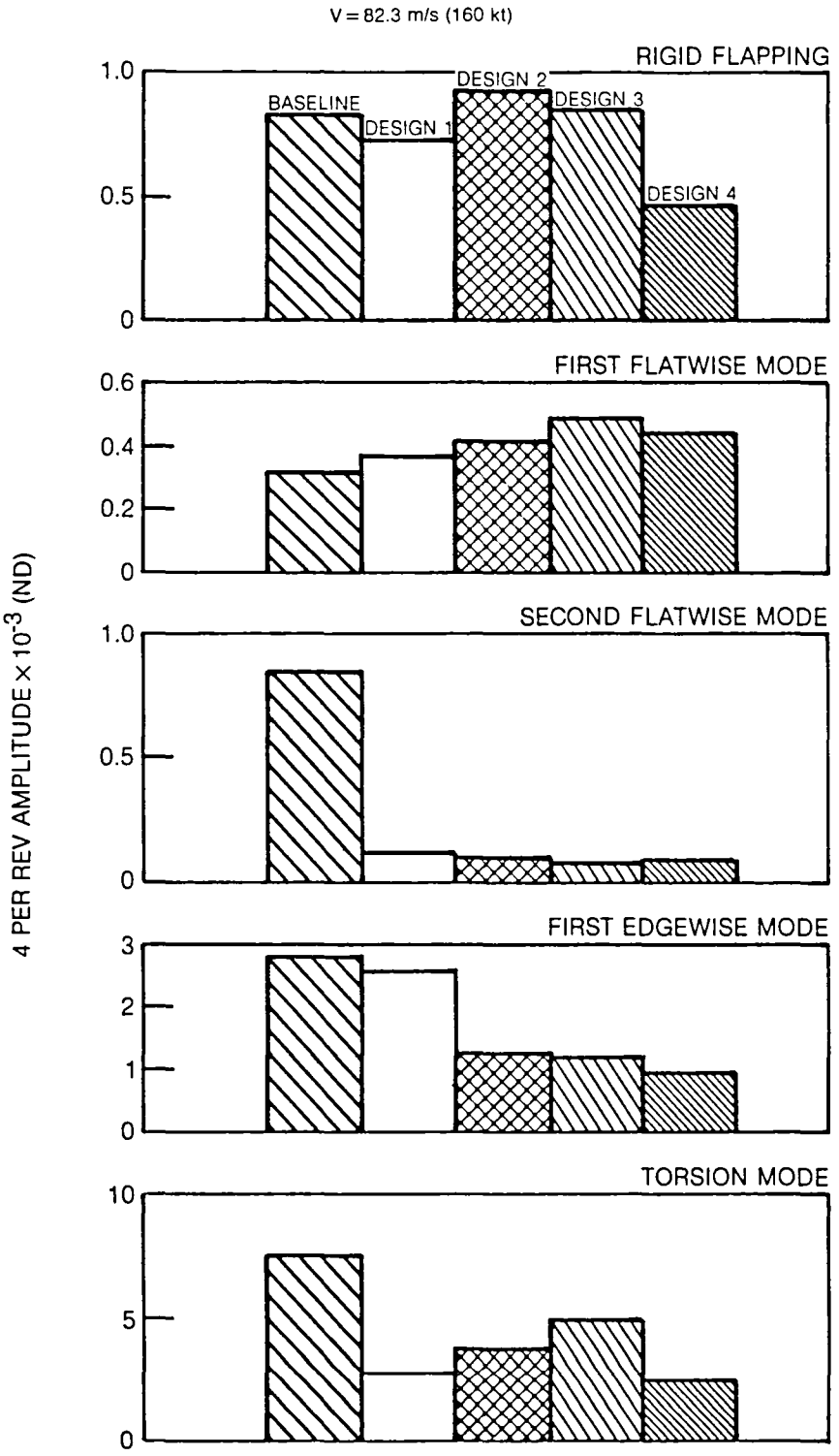

Figure 64. Summary of Predicted 4 Per Rev Modal Response for the High Speed Flight Condition

83-6-38-10

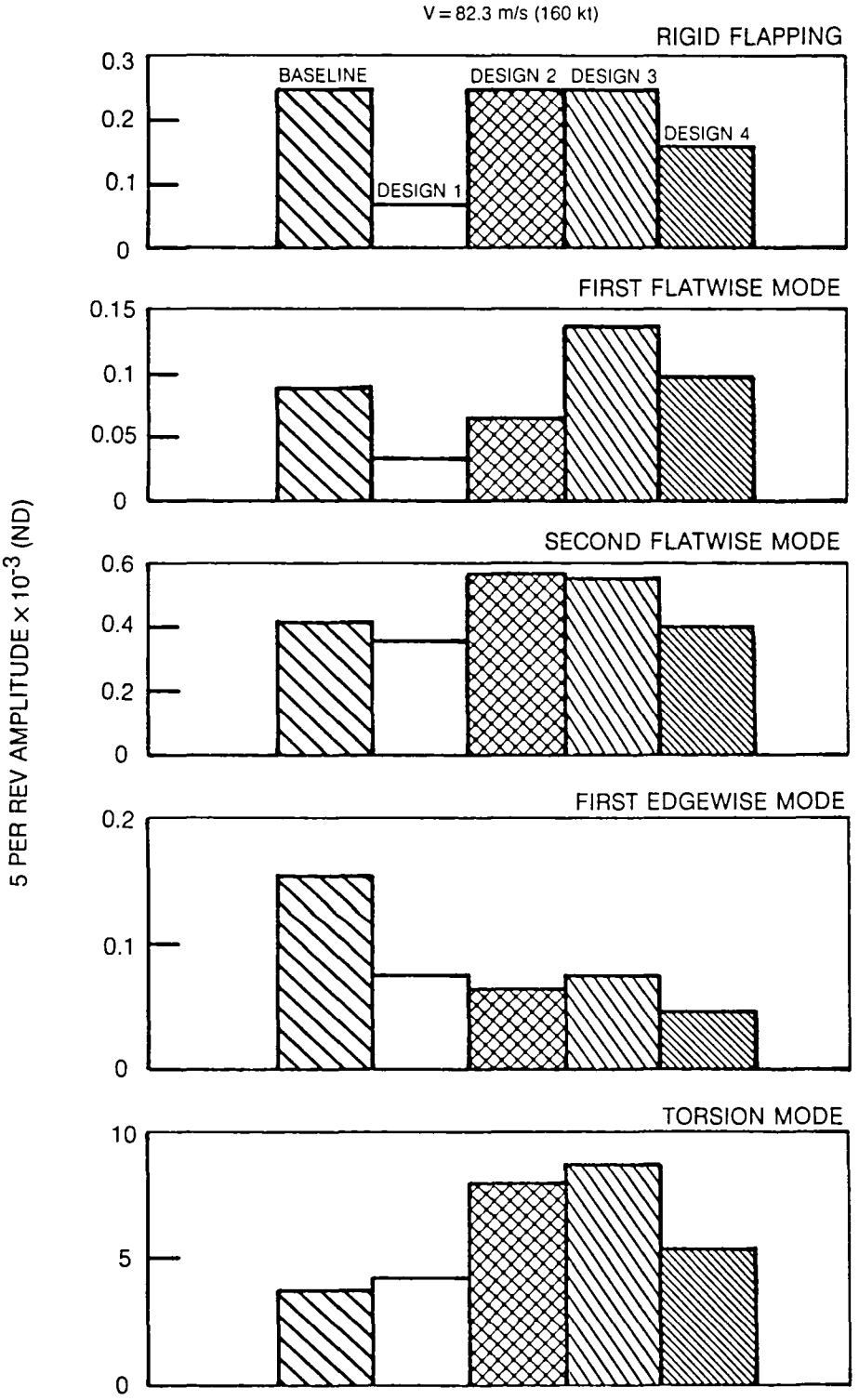

Figure 65. Summary of Predicted 5 Per Rev Modal Response for the High Speed Flight Condition

83-6-38-9

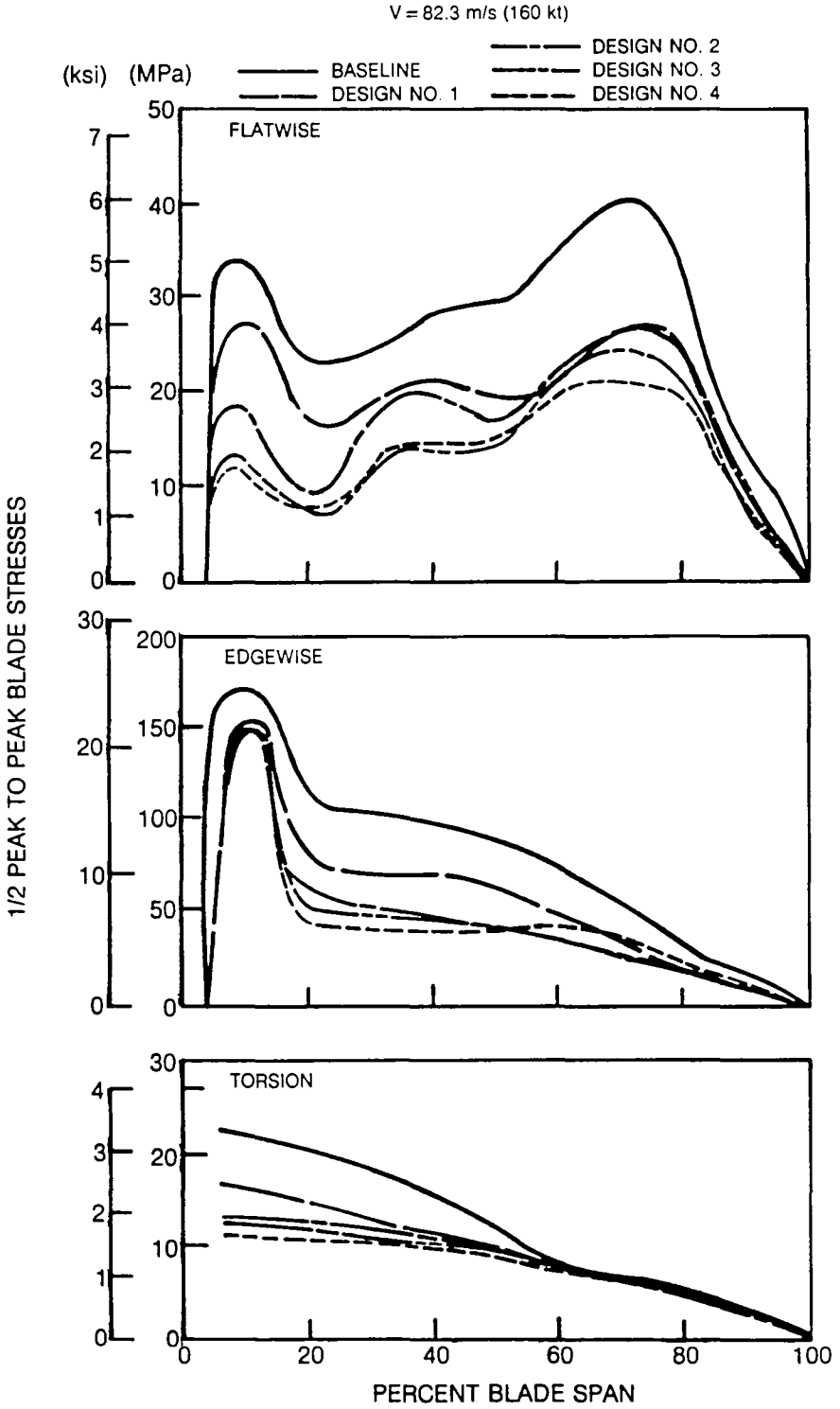

Figure 66. Summary of Predicted Peak-to-Peak Blade Stresses for the Baseline and Modified Designs at the High Speed Flight Condition

83-6-38-31

1. Report No.	2. Government Accession No.	3. Recipient's Catalog No.
NASA CR-3825 AVSCOM TR 84-A-2		

4. Title and Subtitle	5. Report Date
Helicopter Rotor Blade Design for Minimum Vibration	October 1984
	6. Performing Organization Code
7. Author(s)	8. Performing Organization Report No.
Robert B. Taylor	R33-915783-27
	10. Work Unit No.
9. Performing Organization Name and Address	
United Technologies Research Center East Hartford, Connecticut 06108	11. Contract or Grant No. NAS2-11025
	13. Type of Report and Period Covered Contractor Report (Final Report)
12. Sponsoring Agency Name and Address	14. Sponsoring Agency Code
Aeromechanics Laboratory U.S. Army Research & Technology Laboratories (AVSCOM) Ames Research Center, Moffett Field, CA 94035	

15. Supplementary Notes

Points of Contact: Donald L. Kunz, Technical Monitor (415) 965-5891
Ames Research Center, Moffett Field, CA 94035
Anton J. Landgrebe, Manager, Aeromechanics (203) 727-7358
United Technologies Research Center, East Hartford, CT 06108

16. Abstract

An analytical investigation was conducted to develop an understanding of the importance and role played by blade design parameters in rotor vibratory response and to design a minimum vibration blade based upon this understanding. Various design approaches were examined for a 4-bladed articulated rotor operating at a high speed flight condition. Blade modal shaping, frequency placement, structural and aerodynamic coupling, and intermodal cancellation were investigated to systematically identify and evaluate blade design parameters that influence blade airloads, blade modal responses, hub loads, and fuselage vibration.

The relative contributions of the various components of blade force excitation and response to the vibratory hub loads transmitted to the fuselage were determined in order to isolate primary candidates for vibration alleviation. The findings led to blade design changes based on modal shaping and frequency placement which do not follow established design criteria. Through blade design variations in mass distribution, stiffness, and outboard center-of-gravity location, a blade design was achieved which reduced the predicted fuselage vibration from the baseline blade by approximately one-half. This analytical study indicates that new blade designs can be developed that offer significant reductions in vibration (and fatigue stresses) without resorting to special vibration alleviation devices, radical blade geometries, or weight penalties.

17. Key Words (Suggested by Author(s))	18. Distribution Statement
Helicopter Vibration Rotor Blade Design Rotor Dynamics	Unclassified - unlimited STAR Category 05

19. Security Classif. (of this report)	20. Security Classif. (of this page)	21. No. of Pages	22. Price*
Unclassified	Unclassified	127	A07

*For sale by the National Technical Information Service, Springfield, Virginia 22161

NASA-Langley, 1984

National Aeronautics and
Space Administration

Washington, D.C.
20546

Official Business
Penalty for Private Use, $300

THIRD-CLASS BULK RATE

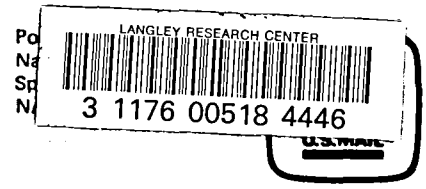

NASA

POSTMASTER: If Undeliverable (Section 158 Postal Manual) Do Not Return